New physics searches at the LHC and a 100 TeV collider

Kazuki Sakurai
(King’s College London)

In collaboration with:
John Ellis, Michihisa Takeuchi, Andreas Papaefstathiou
Ian-Woo Kim, Michele Papucci, Andreas Weiler, Lisa Zeune,
Bobby. Acharya, Krzysztof Bozek, Chakrit Pongkitivanichkul

Outline

- **Higgs measurements:**
  - anomalous ttH coupling in ttH, tHj production

- **Direct BSM searches:**
  - 8 TeV data: Interpretation of the results
  - 13/14 TeV LHC: Wino searches in split SUSY (Bino LSP case)
  - a 100 TeV collider: Wino searches in split SUSY (Higgino LSP case)

Introduction

- The LHC run 1 brought a lot of successes:
  - The discovery of a Higgs boson
  - The Higgs property measurements → SM-like
  - The direct BSM searches → strong limits

more interpretation is needed

- The LHC will resume collecting data with 13 TeV this year.
  - New Higgs property measurements
  - More direct BSM searches

Where should we look at?
How should we look at?
What are the prospects?

Higgs decay modes

- The Higgs is observed in various decay modes.
- The results are consistent with the SM.

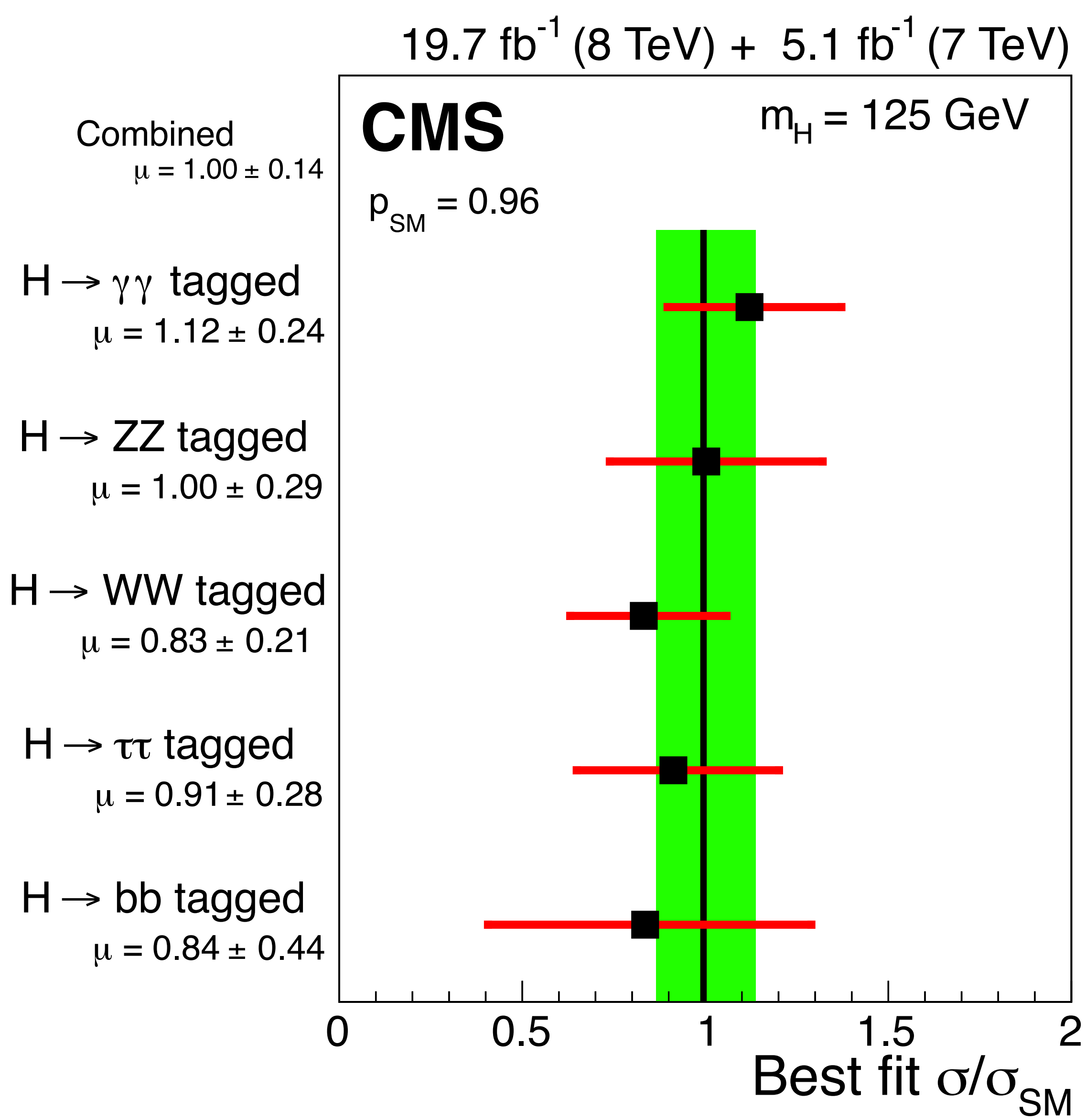

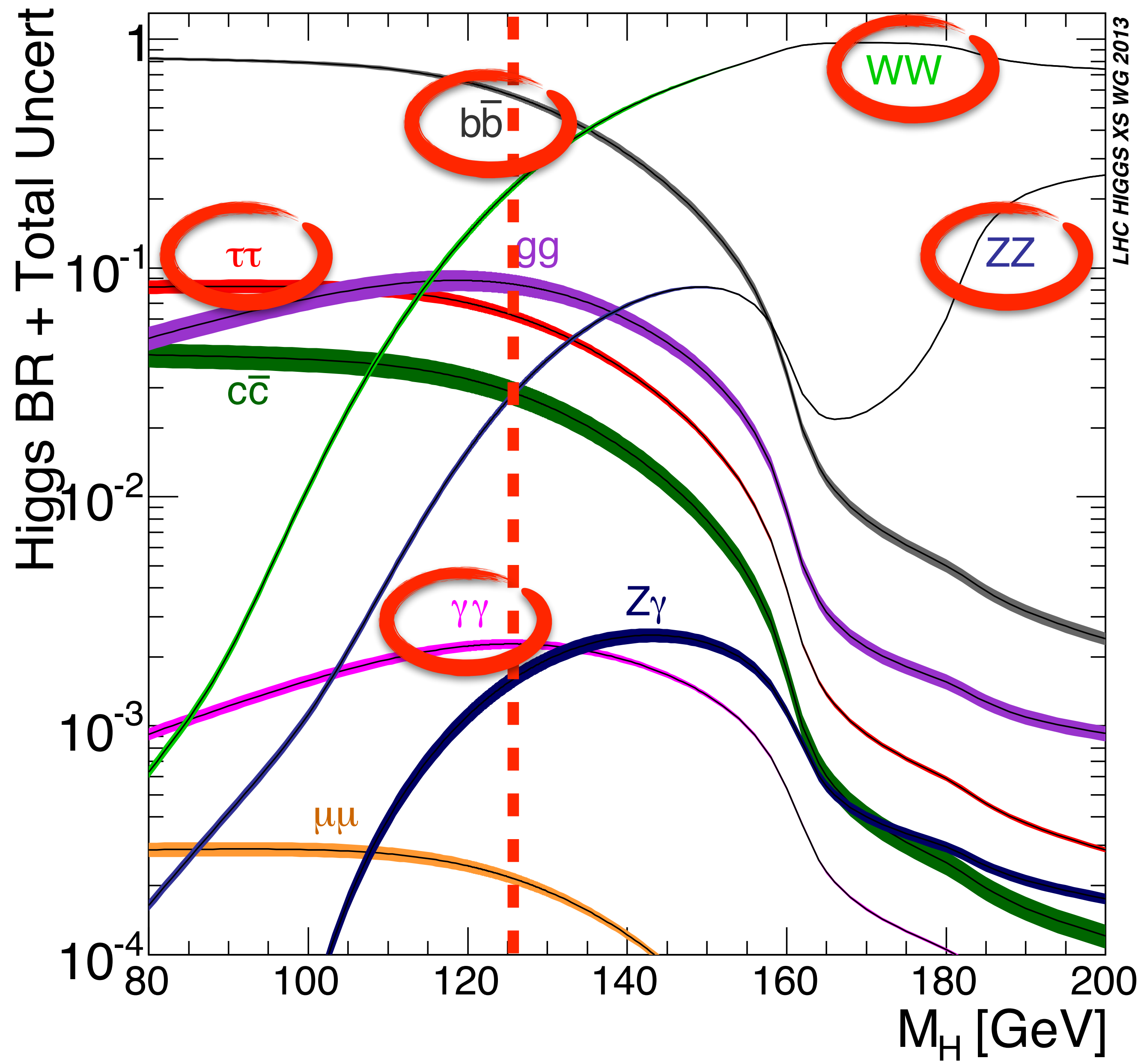

Higgs production modes

- Several Higgs production modes are measured.
- Some processes have not been well or at all observed: ttH, tHj, bbH, HH

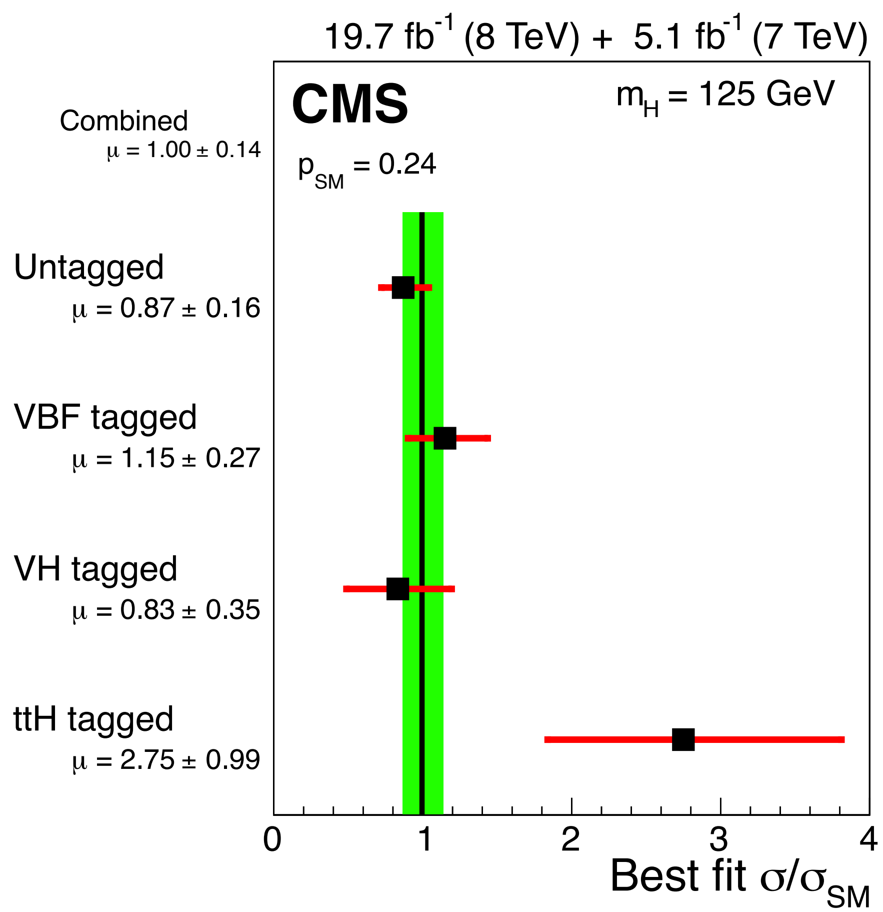

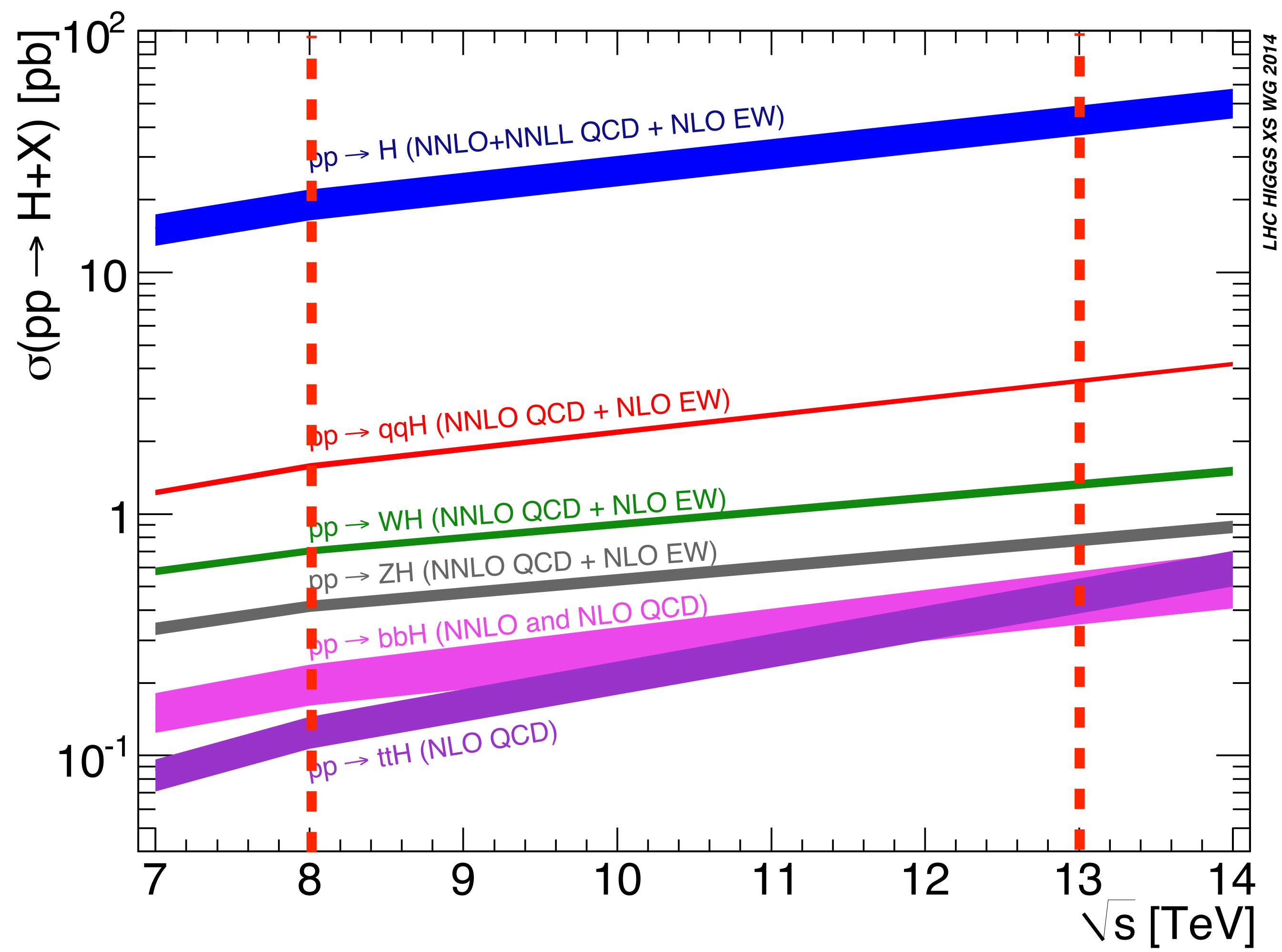

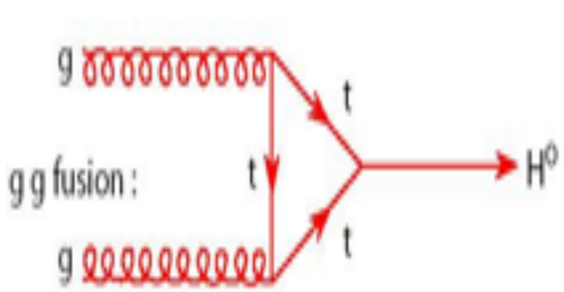

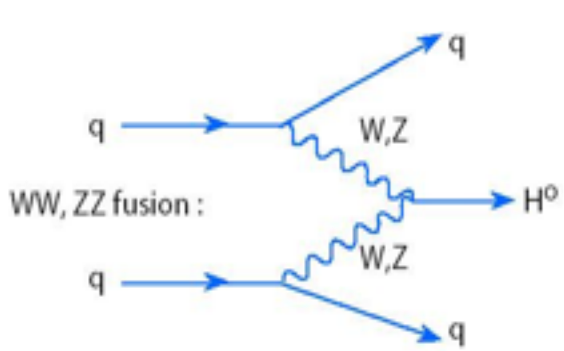

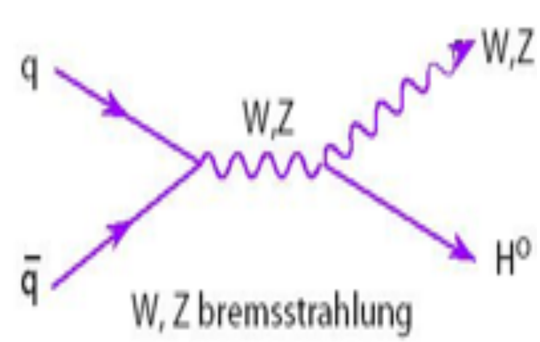

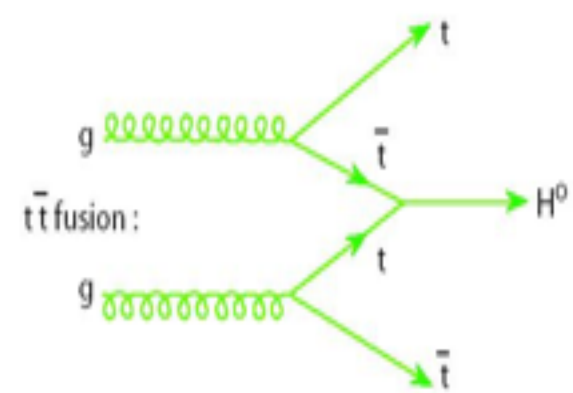

Higgs production modes

- Several Higgs production modes are measured.
- Some processes have not been well or at all observed: ttH, tHj, bbH, HH

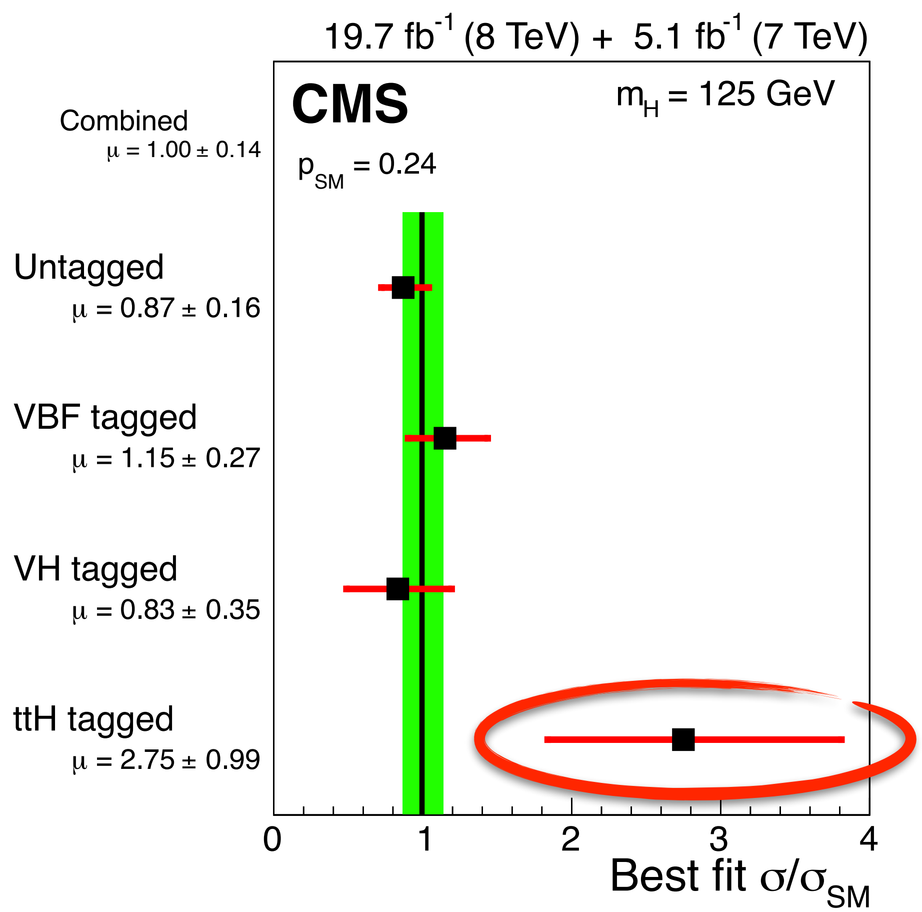

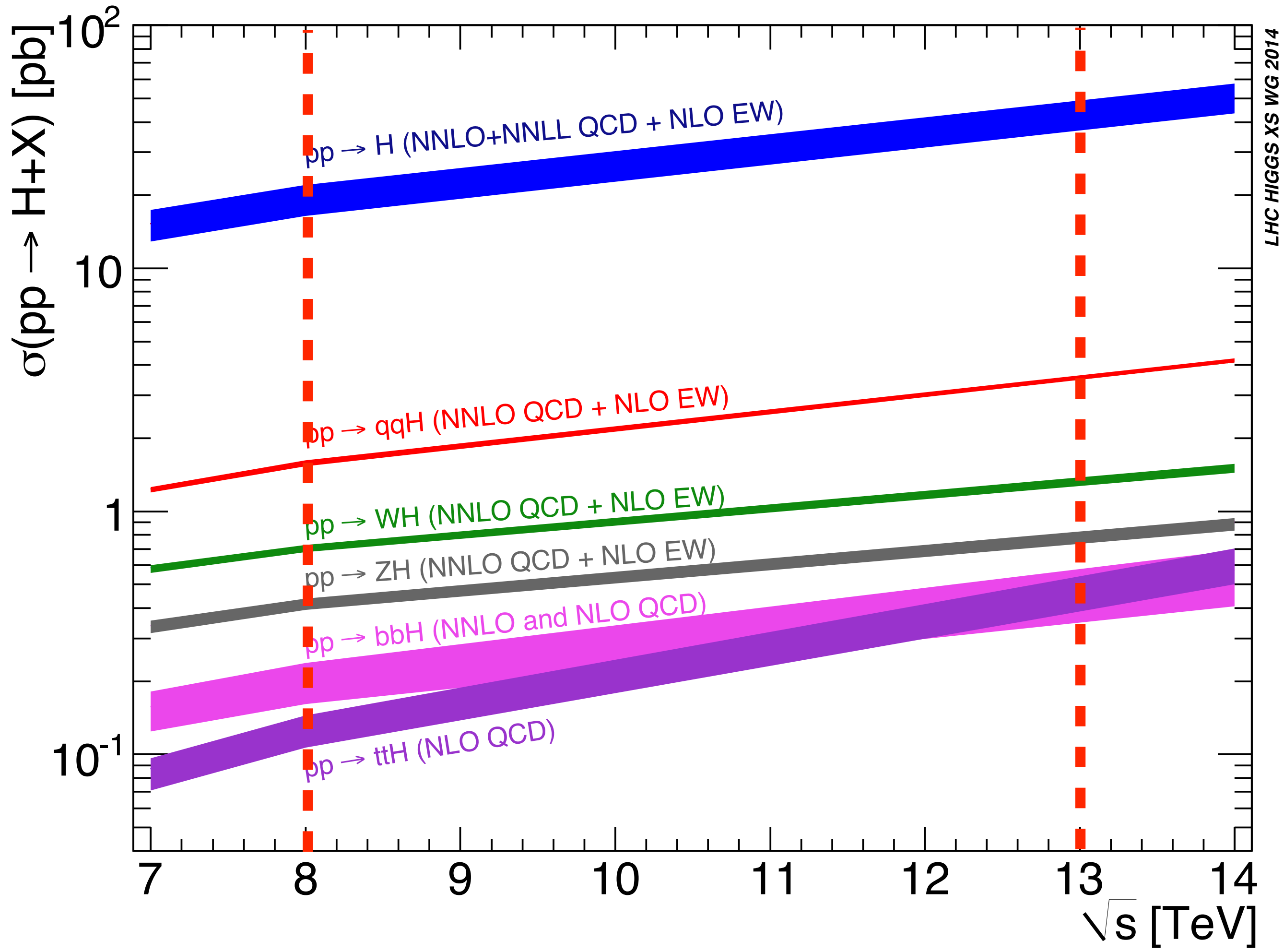

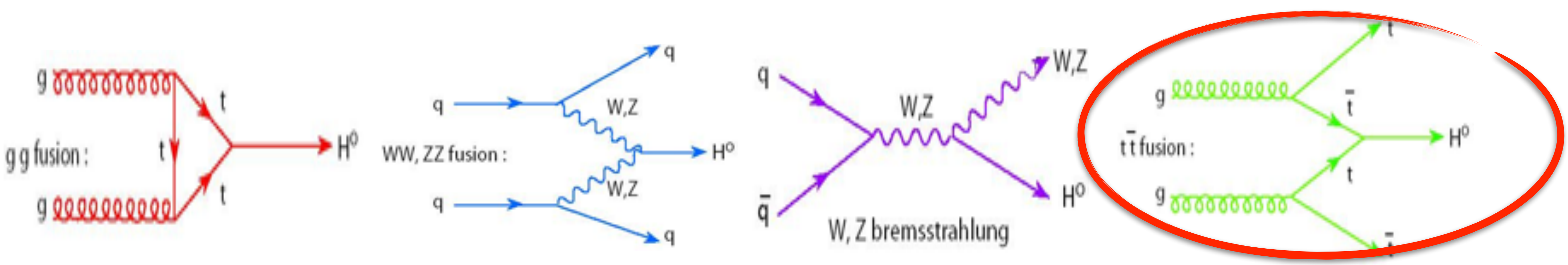

ttH and tHj productions

- The ttH production (σ~130 fb @8TeV) is only poorly measured and the tHj production (σ~18 fb @8TeV) is not measured in the 7 and 8 TeV data.
- At the 13 TeV LHC the cross sections of these processes go up and they become important physics targets at run 2 LHC.
- Observation of these production modes enable us to constrain the ttH coupling.

$$\mathcal{L}_t = -\frac{m_t}{v}(\kappa_t \bar{t}t + i\tilde{\kappa}_t \bar{t}\gamma_5 t)H \qquad \text{SM: } (\kappa_t, \tilde{\kappa}_t) = (1, 0)$$

↑ CPV

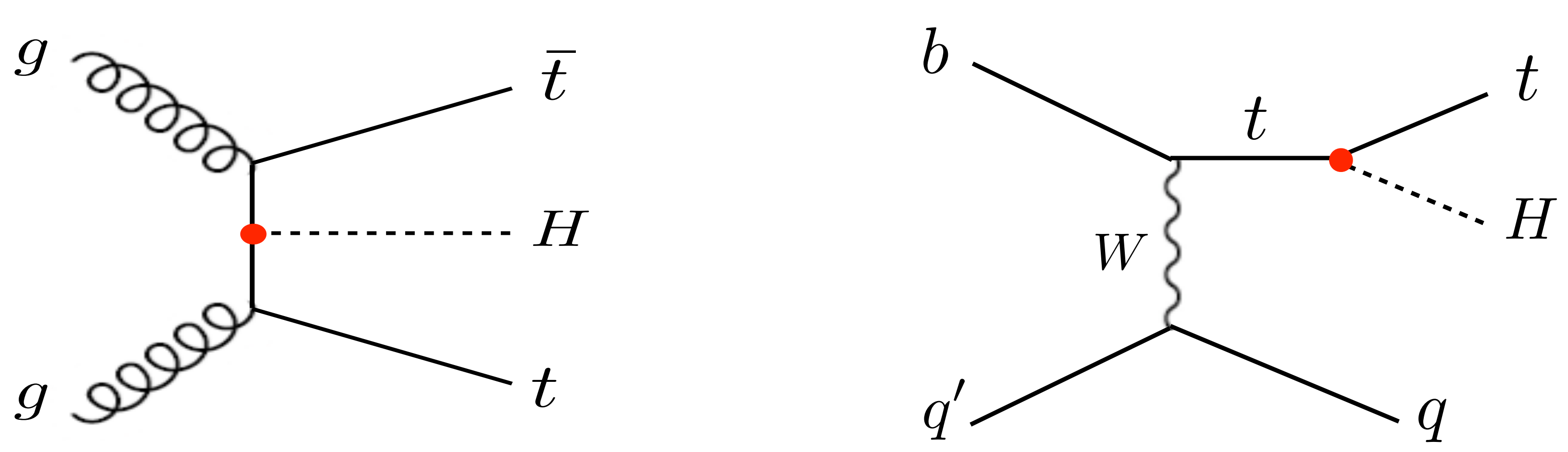

Constraint on ttH coupling

- The ttH coupling is already constrained by the gluon-fusion Higgs production and the Higgs decay into γγ.

$$\mathcal{L}_\Delta = -\left[\frac{\alpha_s}{8\pi} c_g b_g G^a_{\mu\nu} G^{\mu\nu a} + \frac{\alpha_{em}}{8\pi} c_\gamma b_\gamma F_{\mu\nu} F^{\mu\nu}\right]\left(\frac{H}{v}\right)$$

SM: $(c_g, c_\gamma) = (1, 1)$

gg→H production

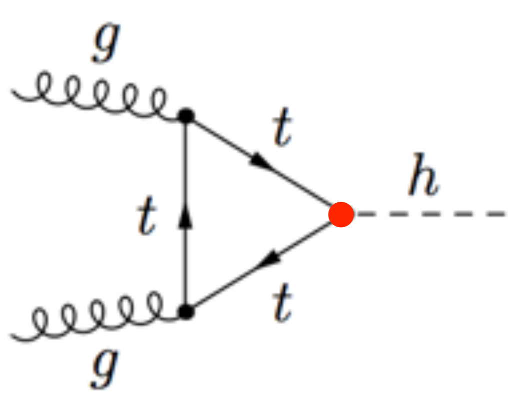

H→γγ decay

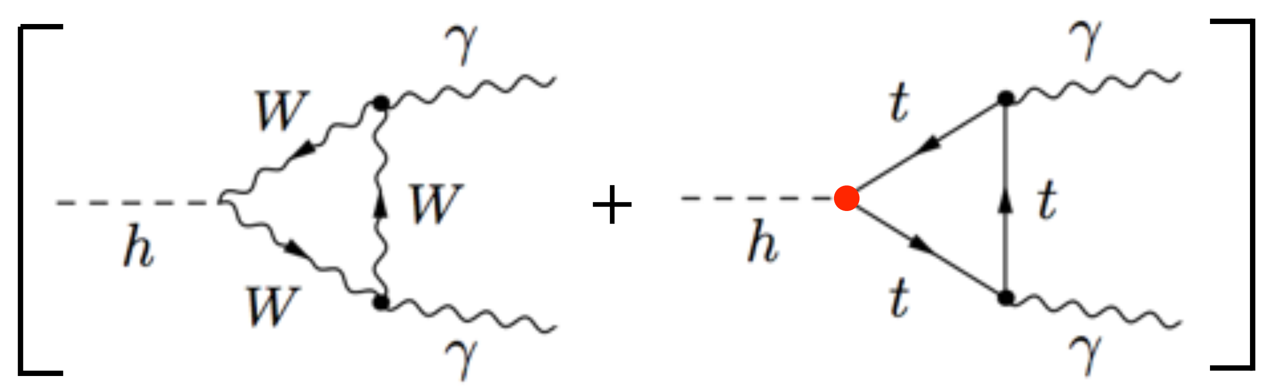

Constraint on ttH coupling

- One can translate the constraint on (c_g, c_γ) into (κ_t, $\tilde{\kappa}_t$).

John Ellis, Tevong You (1303.3879)

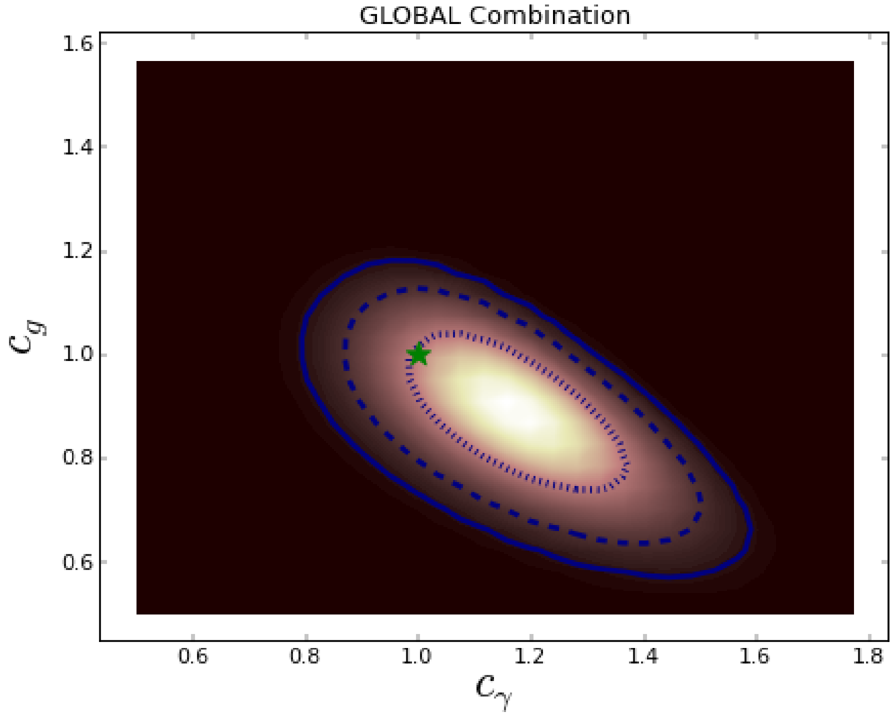

$$\mathcal{L}_\Delta = -\left[\frac{\alpha_s}{8\pi} c_g b_g G^a_{\mu\nu} G^{\mu\nu a} + \frac{\alpha_{em}}{8\pi} c_\gamma b_\gamma F_{\mu\nu} F^{\mu\nu}\right]\left(\frac{H}{v}\right)$$

$$\mathcal{L}_t = -\frac{m_t}{v}(\kappa_t \bar{t} t + i\tilde{\kappa}_t \bar{t}\gamma_5 t) H$$

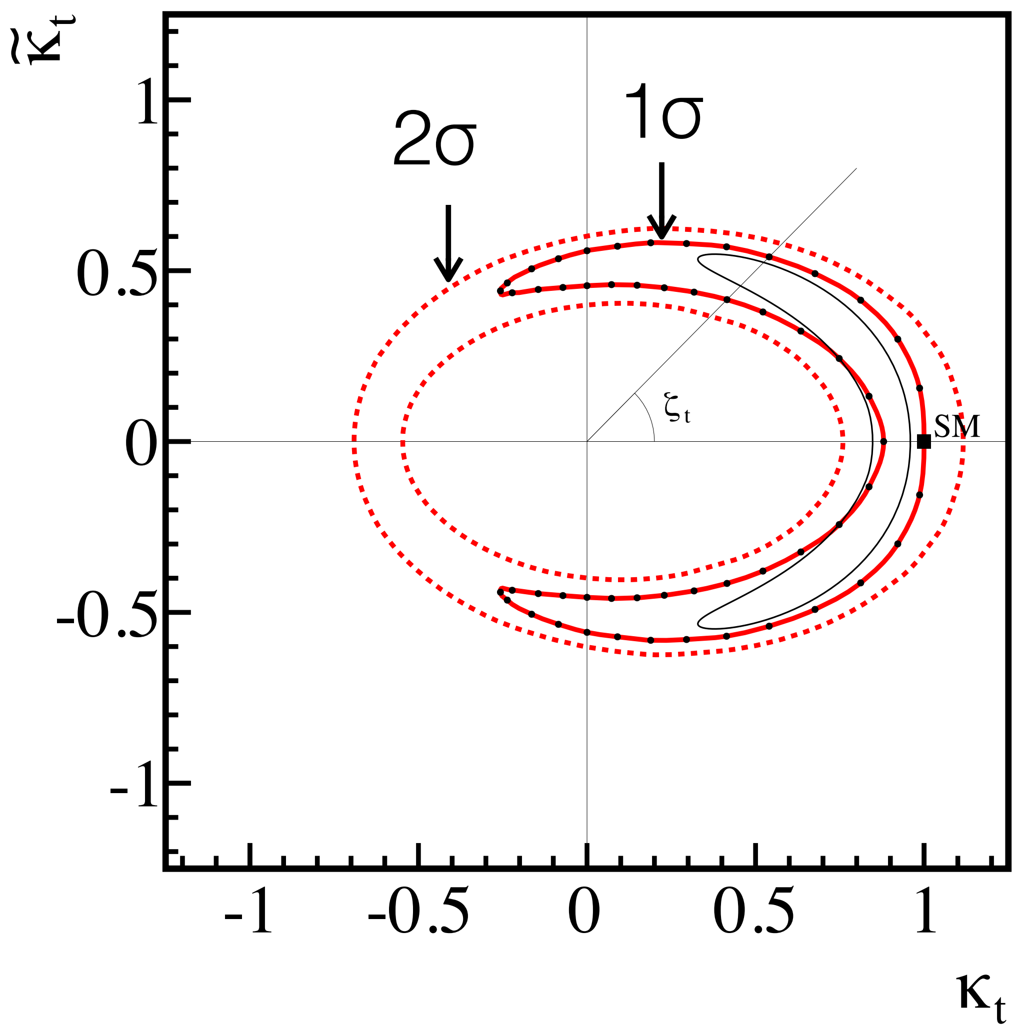

- The CP phase ζ_t is not well constrained.

J. Ellis, KS, D.S. Hwang, M. Takeuchi (1312.5736)

Cross sections

- How are the cross sections affected by the anomalous top-Higgs coupling?

$pp \to \bar{t}tH$

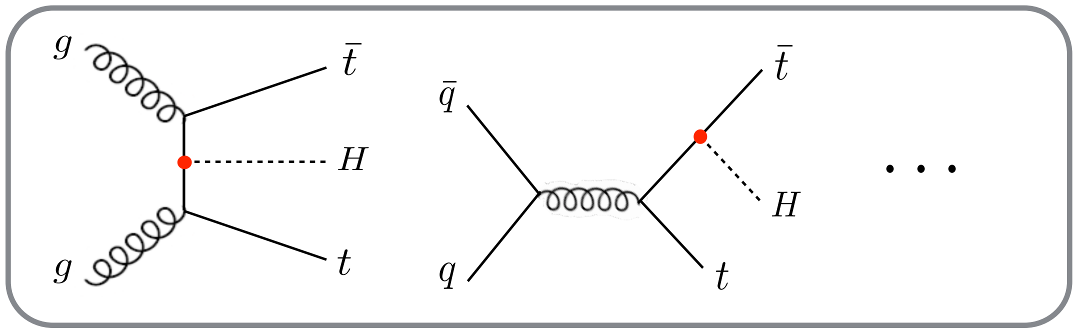

$pp \to tHj\ (\bar{t}Hj)$

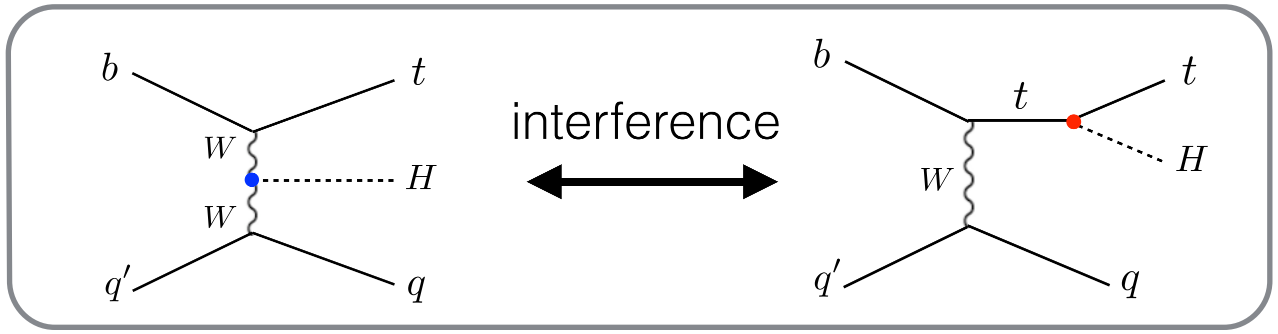

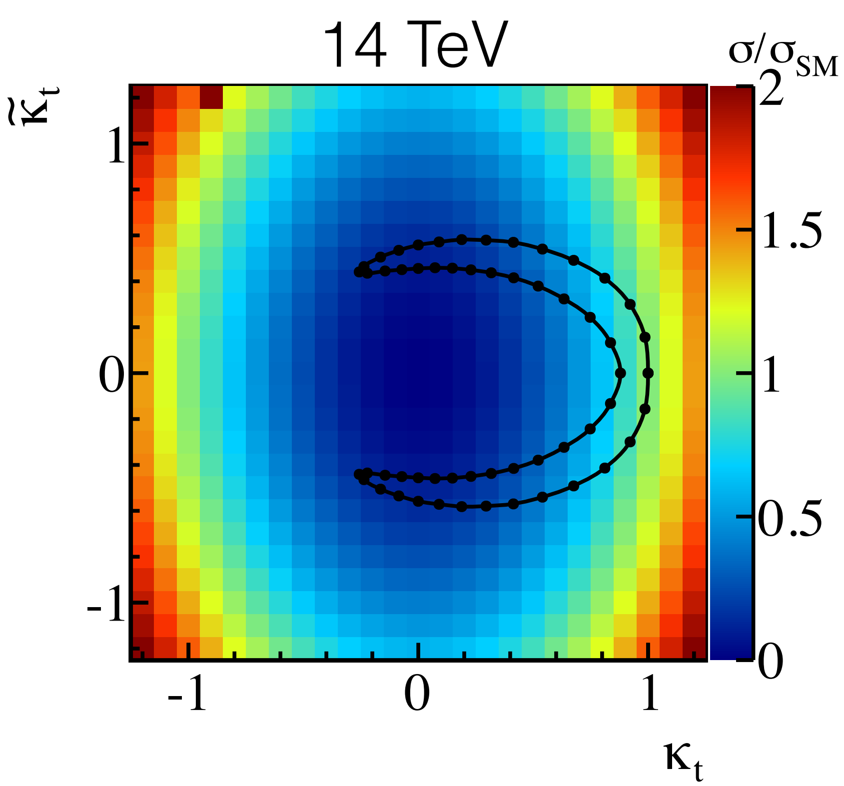

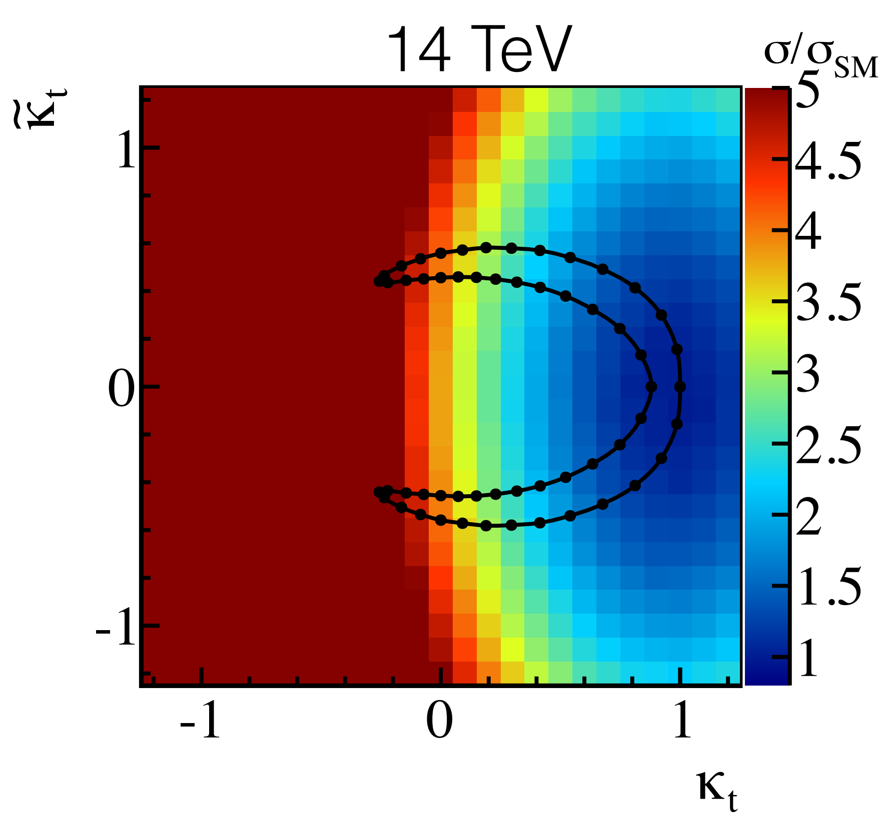

J. Ellis, KS, D.S. Hwang, M. Takeuchi (1312.5736)

Cross sections

- How are the cross sections affected by the anomalous top-Higgs coupling?

$pp \to \bar{t}tH$

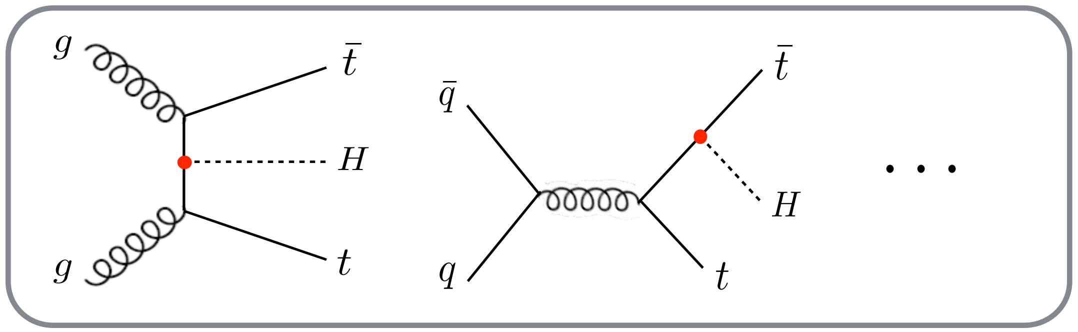

$pp \to tHj\ (\bar{t}Hj)$

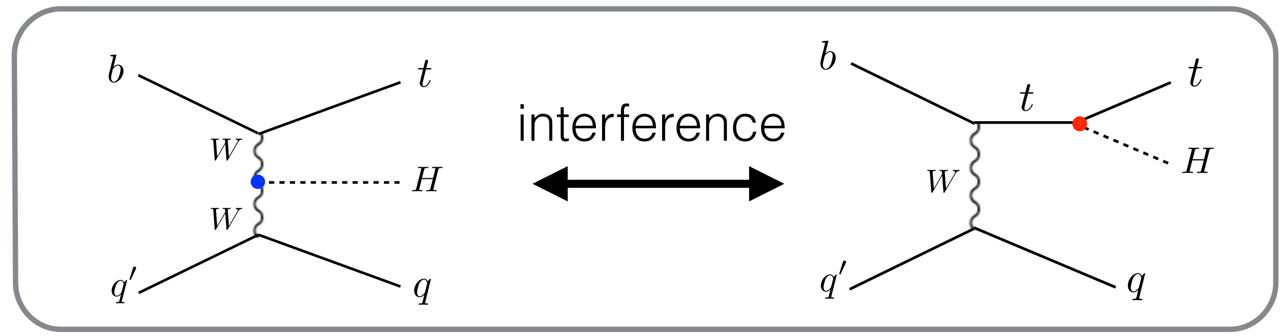

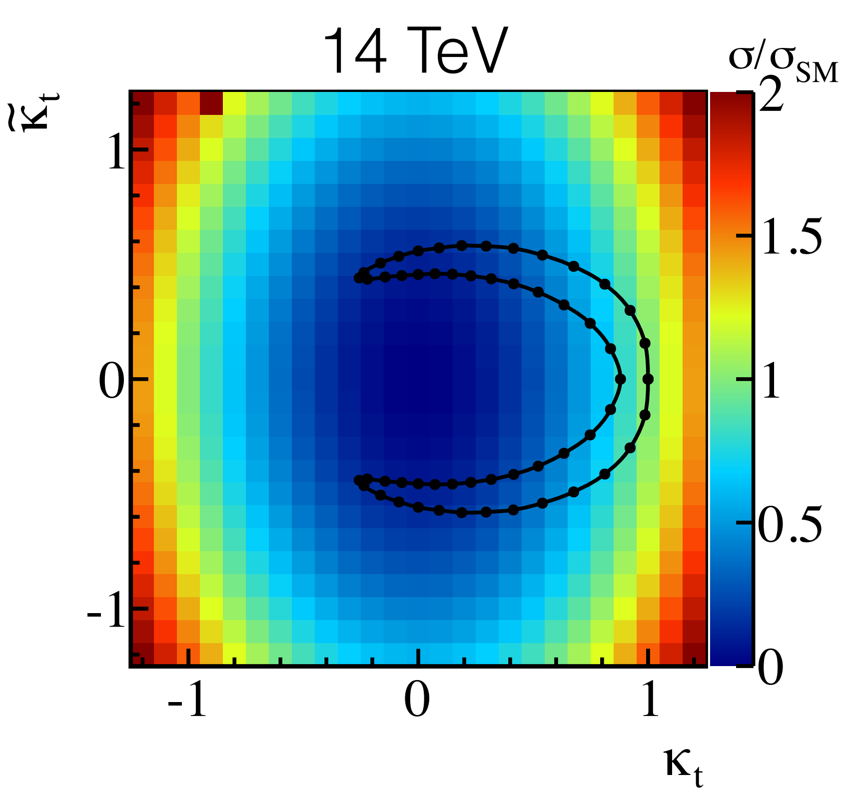

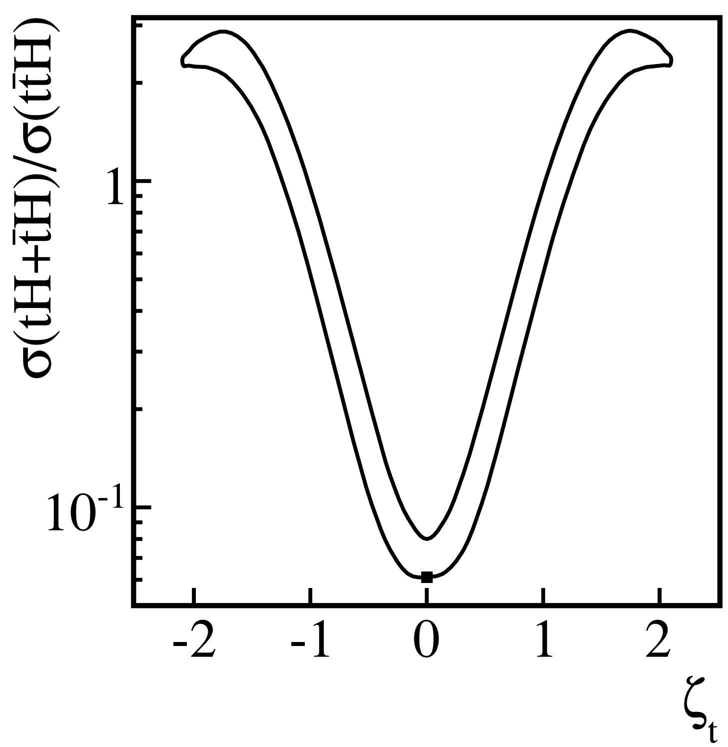

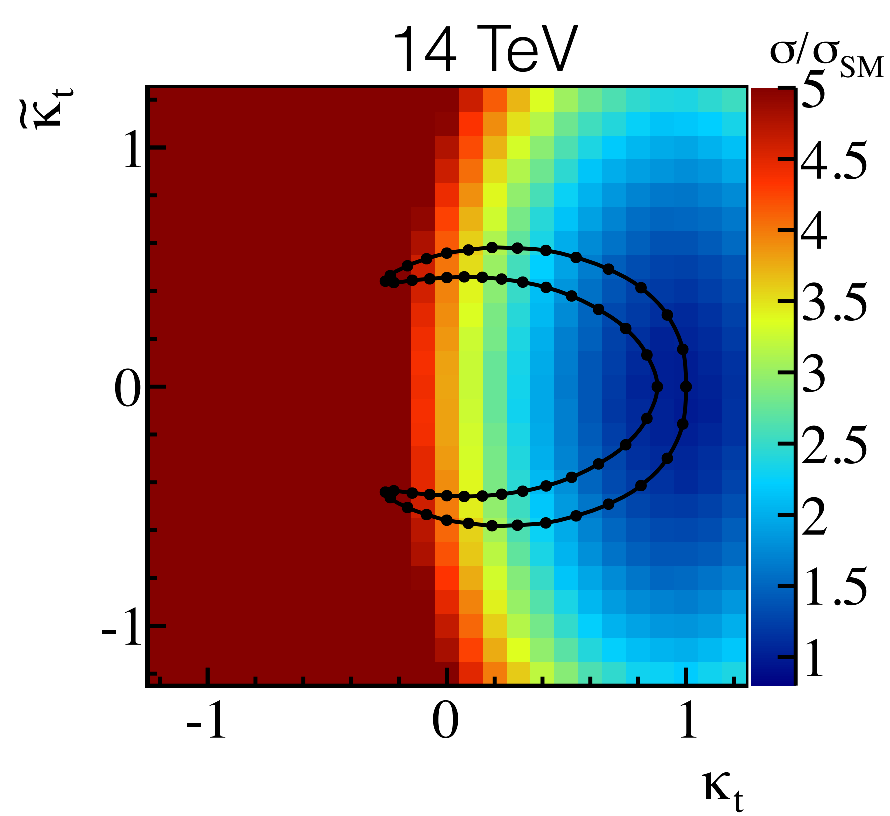

- For ζ_t > 1.2, σ(tHj) can become larger than σ(ttH).
- The difference from the SM is a factor of 20 at the maximum.

Spin measurement in tHj

- In the diagram without ttH coupling the top is dominantly left-handed, whereas it is right-handed in the diagram with ttH. Modification of ttH coupling may affect the top polarisation measurement in tHj.

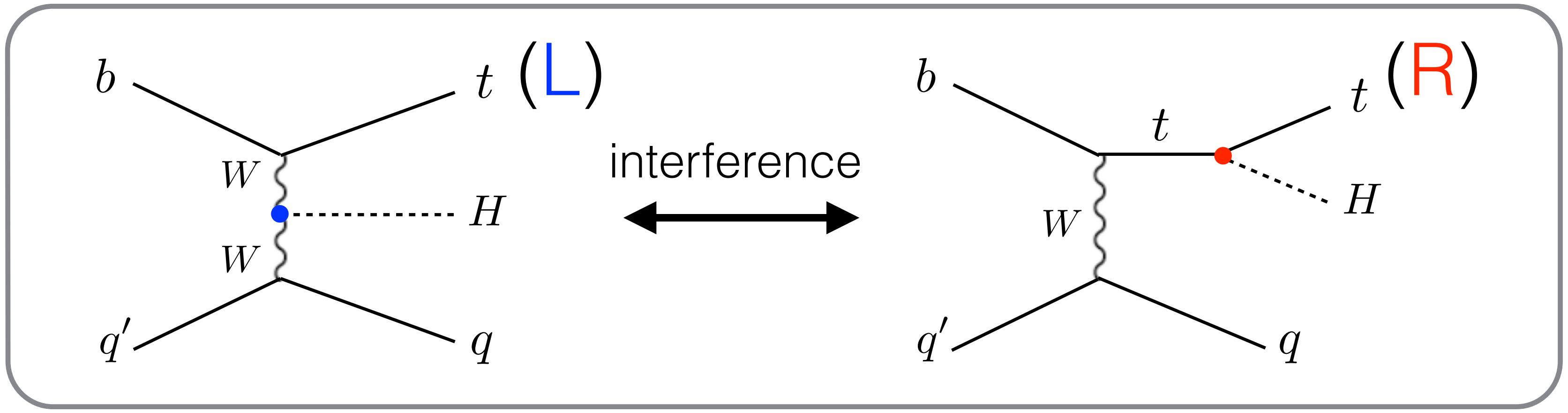

- The top polarisation can be measured by the angle of the lepton w.r.t the top boost direction at the top rest frame.

$$\frac{1}{\Gamma_\ell}\frac{d\Gamma_\ell}{d\cos\theta_\ell} = \frac{1}{2}(1 + P_t\cos\theta_\ell)$$

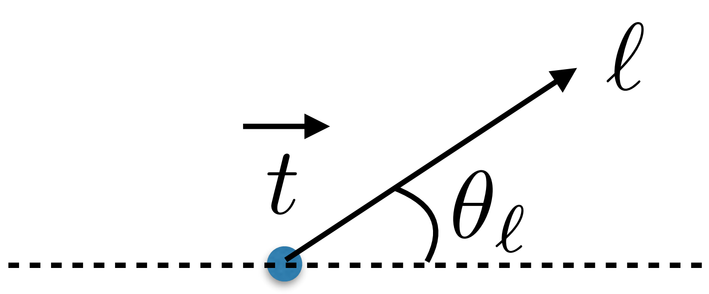

$P_t = \pm 1$ for pure right(left)-handed top

Spin measurement in tHj

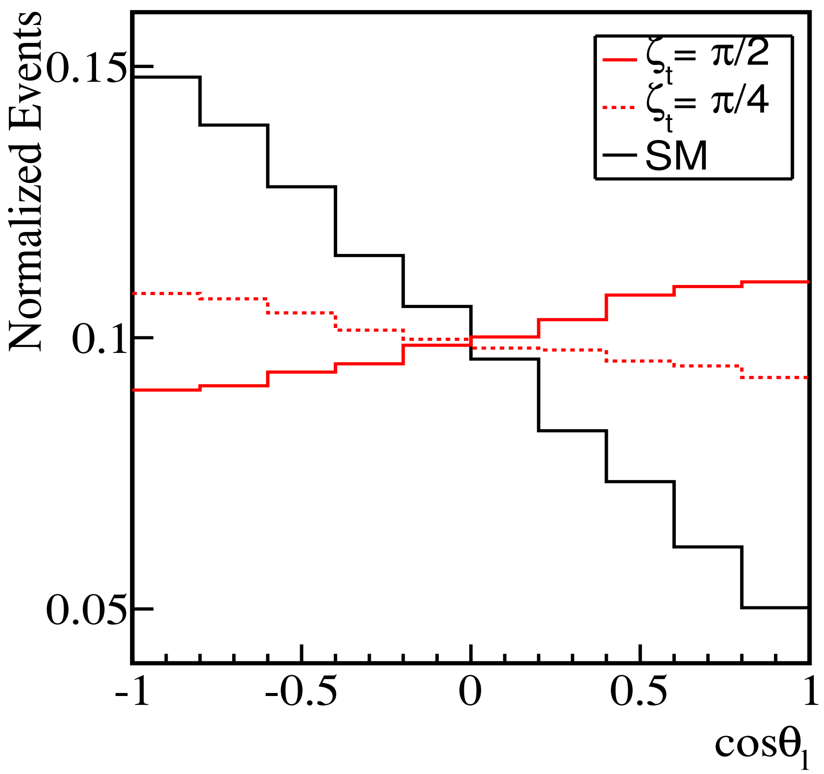

- The $\cos\theta_l$ distribution but in the tHj rest frame
- Some dependency of the CP phase
- In SM the lepton prefers the opposite direction to the top boost direction, whereas for $\zeta_t = \pi/2$, it prefers the same direction.

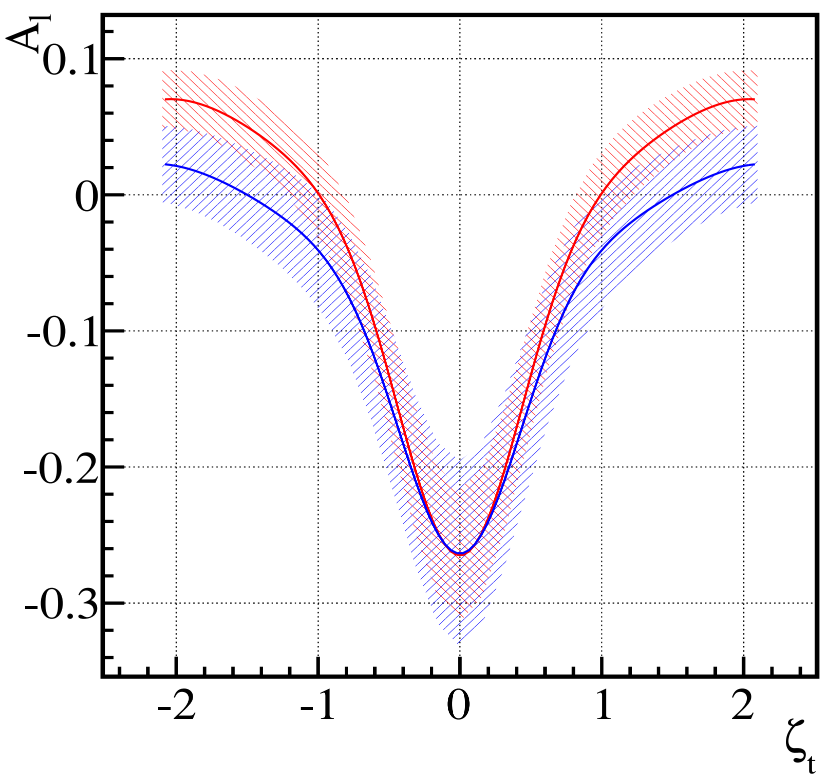

- The asymmetry is an useful measure.

$$A_\ell = \frac{N(\cos\theta_\ell > 0) - N(\cos\theta_\ell < 0)}{N(\cos\theta_\ell > 0) + N(\cos\theta_\ell < 0)}$$

- tHj and tbarHj. The band is the statistic error assuming 14 TeV LHC with 100 fb^{-1}.
- $\zeta_t > 0$ and < 0 are not distinguishable.

J. Ellis, KS, D.S. Hwang, M. Takeuchi (1312.5736)

14 TeV, Parton Level

The angle from prod. plane

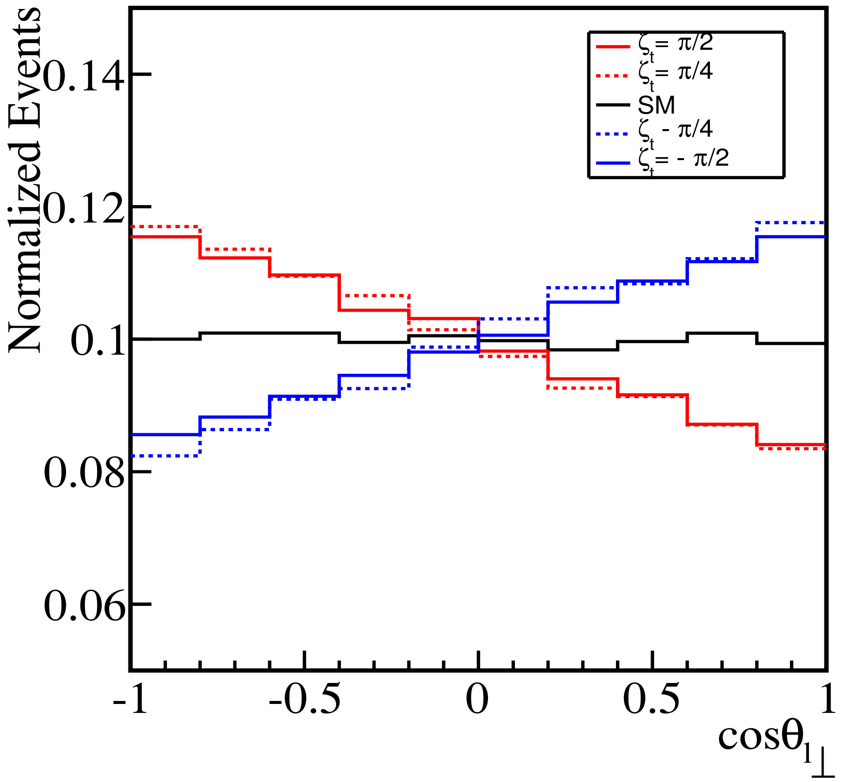

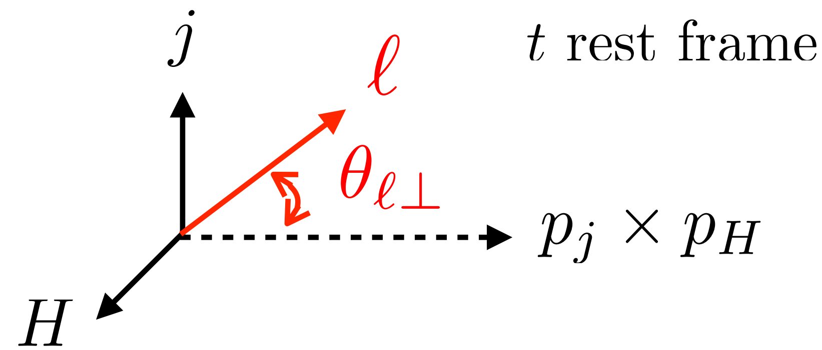

- The SM has a flat distribution => no CPV
- With $\zeta_t \neq 0$, the lepton prefers a particular direction depending on the sign of ζ_t.

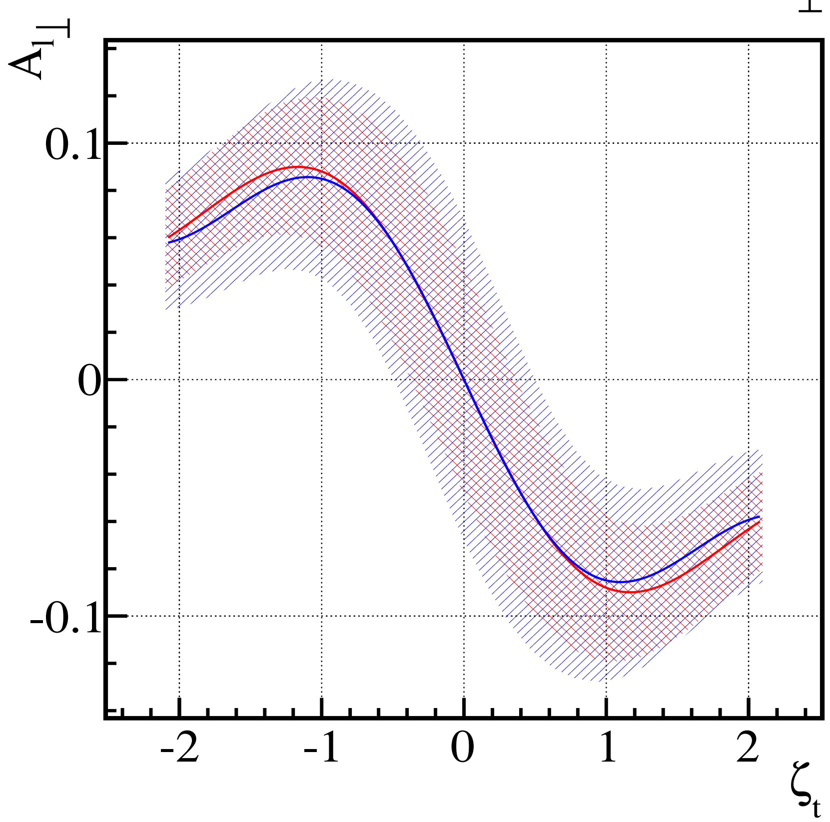

$$A_\ell = \frac{N(\cos\theta_\ell > 0) - N(\cos\theta_\ell < 0)}{N(\cos\theta_\ell > 0) + N(\cos\theta_\ell < 0)}$$

- ζ_t > 0 and < 0 are distinguishable.

J. Ellis, KS, D.S. Hwang, M. Takeuchi (1312.5736)

14 TeV, Parton Level

Spin Correlation in ttH

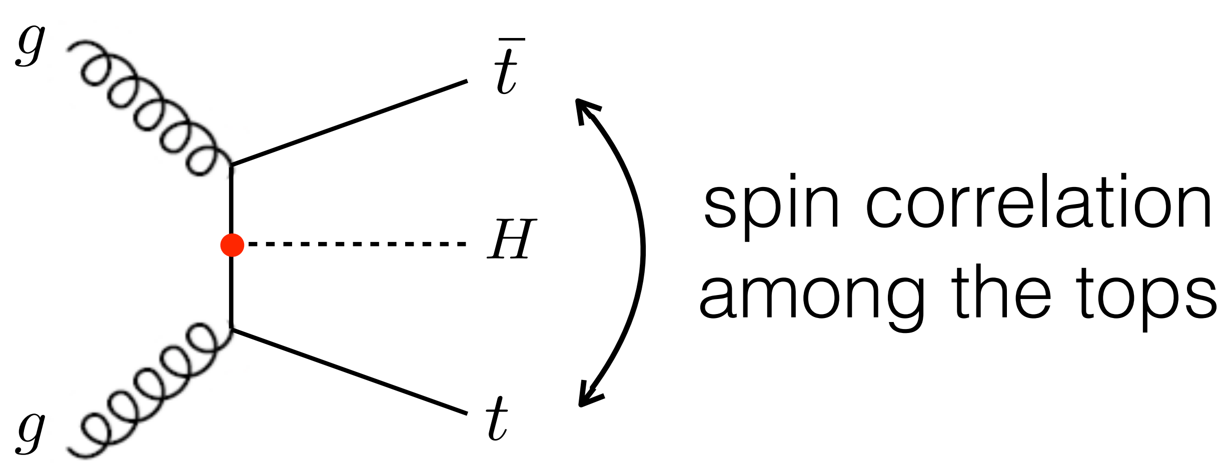

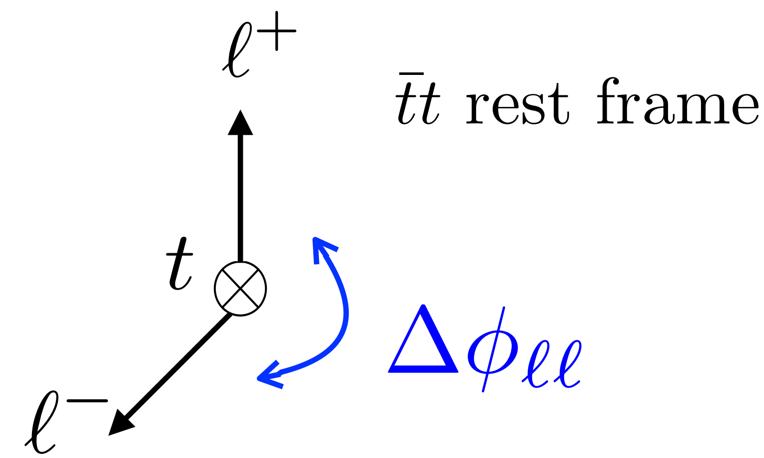

The sign is defined by the direction of the top.
This is important to capture the CP violation.

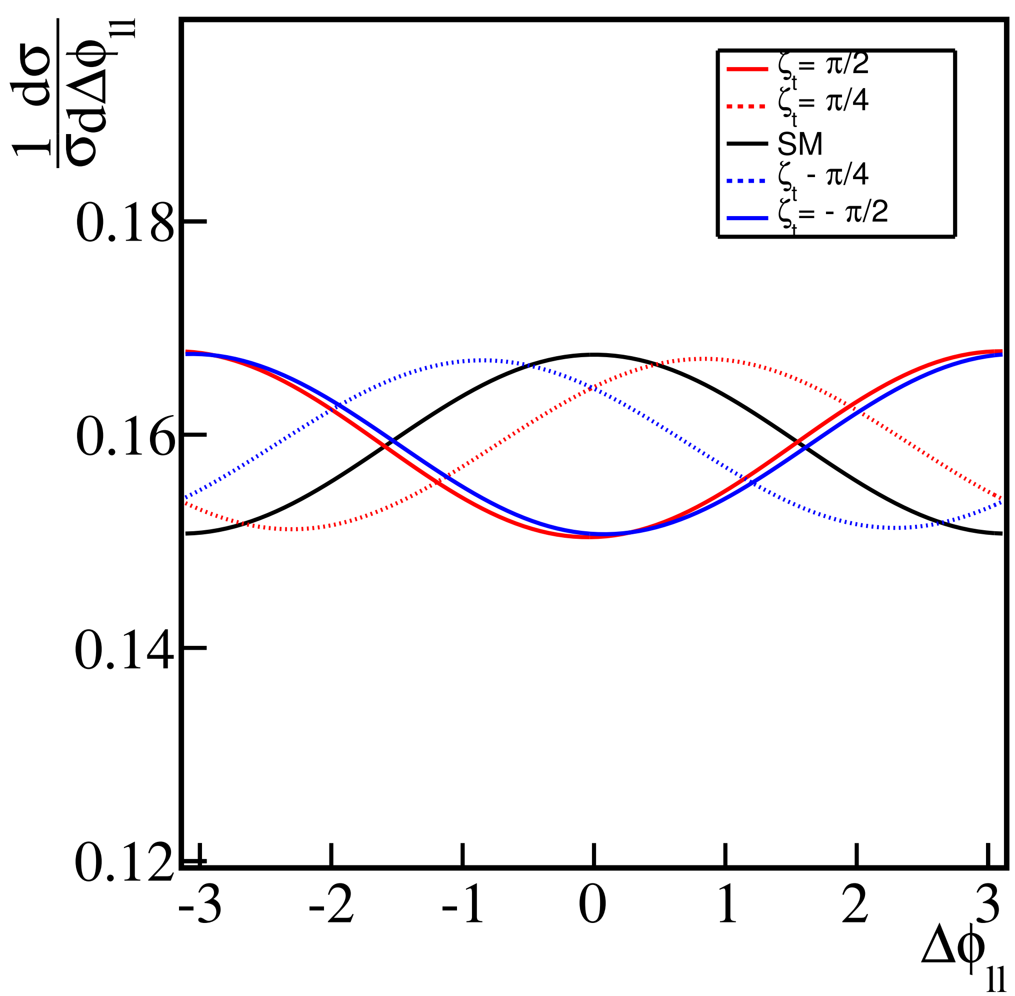

- $\Delta\phi_{\ell\ell}$ can discriminate $\xi_t > 0$ and < 0.
- The fit shows:

$$\frac{d\sigma}{d\Delta\phi_{\ell\ell}} \propto \cos(\Delta\phi_{\ell\ell} - \delta) + \text{const}$$

$$\delta = 2\xi_t - \sin(2\xi_t)/2$$

14 TeV, Parton Level

Direct BSM searches

Supersymmetry

- A number of SUSY searches has been conducted: ~50 analyses (including preliminary ones) using the 8 TeV data.

Supersymmetry

- A number of SUSY searches has been conducted: ~50 analyses (including preliminary ones) using the 8 TeV data.

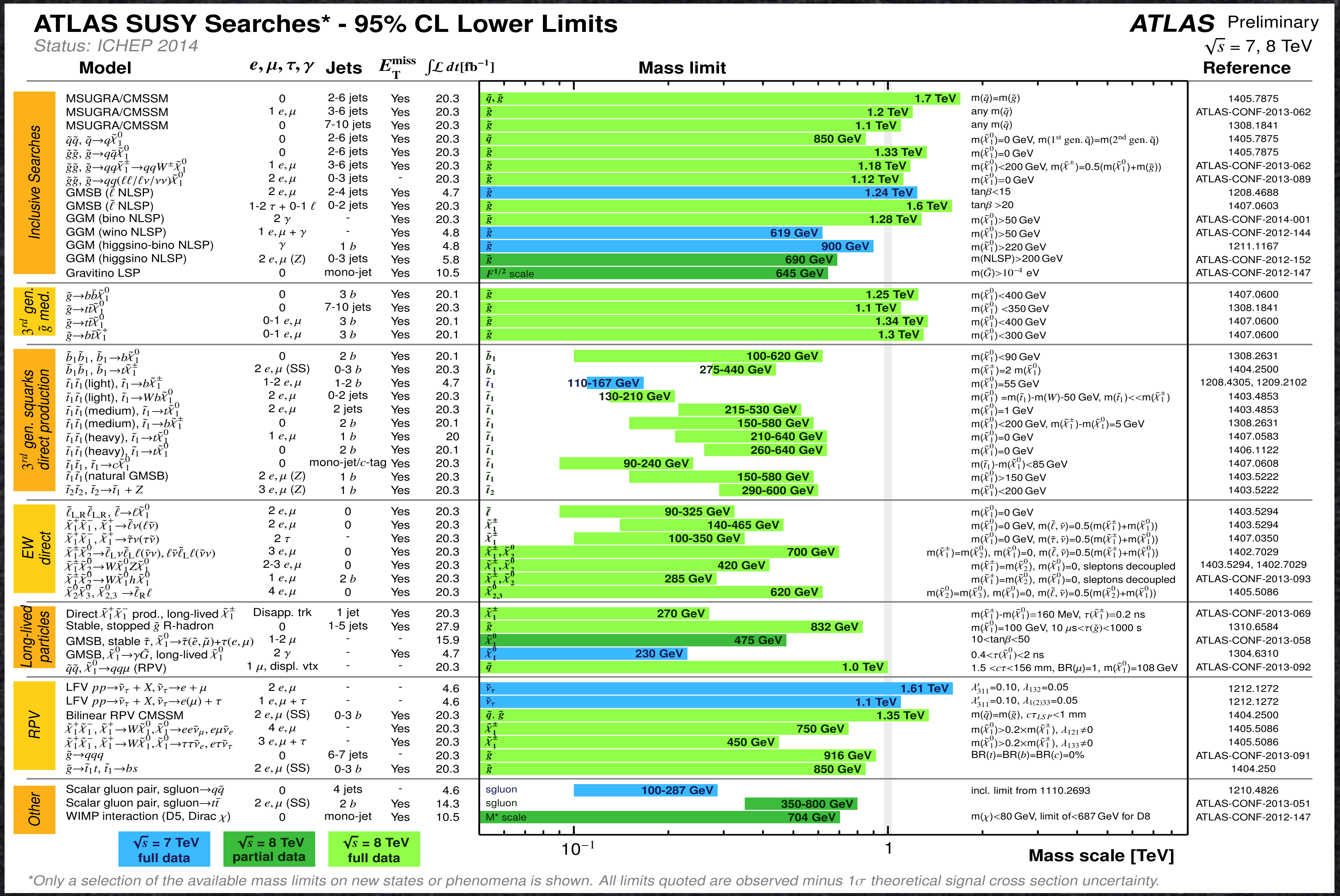

Supersymmetry

- A number of SUSY searches has been conducted: ~50 analyses (including preliminary ones) using the 8 TeV data.

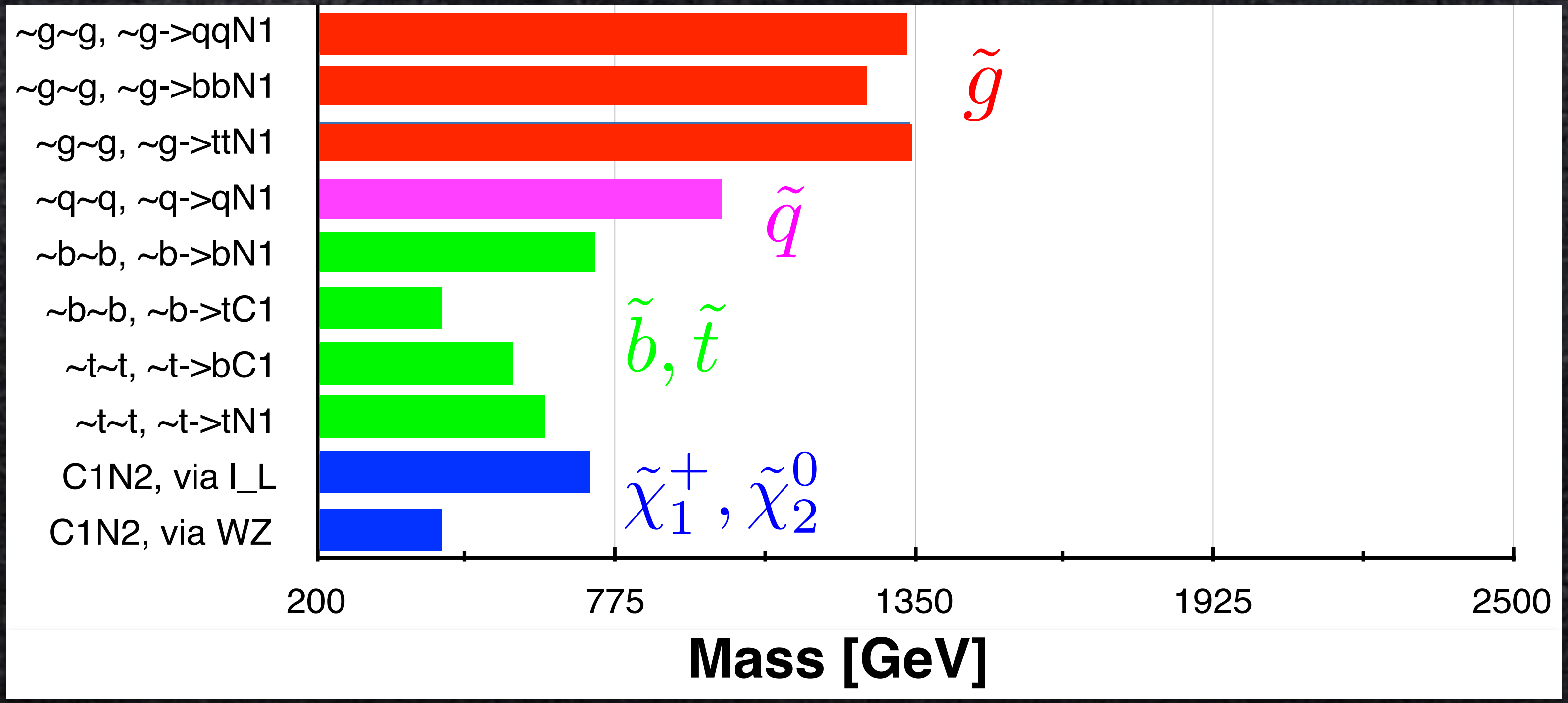

Supersymmetry

E.Halkiadakis, G.Redlinger, D.Shih (1411.1427)

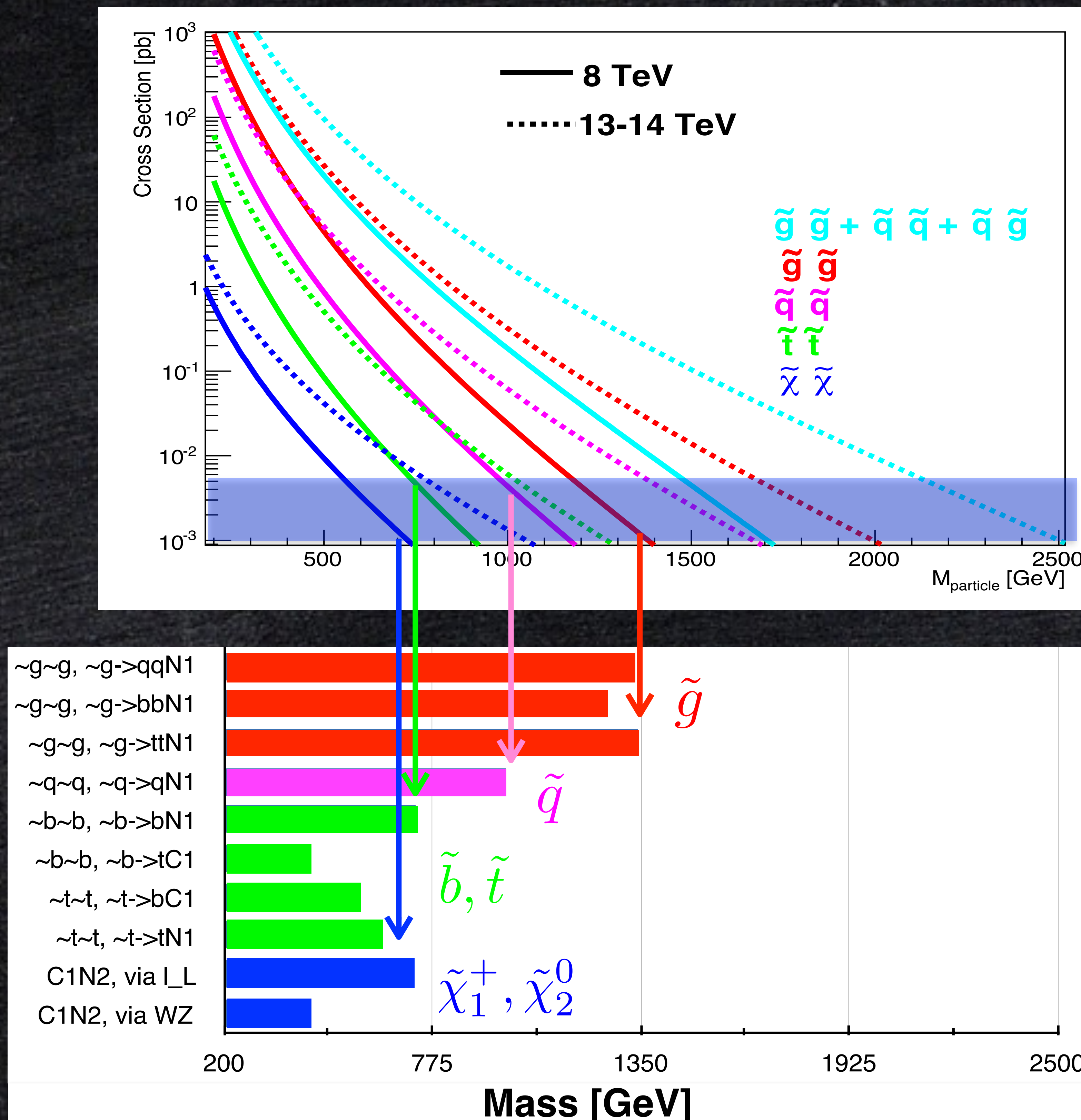

~ 20-100 events at 20 fb^{-1}

Supersymmetry

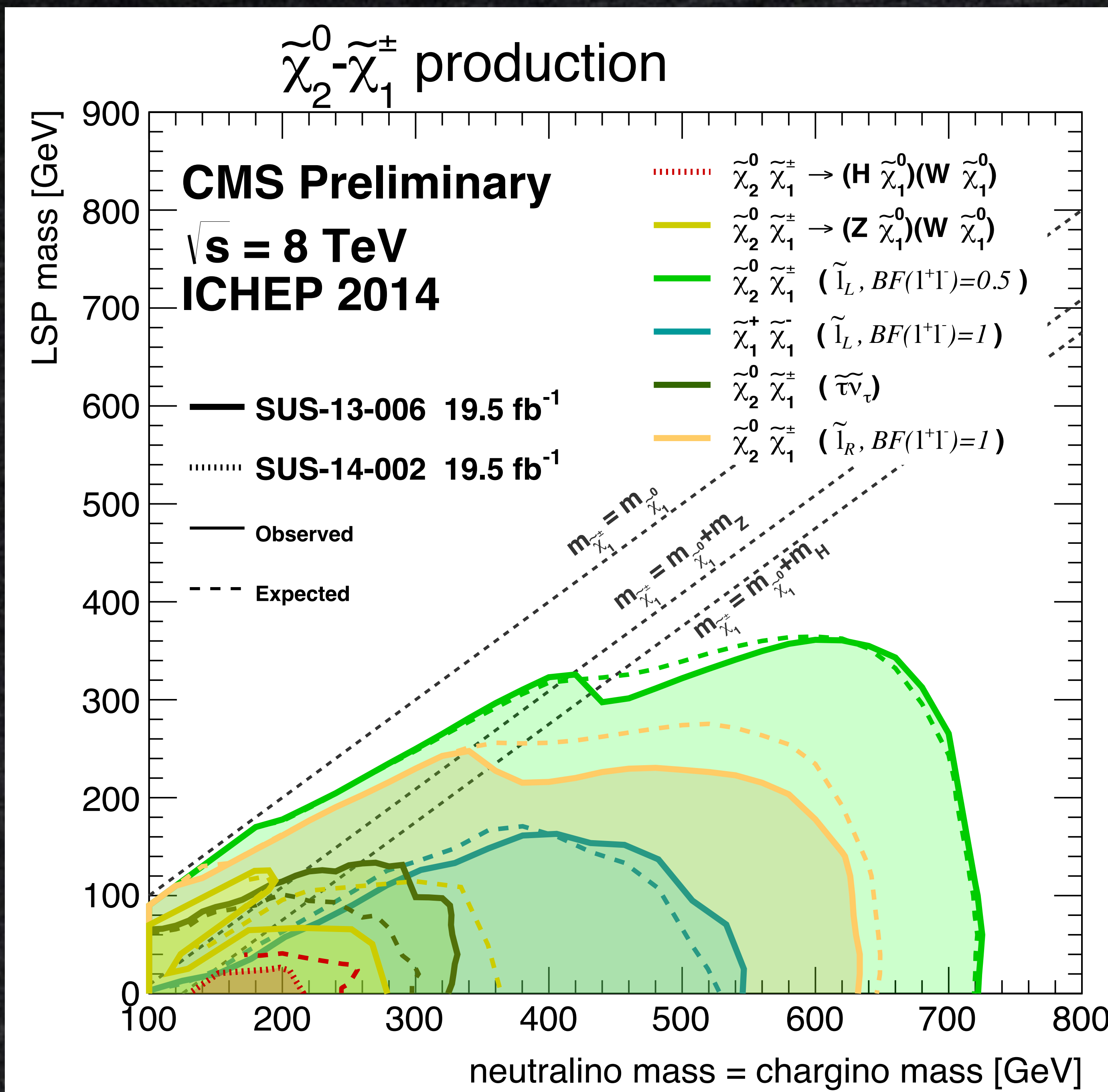

- The actual limit is much more complicated and depends on:
  - the LSP mass
  - the details of decay modes
  - other production modes

Wouldn't it be nice if there is a program, in which you give a SLHA file and press a button, then you get the limits from ATLAS and CMS analyses?

I-W Kim, M.Papucci, KS, A.Weiler

Atom
(Automated Tests Of Models)

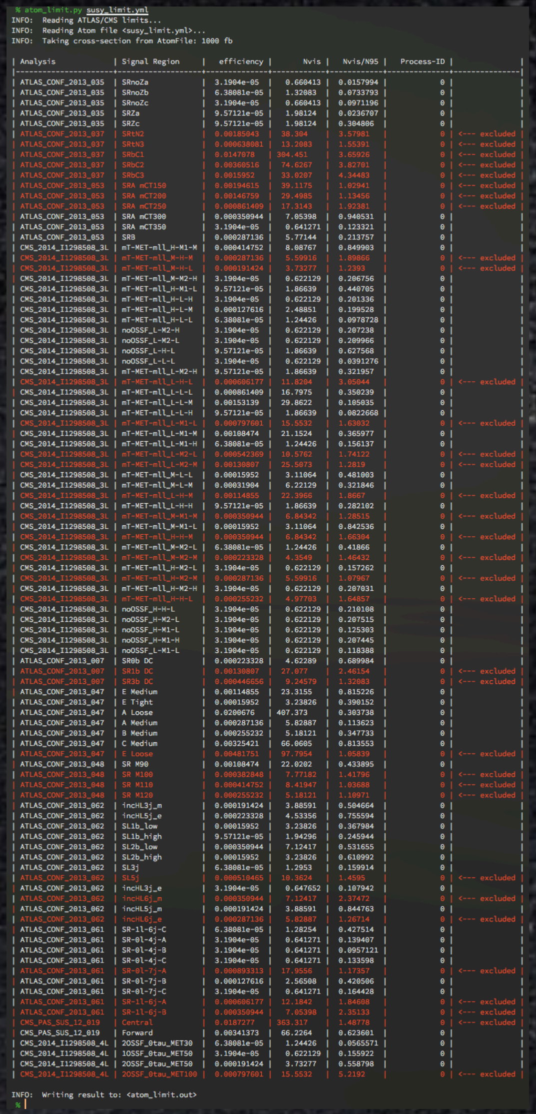

- give HepMC event file
- compute constraints from ATLAS/CMS analyses

Analysis	Signal Region	efficiency	Nvis	Nvis/N95	Process-ID	
ATLAS_CONF_2013_035	SRnoZa	3.1904e-05	0.660413	0.0157994	0	
ATLAS_CONF_2013_035	SRnoZb	6.38081e-05	1.32083	0.0733793	0	
ATLAS_CONF_2013_035	SRnoZc	3.1904e-05	0.660413	0.0971196	0	
ATLAS_CONF_2013_035	SRZa	9.57121e-05	1.98124	0.0236707	0	
ATLAS_CONF_2013_035	SRZc	9.57121e-05	1.98124	0.304806	0	
ATLAS_CONF_2013_037	SRtN2	0.00185043	38.304	3.57981	0	<--- excluded
ATLAS_CONF_2013_037	SRtN3	0.000638081	13.2083	1.55391	0	<--- excluded
ATLAS_CONF_2013_037	SRbC1	0.0147078	304.451	3.65926	0	<--- excluded
ATLAS_CONF_2013_037	SRbC2	0.00360516	74.6267	3.82701	0	<--- excluded
ATLAS_CONF_2013_037	SRbC3	0.0015952	33.0207	4.34483	0	<--- excluded
ATLAS_CONF_2013_053	SRA mCT150	0.00194615	39.1175	1.02941	0	<--- excluded
ATLAS_CONF_2013_053	SRA mCT200	0.00146759	29.4985	1.13456	0	<--- excluded
ATLAS_CONF_2013_053	SRA mCT250	0.000861409	17.3143	1.92381	0	<--- excluded
ATLAS_CONF_2013_053	SRA mCT300	0.000350944	7.05398	0.940531	0	
ATLAS_CONF_2013_053	SRA mCT350	3.1904e-05	0.641271	0.123321	0	

How does it work?

ATLAS-CONF-2011-086

Signal Region	≥ 2 jets	≥ 3 jets	≥ 4 jets
E_T^{miss} [GeV]	> 130	> 130	> 130
Leading jet p_T [GeV]	> 130	> 130	> 130
Second jet p_T [GeV]	> 40	> 40	> 40
Third jet p_T [GeV]	–	> 40	> 40
Fourth jet p_T [GeV]	–	–	> 40
$\Delta\phi(\text{jet}_i, E_T^{miss})_{min}$ $(i = 1, 2, 3)$	> 0.4	> 0.4	> 0.4
E_T^{miss}/m_{eff}	> 0.3	> 0.25	> 0.25
m_{eff} [GeV]	> 1000	> 1000	> 1000

Process	Signal Region		
	≥ 2 jets	≥ 3 jets	≥ 4 jets
SM prediction	12.1 ± 2.8	10.1 ± 2.3	7.3 ± 1.7
Observed	10	8	7
N_{BSM}^{UL}	5.77	4.95	5.77

How does it work?

ATLAS-CONF-2011-086

Signal Region	≥ 2 jets	≥ 3 jets	≥ 4 jets
E_T^{miss} [GeV]	> 130	> 130	> 130
Leading jet p_T [GeV]	> 130	> 130	> 130
Second jet p_T [GeV]	> 40	> 40	> 40
Third jet p_T [GeV]	–	> 40	> 40
Fourth jet p_T [GeV]	–	–	> 40
$\Delta\phi(\text{jet}_i, E_T^{miss})_{min}$ $(i = 1, 2, 3)$	> 0.4	> 0.4	> 0.4
E_T^{miss}/m_{eff}	> 0.3	> 0.25	> 0.25
m_{eff} [GeV]	> 1000	> 1000	> 1000

Process	Signal Region		
	≥ 2 jets	≥ 3 jets	≥ 4 jets
SM prediction	12.1 ± 2.8	10.1 ± 2.3	7.3 ± 1.7
Observed	10	8	7
N_{BSM}^{UL}	5.77	4.95	5.77

Result

How does it work?

ATLAS-CONF-2011-086

Signal Region	≥ 2 jets	≥ 3 jets	≥ 4 jets
E_T^{miss} [GeV]	> 130	> 130	> 130
Leading jet p_T [GeV]	> 130	> 130	> 130
Second jet p_T [GeV]	> 40	> 40	> 40
Third jet p_T [GeV]	–	> 40	> 40
Fourth jet p_T [GeV]	–	–	> 40
$\Delta\phi(\text{jet}_i, E_T^{miss})_{min}$ $(i = 1, 2, 3)$	> 0.4	> 0.4	> 0.4
E_T^{miss}/m_{eff}	> 0.3	> 0.25	> 0.25
m_{eff} [GeV]	> 1000	> 1000	> 1000

Process	Signal Region		
	≥ 2 jets	≥ 3 jets	≥ 4 jets
SM prediction	12.1 ± 2.8	10.1 ± 2.3	7.3 ± 1.7
Observed	10	8	7
N_{BSM}^{UL}	5.77	4.95	5.77

Result

Interpretation

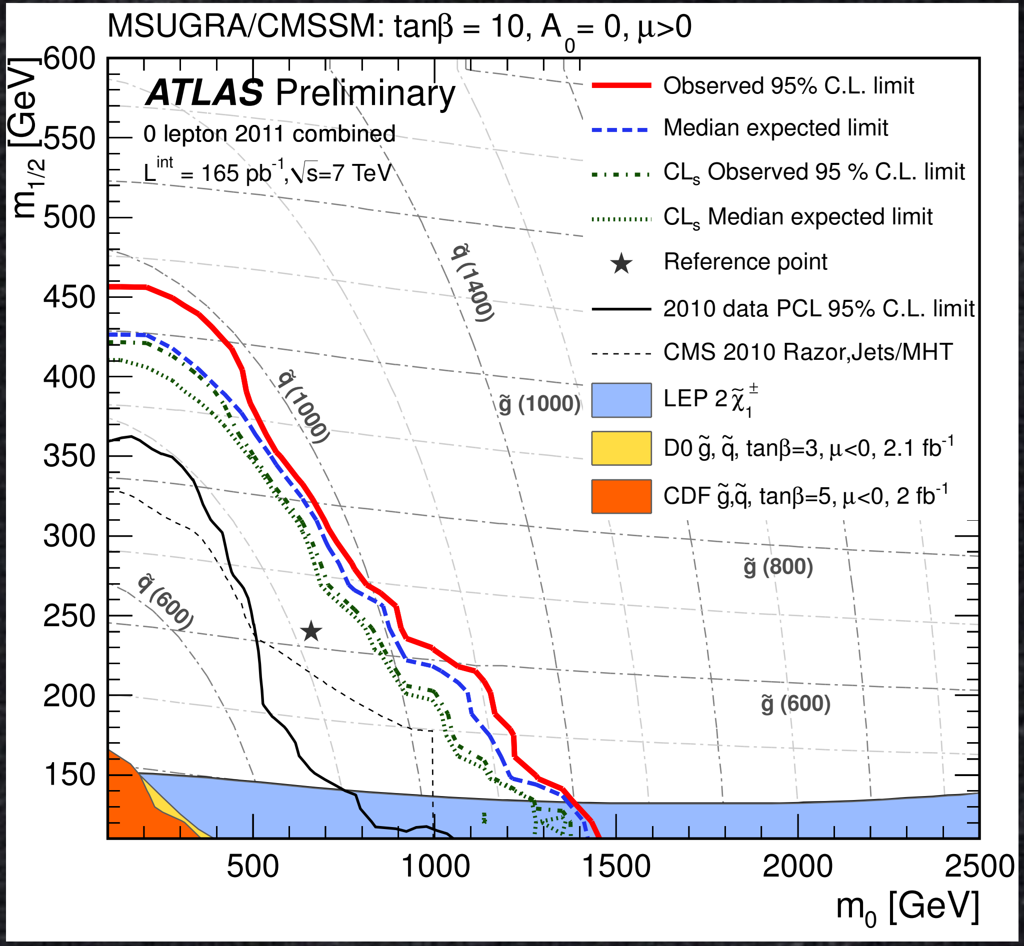

How does it work?

ATLAS-CONF-2011-086

Signal Region	≥ 2 jets	≥ 3 jets	≥ 4 jets
E_T^{miss} [GeV]	> 130	> 130	> 130
Leading jet p_T [GeV]	> 130	> 130	> 130
Second jet p_T [GeV]	> 40	> 40	> 40
Third jet p_T [GeV]	–	> 40	> 40
Fourth jet p_T [GeV]	–	–	> 40
$\Delta\phi(\text{jet}_i, E_T^{miss})_{min}$ $(i = 1, 2, 3)$	> 0.4	> 0.4	> 0.4
E_T^{miss}/m_{eff}	> 0.3	> 0.25	> 0.25
m_{eff} [GeV]	> 1000	> 1000	> 1000

Process	Signal Region		
	≥ 2 jets	≥ 3 jets	≥ 4 jets
SM prediction	12.1 ± 2.8	10.1 ± 2.3	7.3 ± 1.7
Observed	10	8	7
N_{BSM}^{UL}	5.77	4.95	5.77

Result

Interpretation

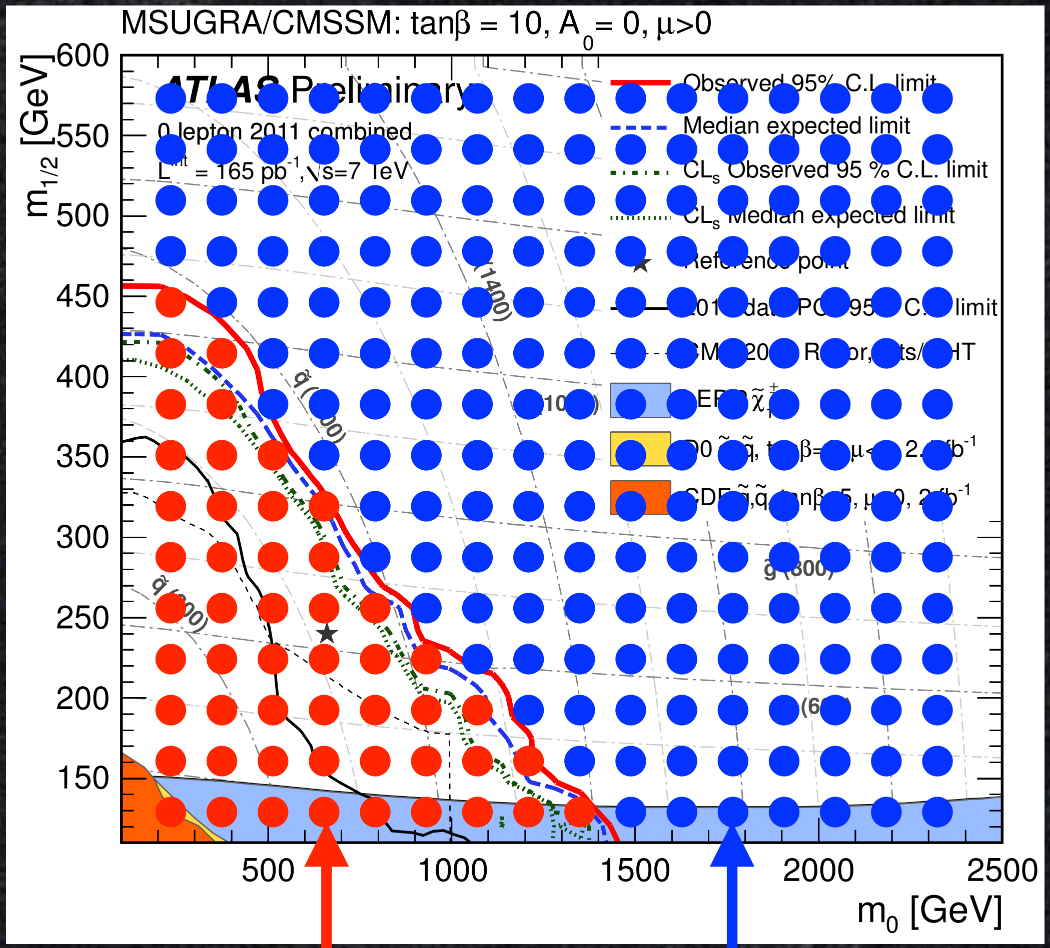

$N_{SUSY} > N_{BSM}^{UL}$ $N_{SUSY} < N_{BSM}^{UL}$

How does it work?

ATLAS-CONF-2011-086

Signal Region	≥ 2 jets	≥ 3 jets	≥ 4 jets
E_T^{miss} [GeV]	> 130	> 130	> 130
Leading jet p_T [GeV]	> 130	> 130	> 130
Second jet p_T [GeV]	> 40	> 40	> 40
Third jet p_T [GeV]	–	> 40	> 40
Fourth jet p_T [GeV]	–	–	> 40
$\Delta\phi(\text{jet}_i, E_T^{miss})_{min}$ $(i = 1, 2, 3)$	> 0.4	> 0.4	> 0.4
E_T^{miss}/m_{eff}	> 0.3	> 0.25	> 0.25
m_{eff} [GeV]	> 1000	> 1000	> 1000

Process	Signal Region		
	≥ 2 jets	≥ 3 jets	≥ 4 jets
SM prediction	12.1 ± 2.8	10.1 ± 2.3	7.3 ± 1.7
Observed	10	8	7
N_{BSM}^{UL}	5.77	4.95	5.77

Result

any interpretation is possible

- GMSB (M_{mess}, Λ)
- AMSB (m_0, $m_{3/2}$)
- gluino simp. model
- stop simp. model
- Little Higgs Model
- ⋮

I-W Kim, M.Papucci, KS, A.Weiler

Atom

- Estimate N_{BSM} for various SRs and confront N_{BSM} with N_{UL}.

$$N_{\rm UL}^{(a)} \longleftrightarrow N_{\rm BSM}^{(a)} = \epsilon_{\rm BSM}^{(a)} \cdot \sigma_{\rm BSM} \cdot \mathcal{L}$$

database of exp. results:
N_{UL}, N_{obs}, N_{sys}, N_{SMBG}

$$\epsilon_{\rm BSM}^{(a)} = \lim_{N_{\rm MC} \to \infty} \frac{N\left(\begin{array}{c}\text{Events fall into}\\ \text{signal region } a\end{array}\right)}{N_{\rm MC}}$$

database of ATLAS and CMS analyses: the selection cuts used in the analyses are implemented.

The effect of detector resolution is taken into account.

I-W Kim, M.Papucci, KS, A.Weiler

Modelling Detector Effects

(1) reconstruct jets, MET, iso-leptons from truth level particles (not from detector cells)

(2) smear the reco-objects according to detector resolutions, apply reco efficiencies (lepton acceptances, b and τ tagging eff.)

momentum smearing

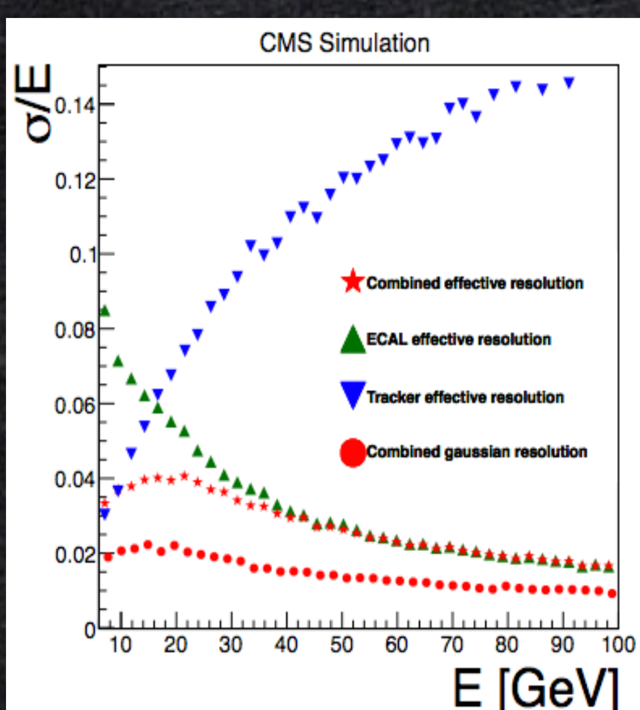

reco-efficiency

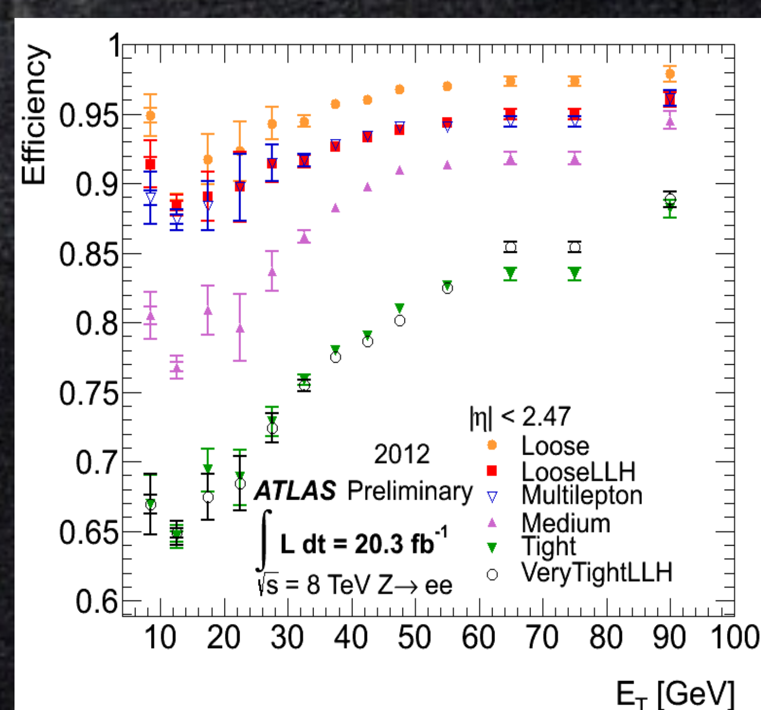

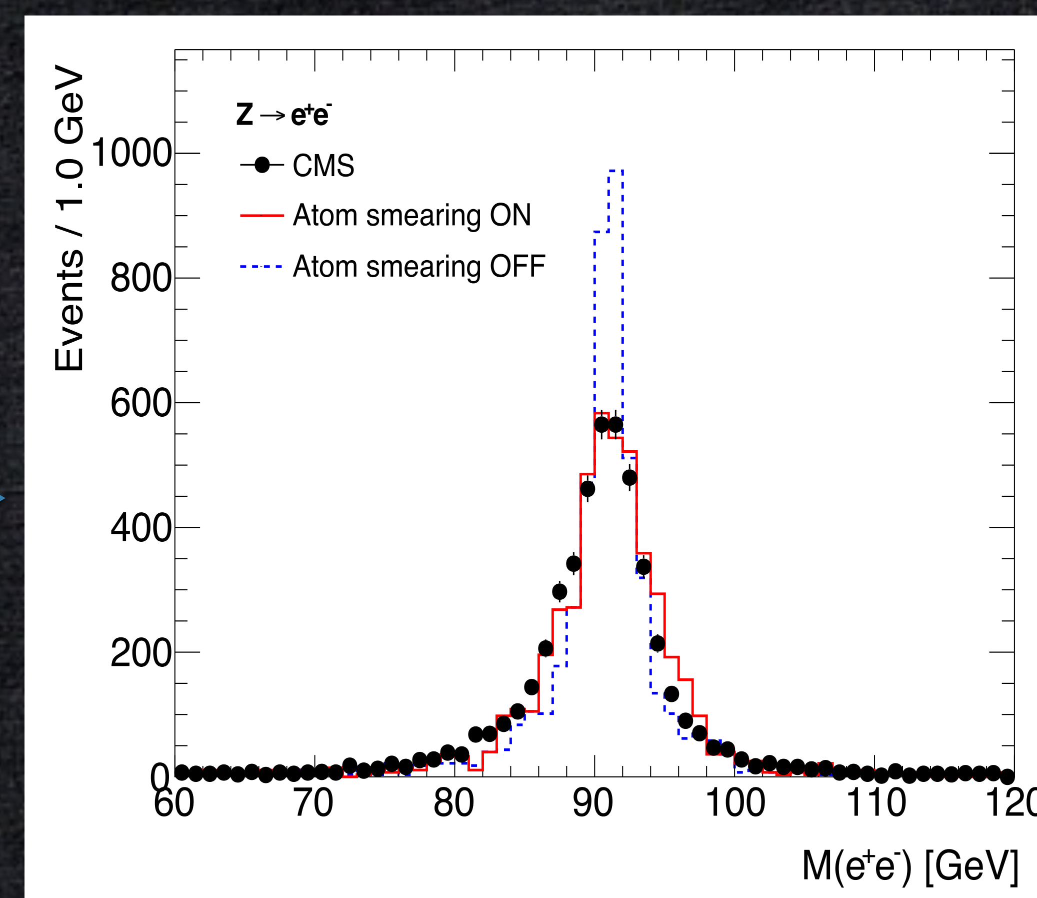

I-W Kim, M.Papucci, KS, A.Weiler

Validation

- The approach works surprisingly well.

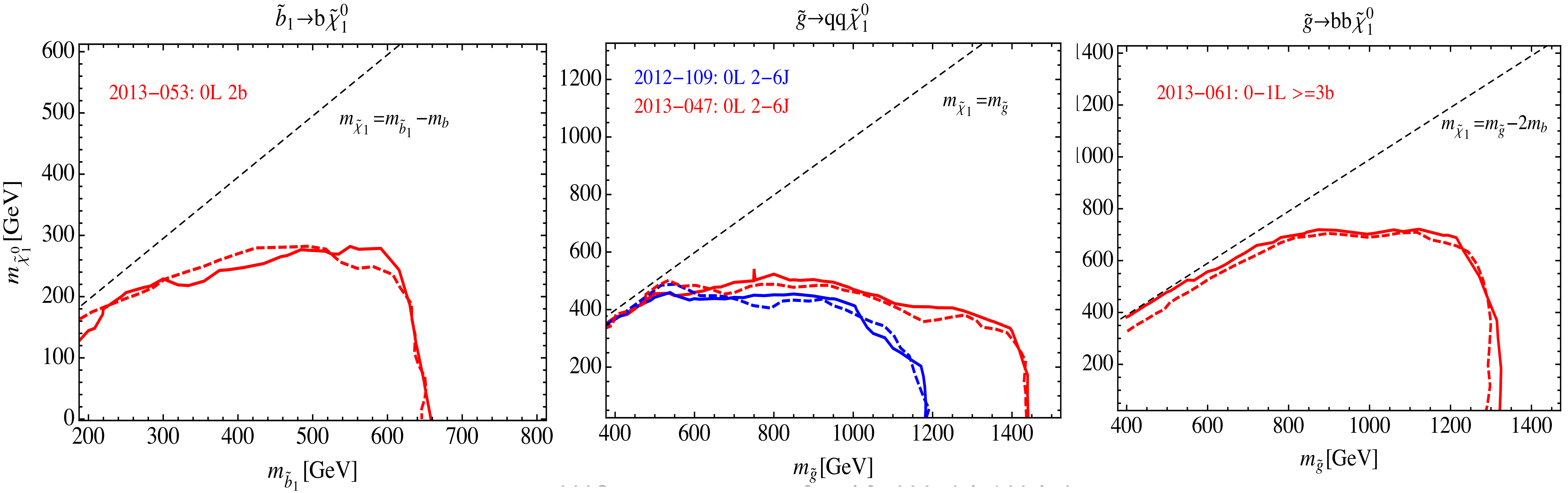

Fitting Excesses

J.S.Kim, K.Rolbiecki, K.Sakurai, J.Tattersall (1406.0858)

Study	SR	Obs	Exp	SM s.d.
ATLAS W^+W^- (7 TeV) [5]	Combined	1325	1219 ± 87	1.1-σ
CMS W^+W^- (7 TeV) [7]	Combined	1134	1076 ± 62	0.8-σ
CMS W^+W^- (8 TeV) [6]	Combined	1111	986 ± 60	1.8-σ
ATLAS Higgs [27]	WW CR	3297	3110 ± 186	0.9-σ
	Higgs SR	3615	3288 ± 220	1.4-σ
ATLAS $\tilde{q}$ and $\tilde{g}$ (1-2 ℓ) [23]	Di-muon	7	1.7 ± 1	2.5-σ
ATLAS Electroweak (3 ℓ) [24]	SR0τa01	36	23 ± 4	2.1-σ
	SR0τa06	13	6.6 ± 1.9	1.9-σ

Description	$\sqrt{s}$ [TeV]	Luminosity [fb^{-1}]	Number of SR	Refs.
ATLAS W^+W^-	7	4.6	1	[arXiv:1210.2979]
CMS W^+W^-	7	4.9	1	[arXiv:1306.1126]
CMS W^+W^-	8	3.5	1	[arXiv:1301.4698]
ATLAS Higgs	8	20.7	2	[ATLAS-CONF-2013-031]
ATLAS Electroweak (2 ℓ)	8	20.3	13	[arXiv:1403.5294]
ATLAS $\tilde{q}$ and $\tilde{g}$ (1-2 ℓ)	8	20.1	19	[ATLAS-CONF-2013-062]
ATLAS $\tilde{q}$ and $\tilde{g}$ razor (2 ℓ)	8	20.3	6	[ATLAS-CONF-2013-089]
ATLAS Electroweak (3 ℓ)	8	20.3	20	[arXiv:1402.7029]
ATLAS $\tilde{t}$ (1 ℓ)	8	20.7	8	[ATLAS-CONF-2013-037]
ATLAS $\tilde{t}$ (2 ℓ)	8	20.3	12	[arXiv:1403.4853]
CMS $W^\pm Z^0$	8	19.6	4	[CMS-PAS-12-006]
ATLAS $W^\pm Z^0$	8	13.0	4	[ATLAS-CONF-2013-021]
ATLAS $\tilde{t} \to b\nu_\tau\tilde{\tau}_1$	8	20.3	1	[ATLAS-CONF-2014-014]

- ATLAS and CMS have observed excesses in some of the SRs.
- We fit the excess using *Checkmate* and Atom taking the relevant constraints into account.
- The following processes are included in the scan:

$$pp \to \tilde{t}_1\tilde{t}_1 : \tilde{t}_1 \to bW^{(*)}\tilde{\chi}_1^0 \text{ (via } \tilde{\chi}_1^\pm)$$

$$pp \to \tilde{\chi}_1^+\chi_1^- : \tilde{\chi}_1^\pm \to W^{(*)}\tilde{\chi}_1^0$$

$$pp \to \tilde{\chi}_1^+\tilde{\chi}_2^0 : \tilde{\chi}_2^0 \to Z^{(*)}\tilde{\chi}_1^0$$

Fitting Excesses

$m_{\tilde{\chi}_1^\pm} = m_{\tilde{\chi}_2^0} = m_{\tilde{t}_1} - 7\text{GeV}$

J.S.Kim, K.Rolbiecki, K.Sakurai, J.Tattersall (1406.0858)

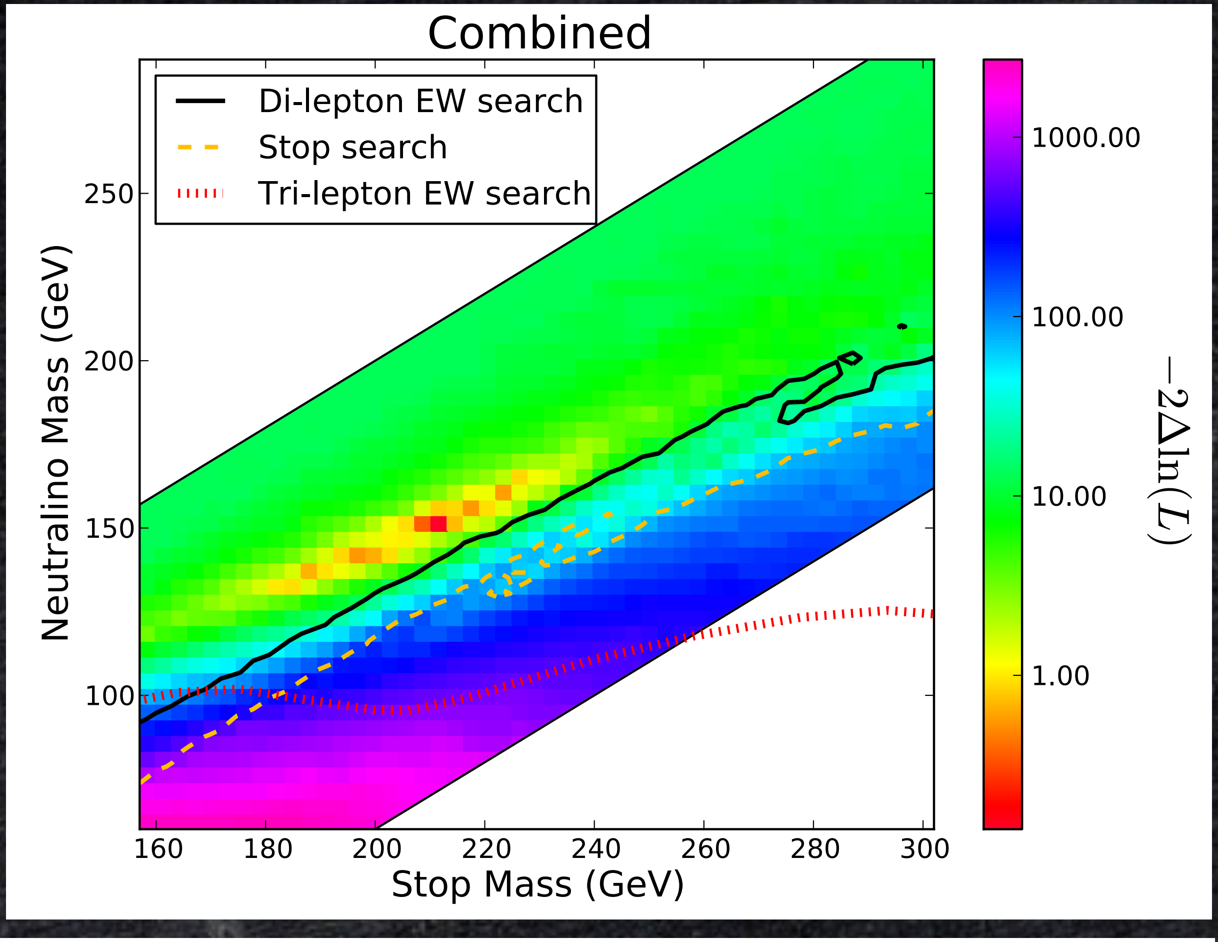

Best fit point:

$m_{\tilde{t}_1} = 212^{+35}_{-35}$ GeV

$m_{\tilde{\chi}_1^0} = 150^{+30}_{-20}$ GeV

Study	SR	Obs	Exp	SM s.d.	Best fit exp	Best fit s.d
ATLAS W^+W^- (7 TeV) [5]	Combined	1325	1219 ± 87	1.1-σ	119	0.1-σ
CMS W^+W^- (7 TeV) [7]	Combined	1134	1076 ± 62	0.8-σ	89	0.4-σ
CMS W^+W^- (8 TeV) [6]	Combined	1111	986 ± 60	1.8-σ	83	0.6-σ
ATLAS Higgs [27]	WW CR	3297	3110 ± 186	0.9-σ	374	0.9-σ
	Higgs SR	3615	3288 ± 220	1.4-σ	501	0.6-σ
ATLAS $\tilde{q}$ and $\tilde{g}$ (1-2 ℓ) [23]	Di-muon	7	1.7 ± 1	2.5-σ	2.7	1.2-σ
ATLAS Electroweak (3 ℓ) [24]	SR0τa01	36	23 ± 4	2.1-σ	2.8	1.6-σ
	SR0τa06	13	6.6 ± 1.9	1.9-σ	1.5	1.4-σ

A fast model testing method

- Testing model points by MC simulation is time consuming.

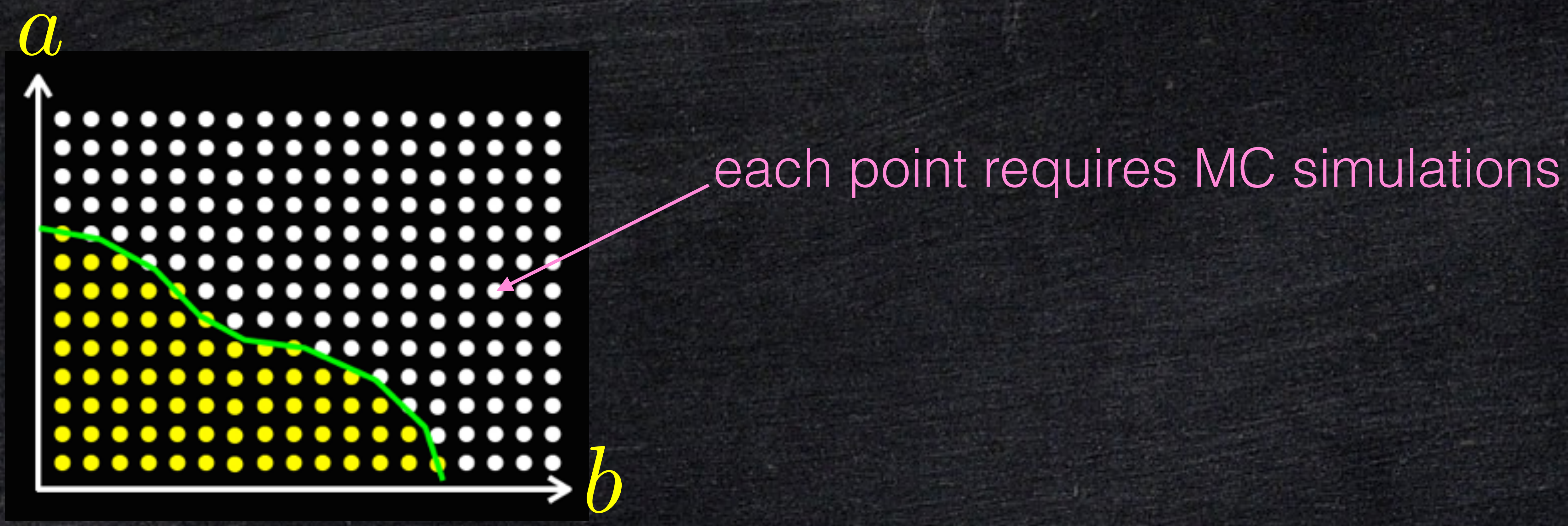

We need a fast model testing method.

Idea

$Q = \tilde{q}$

$G = \tilde{g}$

$\mathrm{N1} = \tilde{\chi}_1^0$

$$N^{(a)}_{\mathrm{BSM}} = \begin{cases} N^{(a)}_{\mathrm{QqN1:QqN1}} \\ + \\ N^{(a)}_{\mathrm{GqqN1:GqqN1}} \\ + \\ N^{(a)}_{\mathrm{GqqN1:QqN1}} \\ \vdots \end{cases}$$

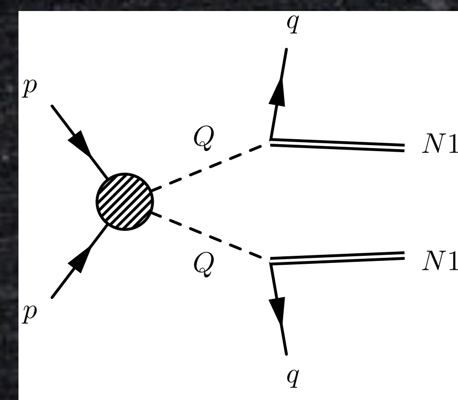

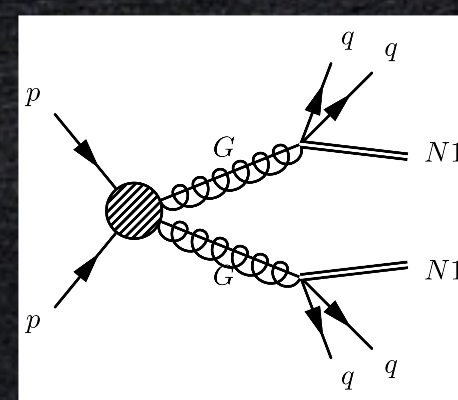

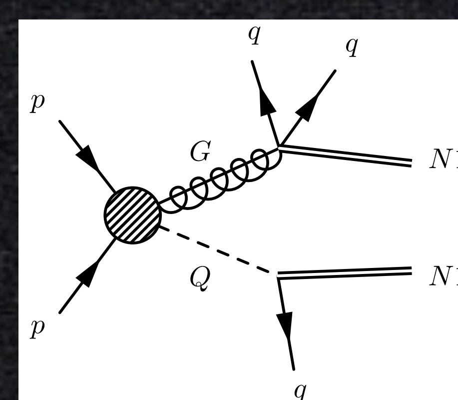

Idea

$\mathrm{Q} = \tilde{q}$
$\mathrm{G} = \tilde{g}$
$\mathrm{N1} = \tilde{\chi}_1^0$

dominantly depends on BSM particle masses

$$N^{(a)}_{\mathrm{BSM}} = \begin{cases} N^{(a)}_{\mathrm{QqN1:QqN1}} = \epsilon^{(a)}_{\mathrm{QqN1:QqN1}}(m_{\mathrm{Q}}, m_{\mathrm{N1}}) \cdot \sigma_{\mathrm{QQ}} \cdot BR \cdot \mathcal{L} \\ + \\ N^{(a)}_{\mathrm{GqqN1:GqqN1}} = \epsilon^{(a)}_{\mathrm{GqqN1:GqqN1}}(m_{\mathrm{G}}, m_{\mathrm{N1}}) \cdot \sigma_{\mathrm{GG}} \cdot BR \cdot \mathcal{L} \\ + \\ N^{(a)}_{\mathrm{GqqN1:QqN1}} = \epsilon^{(a)}_{\mathrm{GqqN1:QqN1}}(m_{\mathrm{G}}, m_{\mathrm{Q}}, m_{\mathrm{N1}}) \cdot \sigma_{\mathrm{GQ}} \cdot BR \cdot \mathcal{L} \\ \vdots \end{cases}$$

Idea

$Q = \tilde{q}$
$G = \tilde{g}$
$N1 = \tilde{\chi}^0_1$

$$N^{(a)}_{\mathrm{BSM}} = \begin{cases} N^{(a)}_{\mathrm{QqN1:QqN1}} = \\ + \\ N^{(a)}_{\mathrm{GqqN1:GqqN1}} = \\ + \\ N^{(a)}_{\mathrm{GqqN1:QqN1}} = \\ \vdots \end{cases}$$

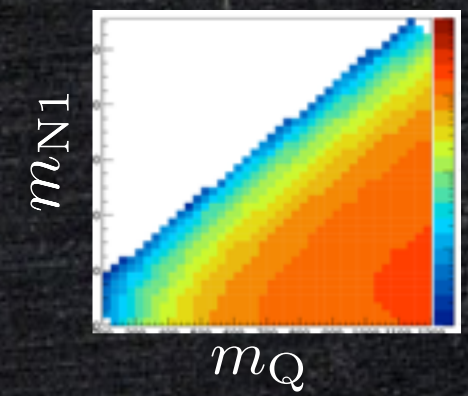

$\sigma_{\mathrm{QQ}} \cdot BR \cdot \mathcal{L}$

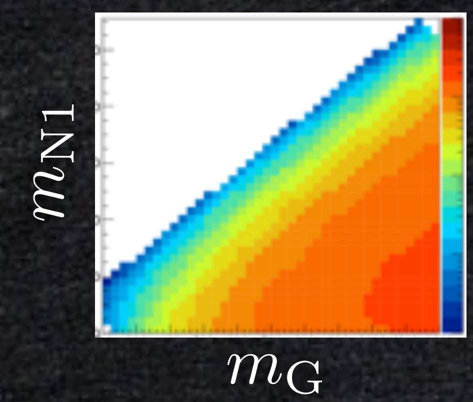

$\sigma_{\mathrm{GG}} \cdot BR \cdot \mathcal{L}$

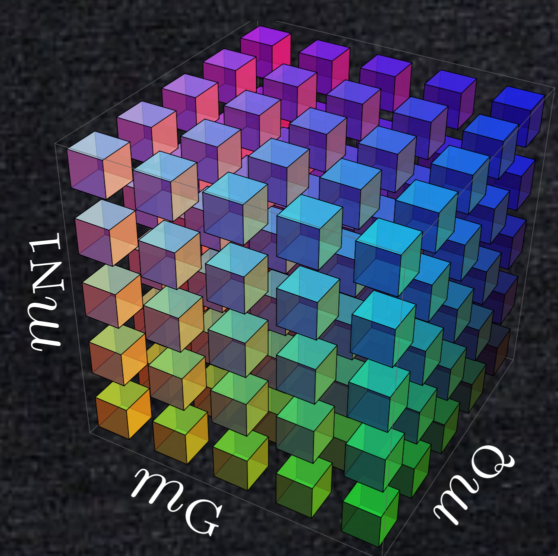

$\sigma_{\mathrm{GQ}} \cdot BR \cdot \mathcal{L}$

Fastlim

Papucci, KS, Weiler, Zeune 1402.0492

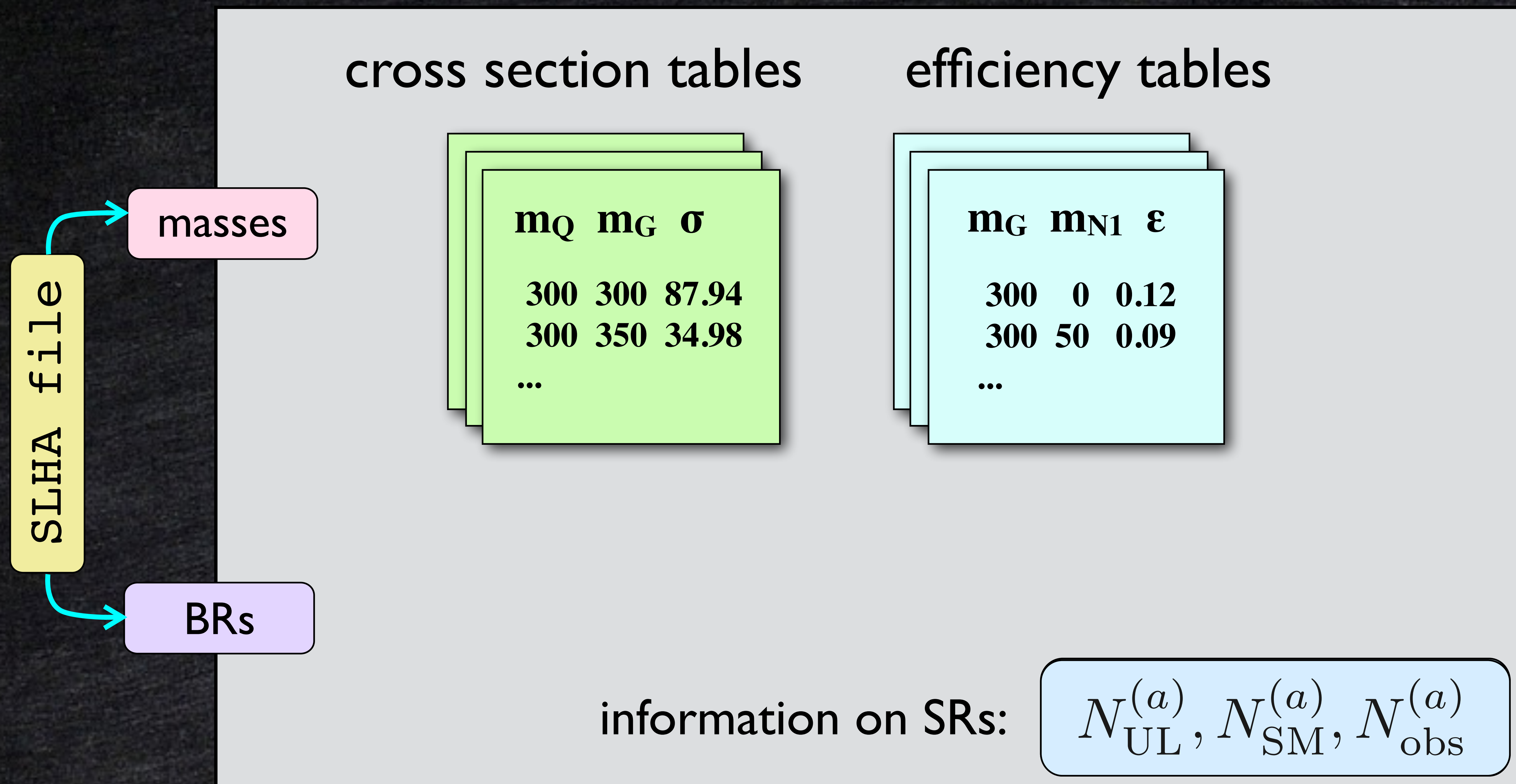

Papucci, KS, Weiler, Zeune 1402.0492

Fastlim

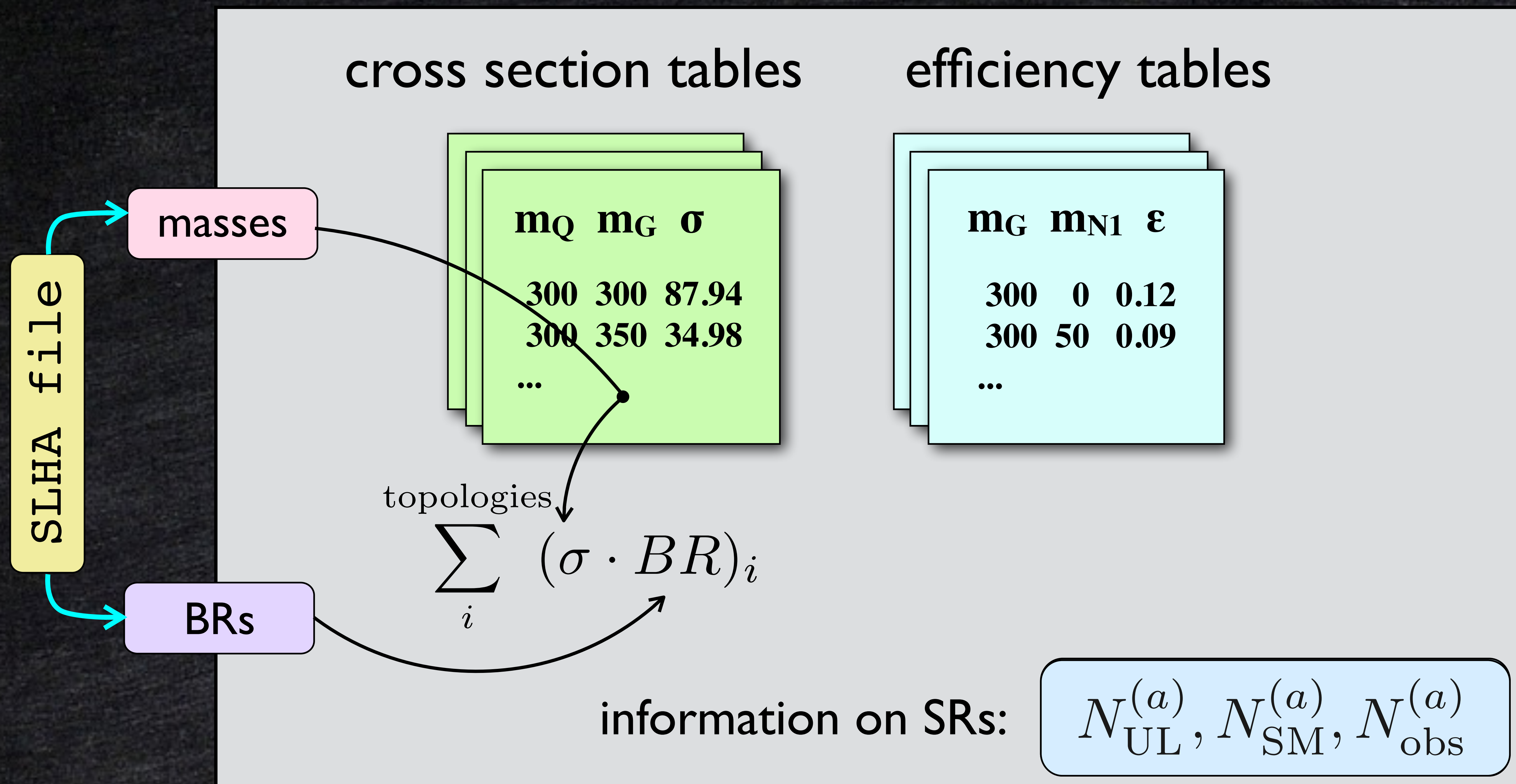

Fastlim

Papucci, KS, Weiler, Zeune 1402.0492

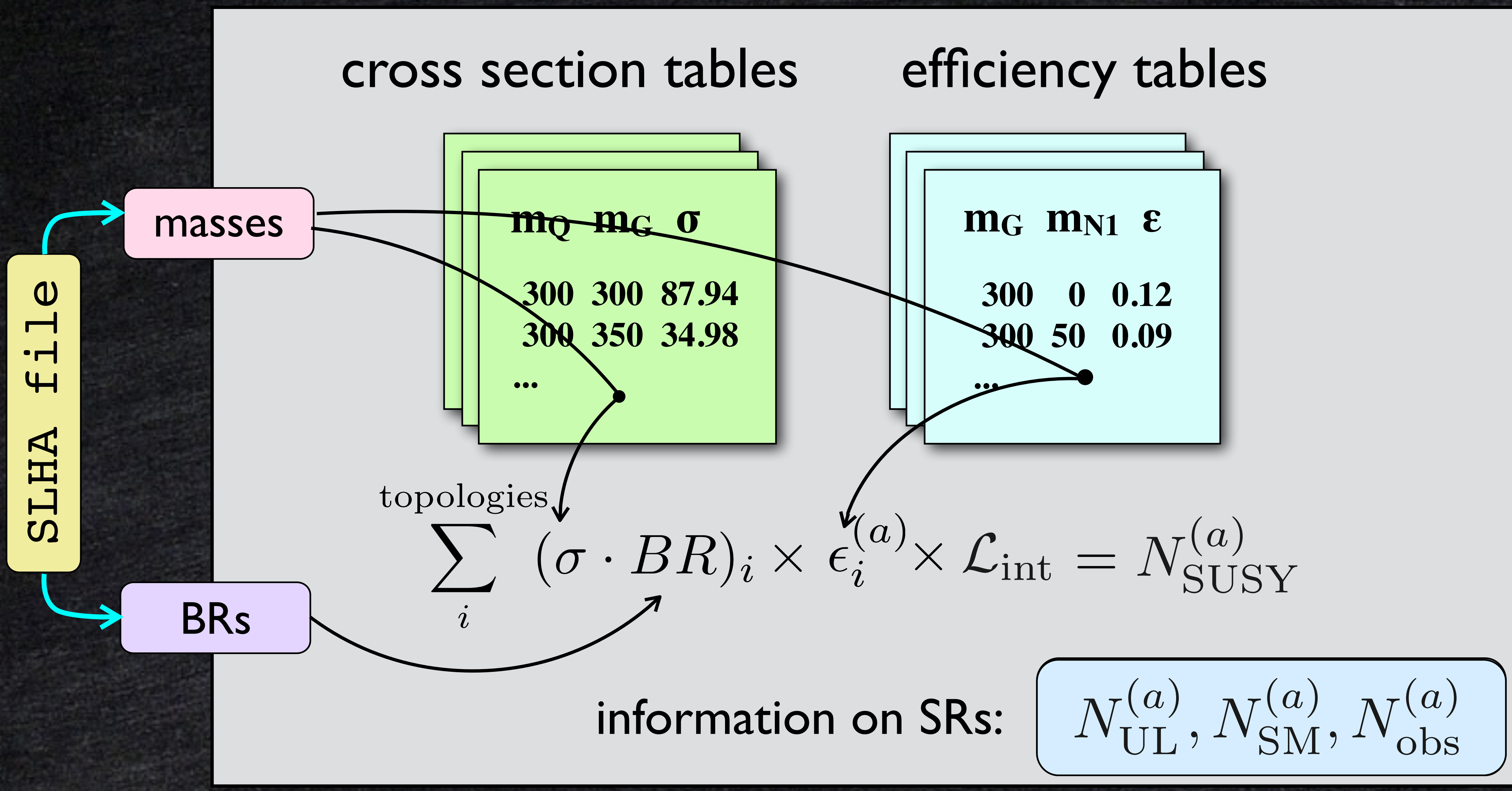

Fastlim

Papucci, KS, Weiler, Zeune 1402.0492

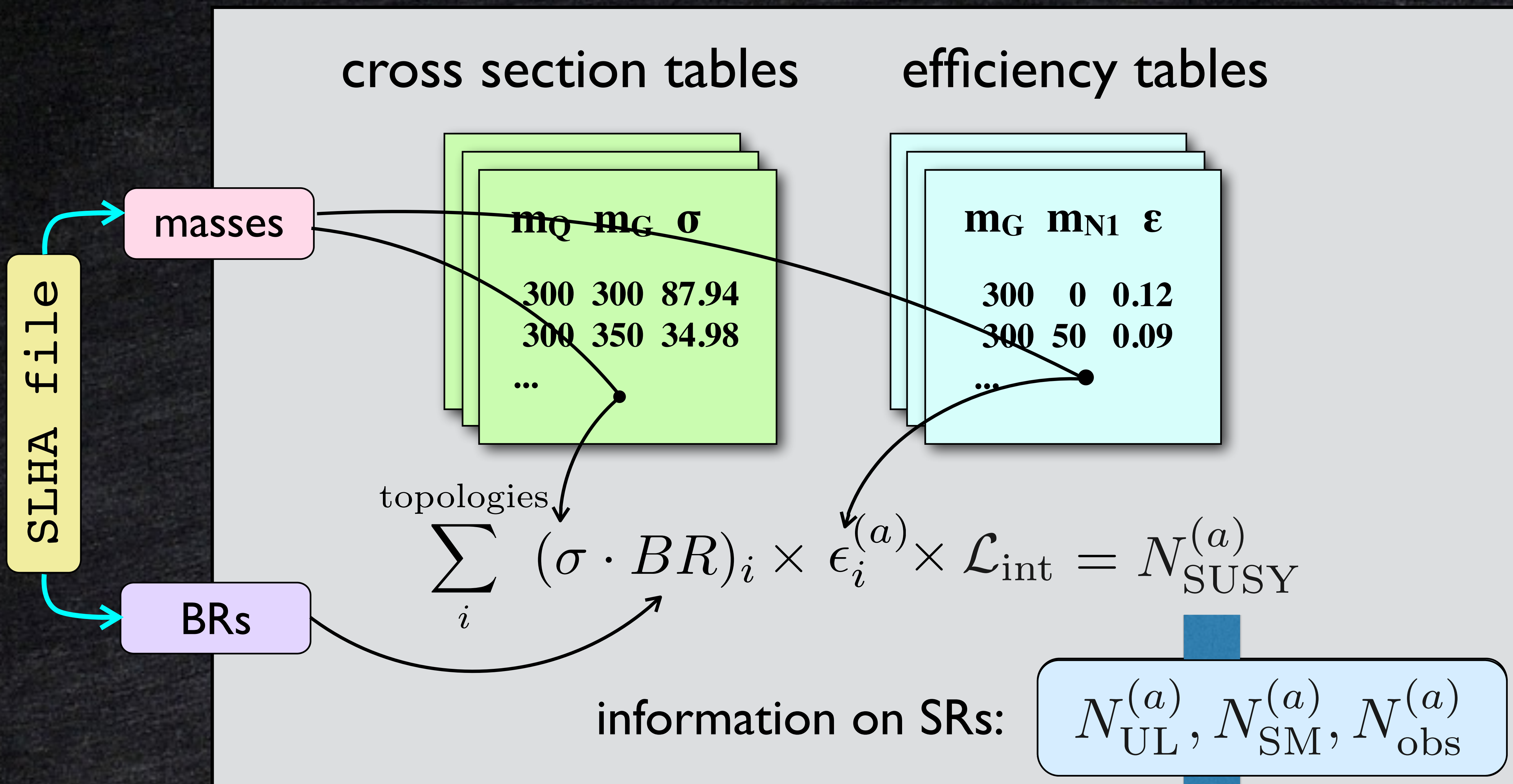

No MC sim. required

output: $N_{\text{SUSY}}^{(a)}/N_{\text{UL}}^{(a)}, CL_s^{(a)}$

http://fastlim.web.cern.ch/fastlim/

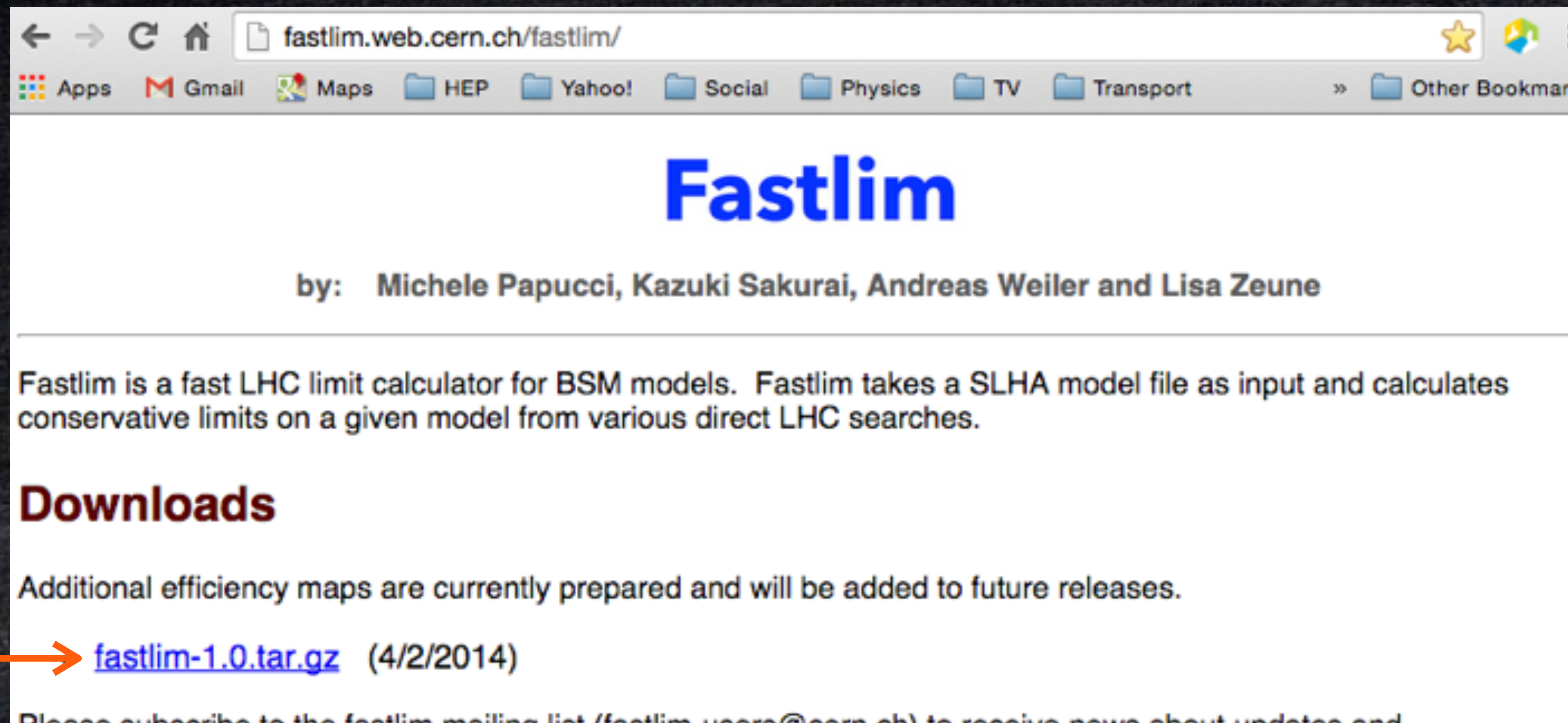

download →

give SLHA →

```
1. zsh
% kazuki Kazukis-MBP in ~/fastlim-1.0
$ ./fastlim.py slha_files/testspectrum.slha
```

works →

```
----------    Cross Section    ----------
Ecm        Total    Implemented    Coverage
8TeV     20.234fb       20.23fb      99.98%

-------------------------------------------------------------------------------------------
            Analysis  E/TeV  L*fb          Signal Region:  Nev/N_UL     CLs
-------------------------------------------------------------------------------------------
ATLAS_CONF_2013_024      8   20.5        SR1: MET > 200:     0.6946  0.1218
ATLAS_CONF_2013_024      8   20.5        SR2: MET > 300:     1.5321      --    <== Exclude
ATLAS_CONF_2013_024      8   20.5        SR3: MET > 350:     1.1153  0.0144    <== Exclude
ATLAS_CONF_2013_035      8   20.7                SRnoZa:     0.0000      --
ATLAS_CONF_2013_035      8   20.7                SRnoZb:     0.0000      --
```

no headache of "make install"

Limit on Natural SUSY

- Light stop, sbottom and Higgsinos (charginos, neutralinos).

$\mu = 100\text{GeV}, \ M_{Q_3} = M_{U_3}$

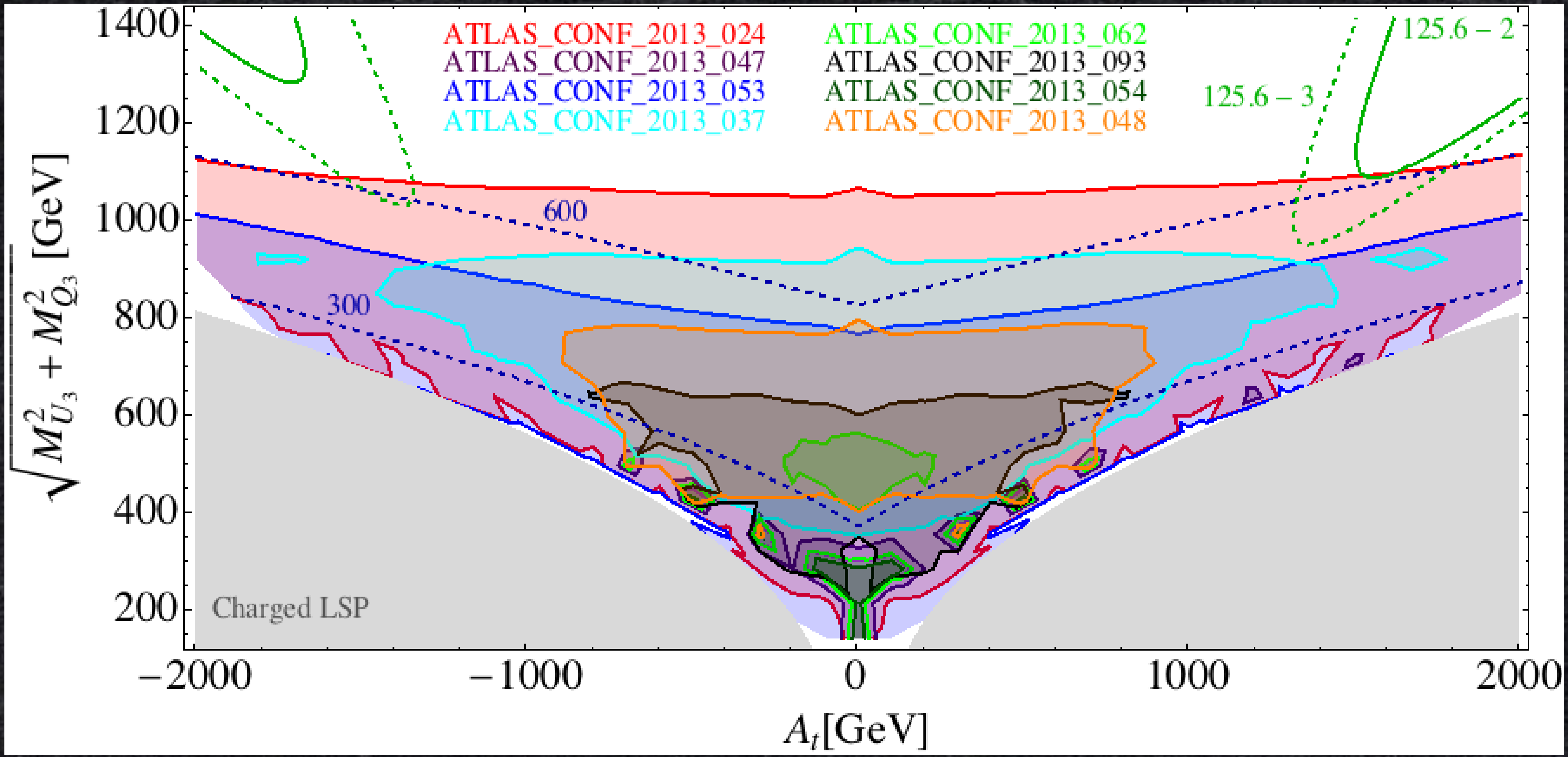

- Distance from the origin is sensitive to the fine-tuning

$$\Delta m_{H_u}^2 \simeq -\frac{3y_t^2}{8\pi^2}(M_{U_3}^2 + M_{Q_3}^2 + A_t^2)\ln\left(\frac{\Lambda}{m_{\tilde{t}}}\right)$$

BSM searches
Prospect

Where to look at?

G.Giudice, A.Strumia (1108.6077)

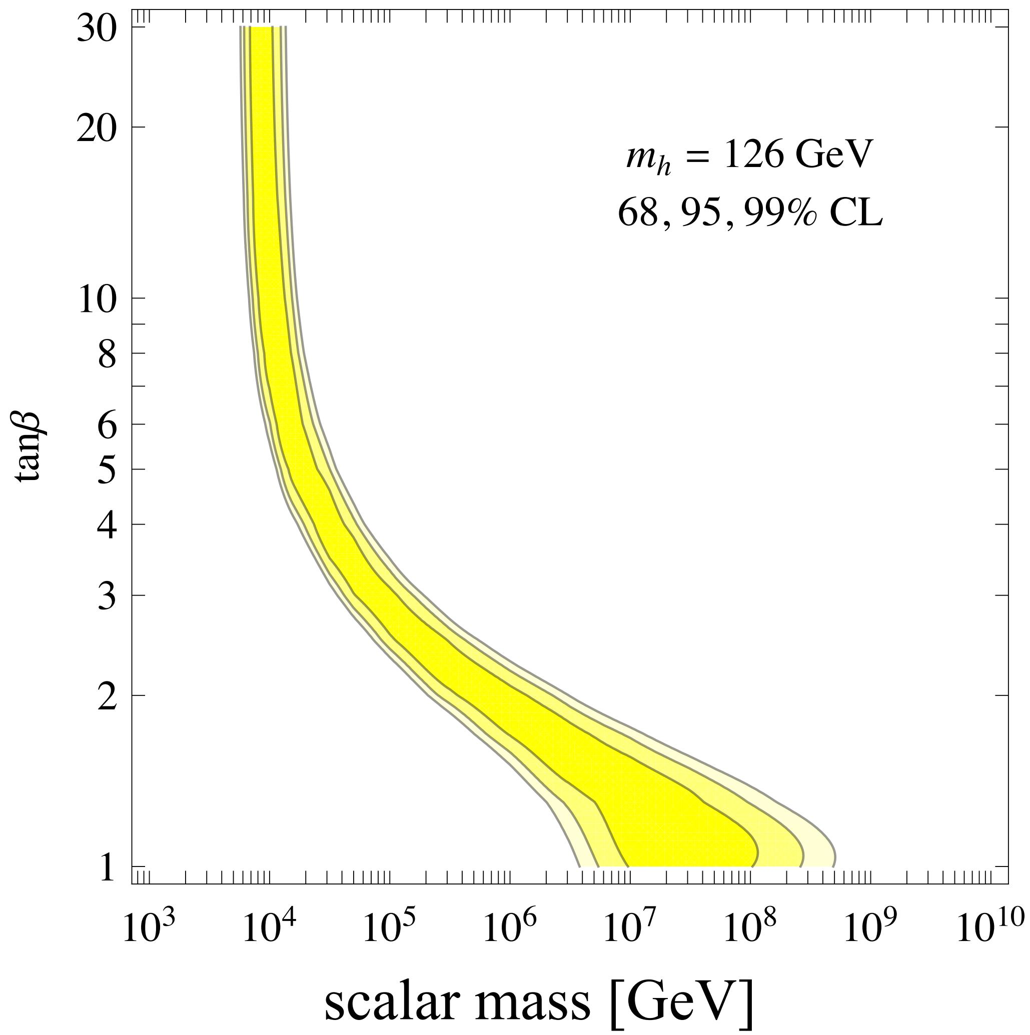

- The measured Higgs mass (~125GeV) may indicate that scalars are heavy.
- This assumption is consistent with other measurements: FCNC, CPV, direct SUSY searches, etc..
- Gauginos (Higgsinos) can still be light. → good for gauge coupling unification.
- In concrete models, gaugino masses are often loop suppressed compared to the scalar mass. Split SUSY
- Among the gauginos, gluinos often become the heaviest due to its colour charge. e.g. $M_3 : M_2 : M_1 = 7 : 2 : 1$.
- Wino, Bino (or Higginos) can be accessible at the LHC.

Wino cross section

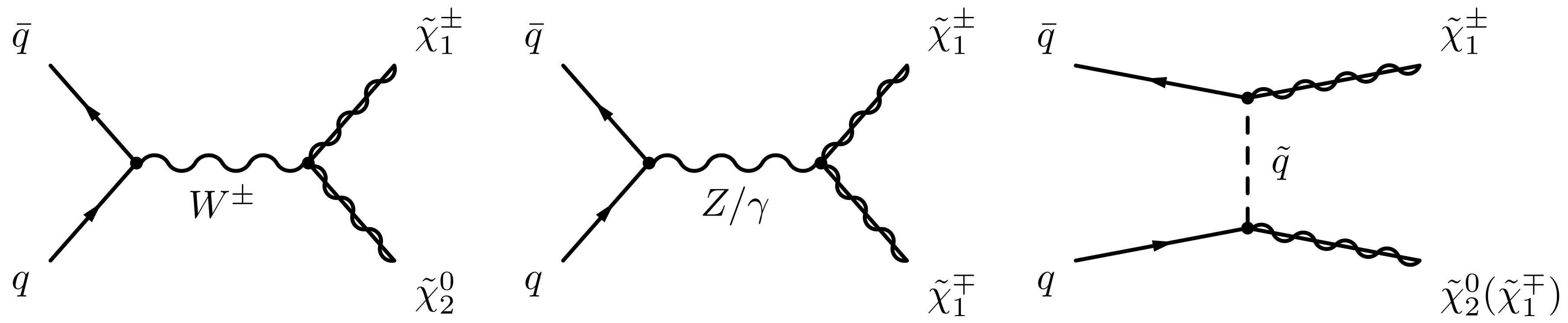

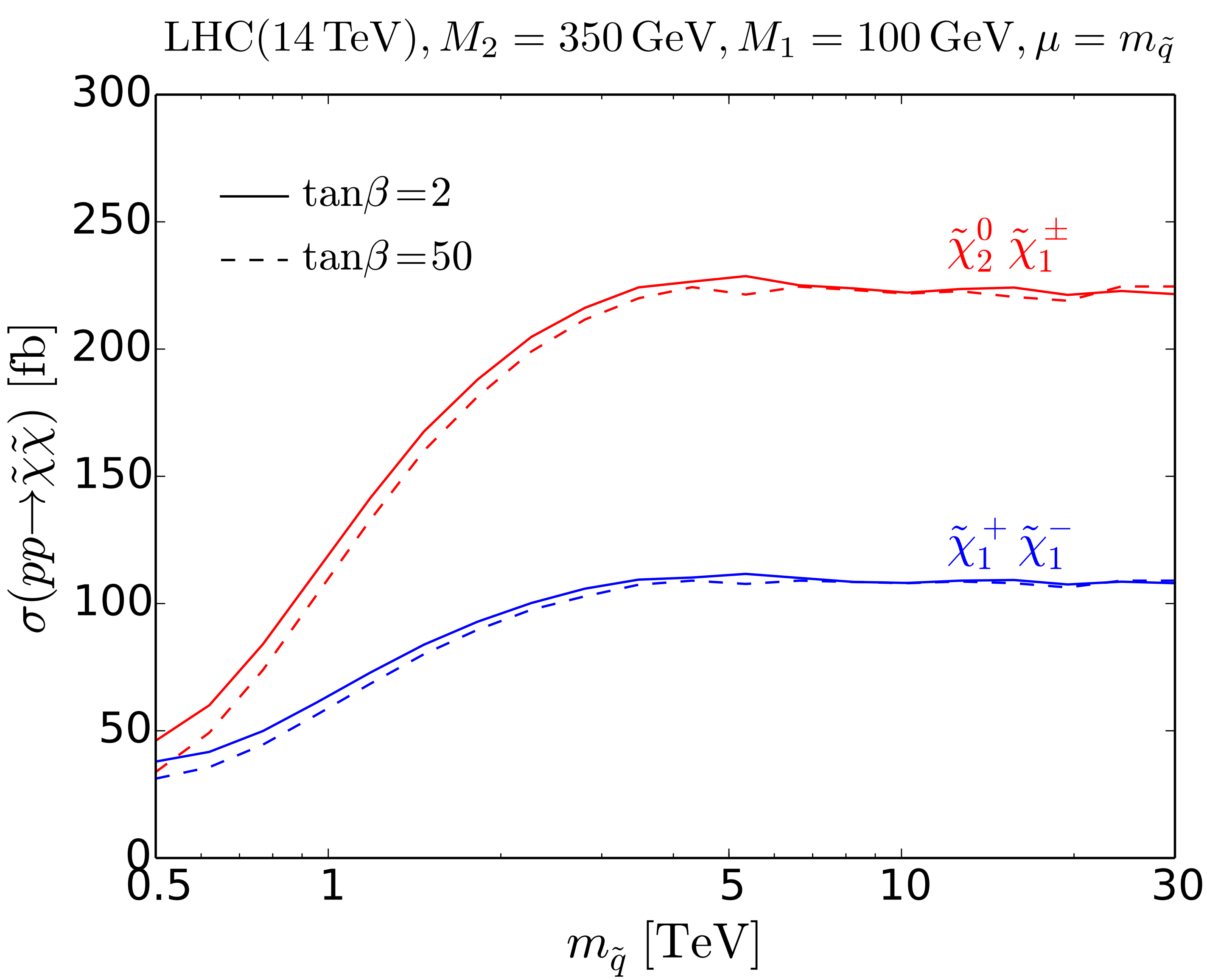

A.Papaefstathiou, KS, M.Takeuchi (1404.1077)

Wino cross section

$\text{LHC}(14\,\text{TeV}), M_3 : M_2 : M_2 = 7 : 2 : 1, \mu = m_{\tilde{q}} = 3\,\text{TeV}$

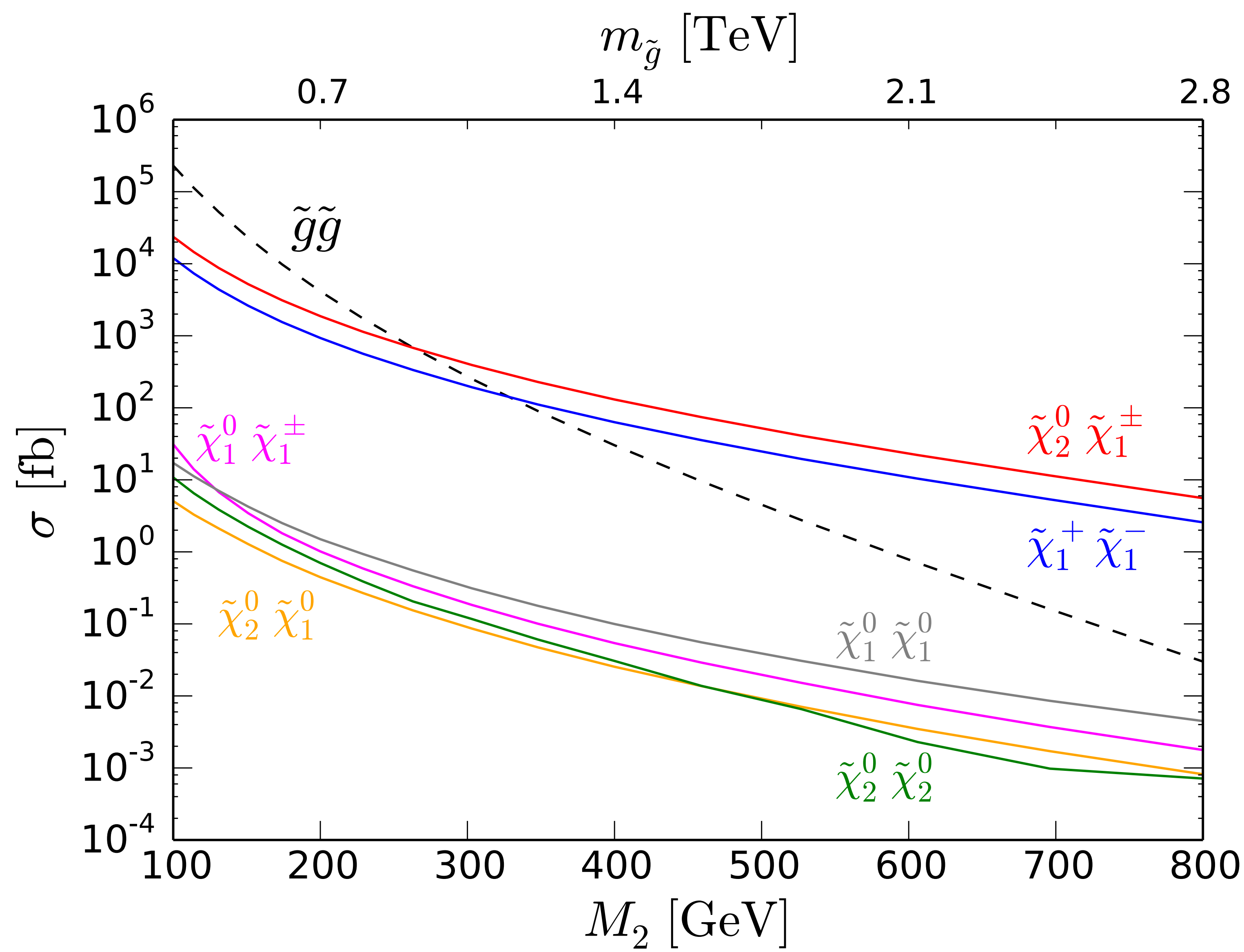

The chargino-neutralino production exceeds the gluino production at M_2 ~ 300 GeV.

A.Papaefstathiou, KS, M.Takeuchi (1404.1077)

Wino → Bino decay

The chargino decay is unique: $\tilde{\chi}_1^\pm \to W^\pm \tilde{\chi}_1^0$ (100%)

There are two possible decays from $\tilde{\chi}_2^0$: $\tilde{\chi}_2^0 \to h\tilde{\chi}_1^0, Z\tilde{\chi}_1^0$

$$H^\dagger e^V H|_{\theta^4} \supset \tilde{H} \not{D} \tilde{H}, \tilde{H}\tilde{\lambda}h, \cancel{\tilde{H}\tilde{\lambda}V}$$

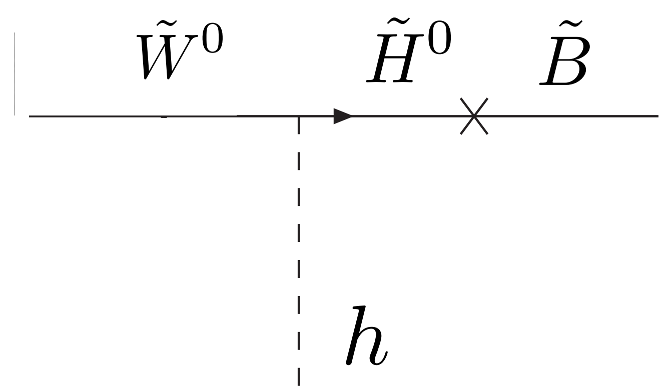

$\gg$

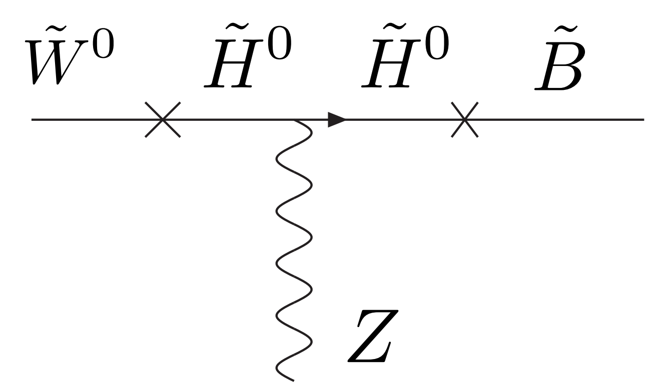

$$|C_{\tilde{\chi}_1^0\tilde{\chi}_2^0 h}| \simeq \frac{e}{2}\frac{m_Z}{|\mu|}\left|2\sin 2\beta + \frac{M_1 + M_2}{\mu}\right|$$

$$|C_{\tilde{\chi}_1^0\tilde{\chi}_2^0 Z}| \simeq \frac{e}{2}\frac{m_Z^2}{|\mu|^2}$$

A.Papaefstathiou, KS, M.Takeuchi (1404.1077)

Wino → Bino decay

$$|C_{\tilde{\chi}_1^0 \tilde{\chi}_2^0 Z}| \simeq \frac{e}{2} \frac{m_Z^2}{|\mu|^2},$$

$$|C_{\tilde{\chi}_1^0 \tilde{\chi}_2^0 h}| \simeq \frac{e}{2} \frac{m_Z}{|\mu|} \left| 2 \sin 2\beta + \frac{M_1 + M_2}{\mu} \right|,$$

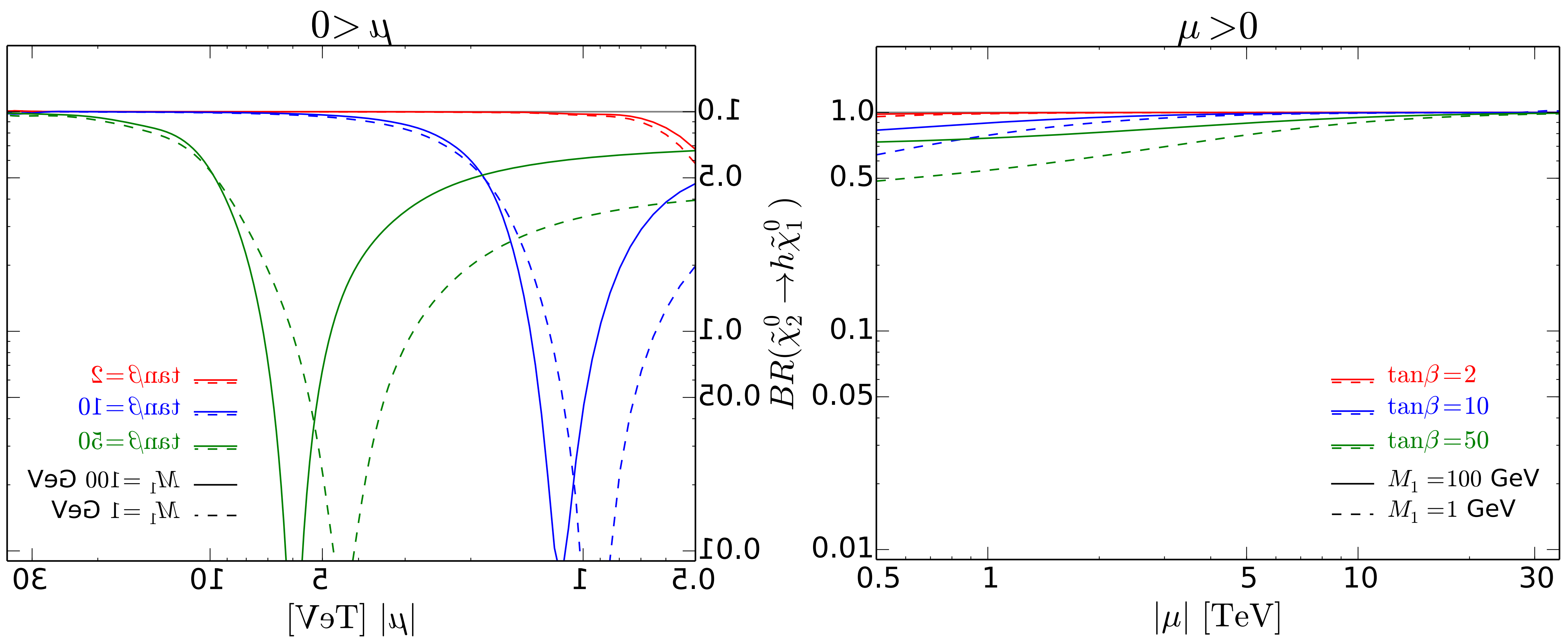

The neutralino2 decays into Higgs predominantly (except for the cancellation region)

A.Papaefstathiou, KS, M.Takeuchi (1404.1077)

h→ττ mode

- In the split SUSY with large μ-term, we have
  $pp \to \tilde{\chi}_1^{\pm}\tilde{\chi}_2^0 \to W^{\pm}\tilde{\chi}_1^0 h\tilde{\chi}_1^0$
- We consider $W^{\pm} \to \ell^{\pm}\nu, h \to \tau^{+}\tau^{-}$ channel
- The BR is small (BR(h→ττ) = 6.3×10^{-2}), but the ttbar background can be controlled by b-jet veto and the requirement of τs.

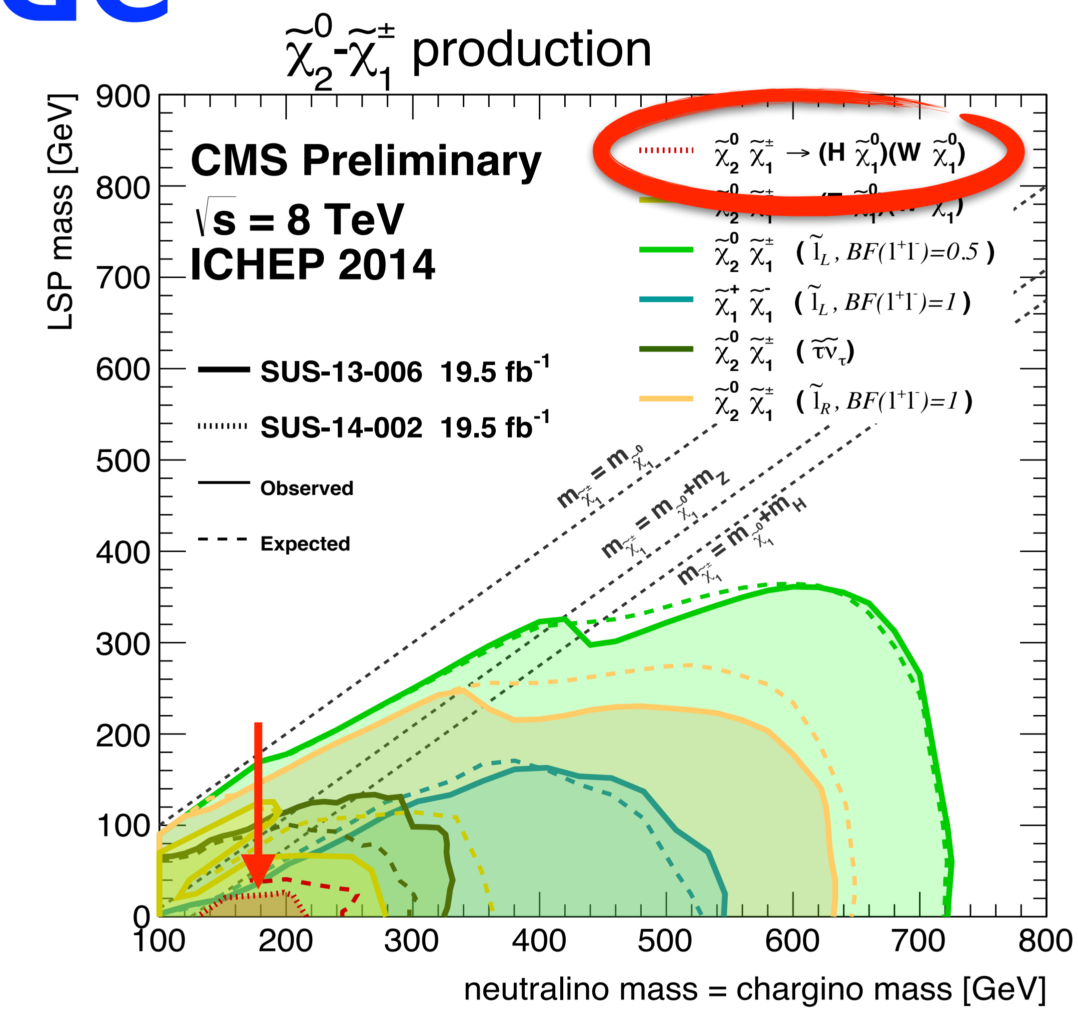

sample	σ_{initial} (fb)
SUSY **C350-100**	5.7
WZ	767
$W(\to \ell\nu_\ell)$+jets	$\sim 600 \times 10^3$
$W(\to \tau\nu_\tau)$+jets	$\sim 300 \times 10^3$
hV	443
$t\bar{t}h$	3.4
$t\bar{t}$	8600
$Z(\to \ell\ell)$+jets	$\sim 600 \times 10^3$
$Z(\to \tau\tau)$+jets	$\sim 300 \times 10^3$

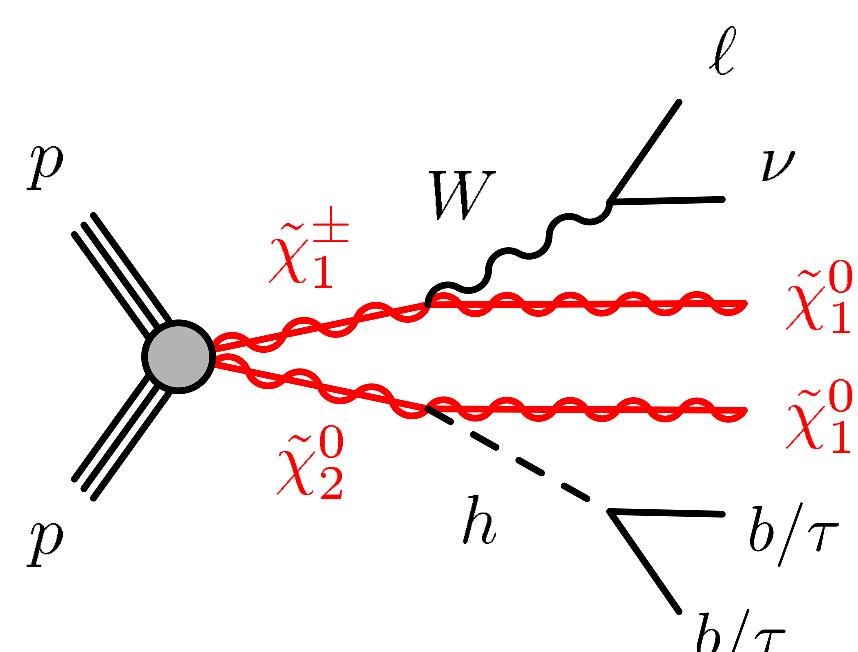

τ-tagging

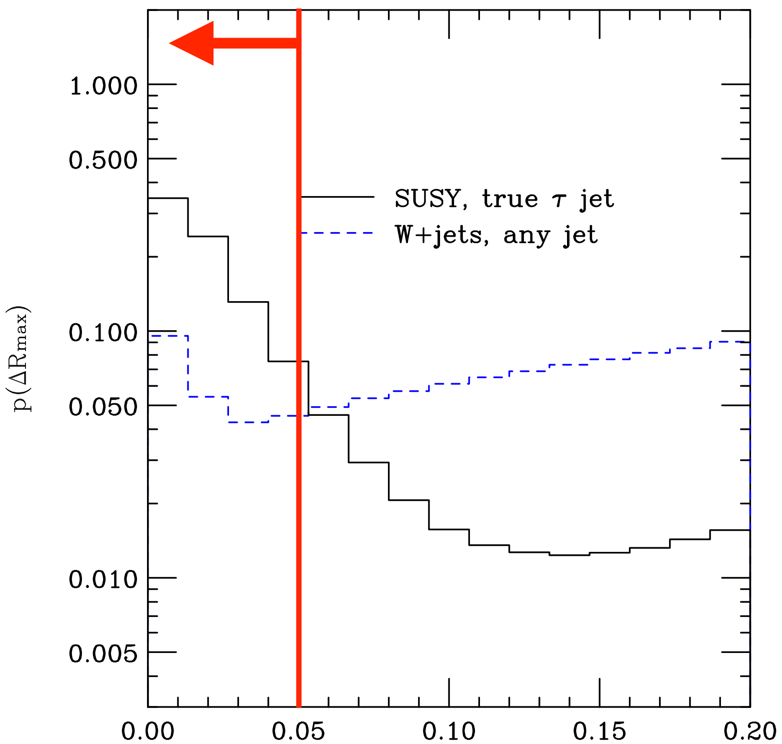

ΔR_{max}

the distance between the jet axis and the furthest track in the jet

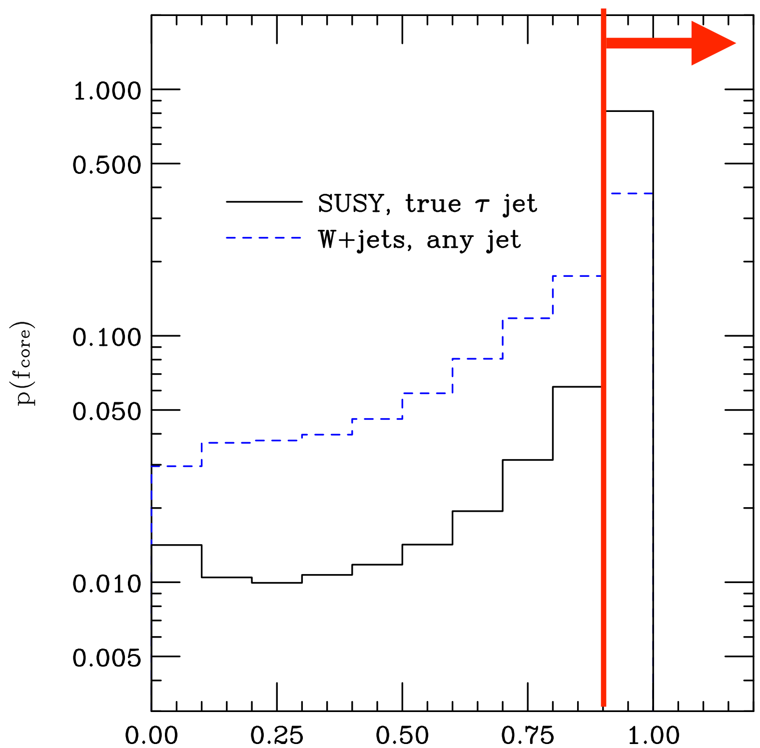

f_{core}

E(ΔR<0.1)/E(jet)

tagging efficiency = 0.5

rejection = 50

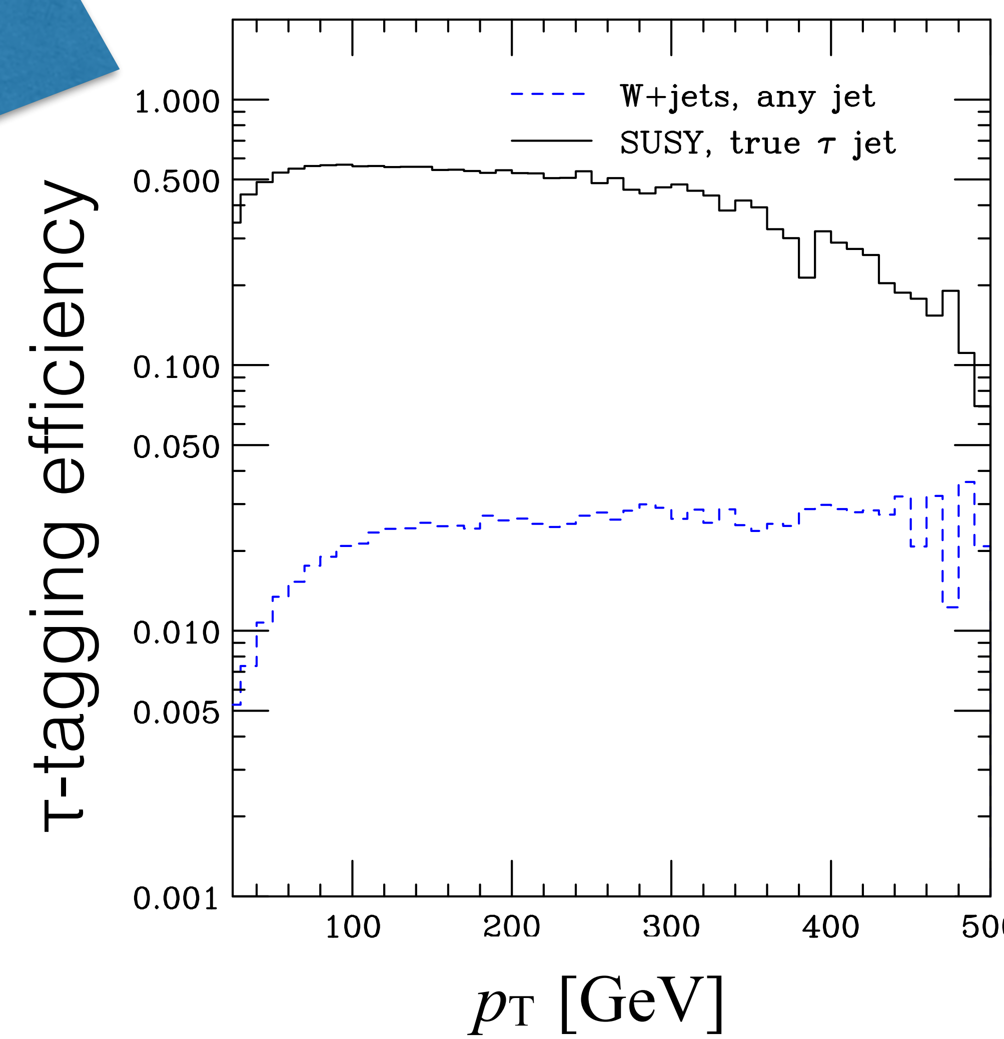

$M_{\min}$ for WZ background

$\theta \equiv \arctan\left(\frac{a}{b}\right)$

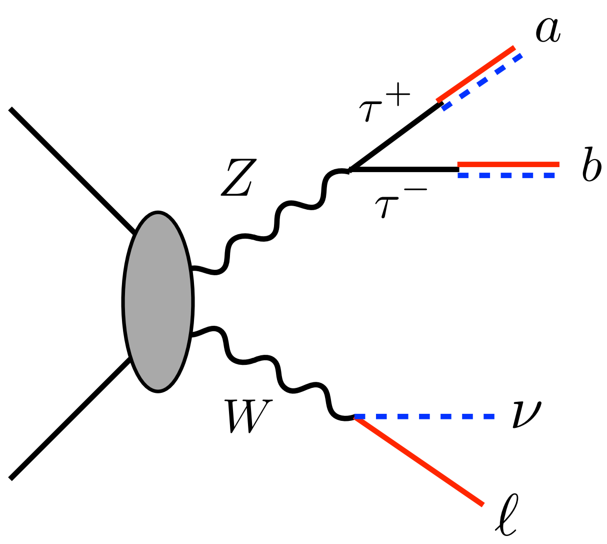

— collinear approx. —

$$p_{\tau^+} = p_{\rho_1}/a, \quad p_{\tau^-} = p_{\rho_2}/b,$$
$$p_{\nu_1} = (1/a - 1)p_{\rho_1}, \quad p_{\nu_2} = (1/b - 1)p_{\rho_2},$$

$a,\ b,\ \mathbf{p}_\nu$: 5 unknowns

$m_Z,\ m_W,\ p^x_{\rm miss},\ p^y_{\rm miss}$: 4 constraints

the system can be parametrised by a single parameter θ

- We define $M_{\min}$ so that it minimises the total energy in terms of θ.

$$M_{\min} \equiv \min_\theta \left[M_{\rm inv}(\theta)\right]$$

$$M^2_{\rm inv}(\theta) = [p_\ell + p_\nu(\theta) + p^+_\tau(\theta) + p^-_\tau(\theta)]^2$$

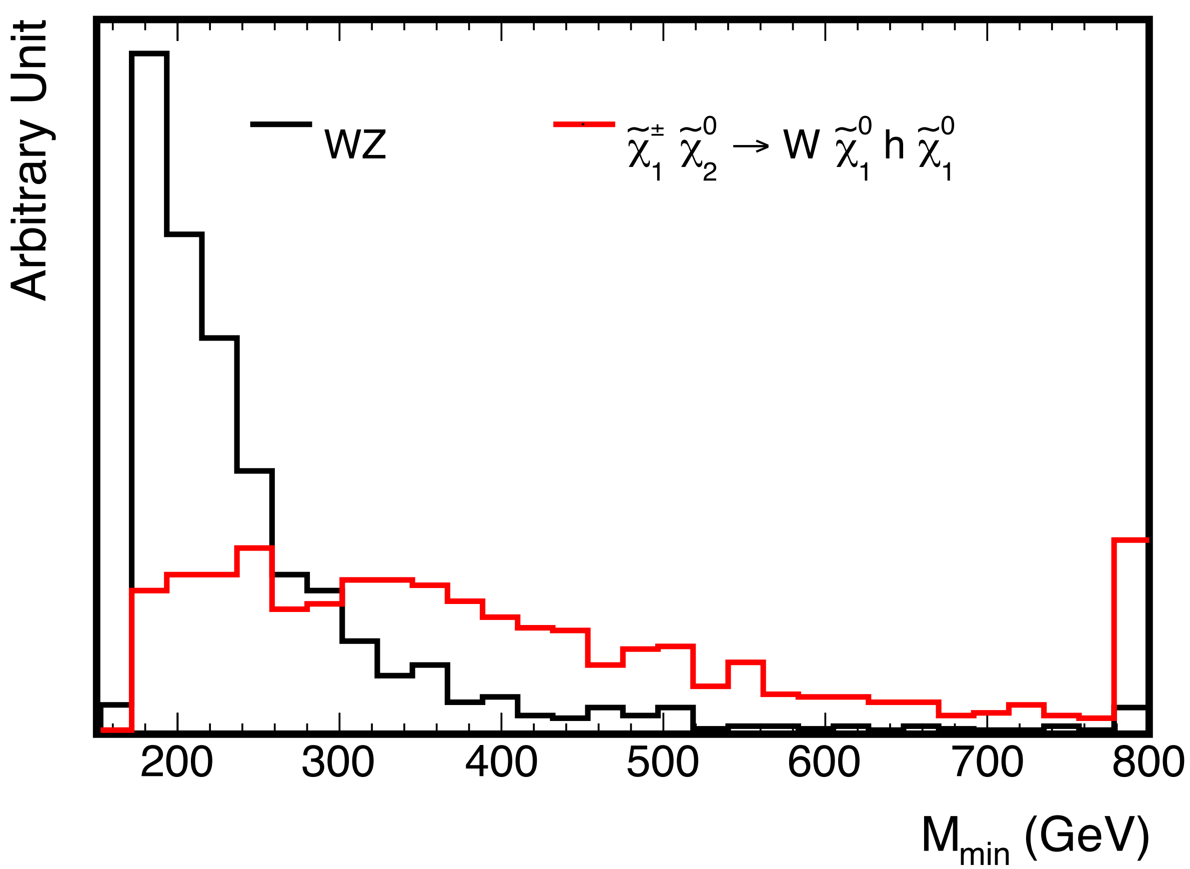

A.Papaefstathiou, KS, M.Takeuchi (1404.1077)

Result

variable	SR1	SR2	SR3	SR4	SR5	SR6	SR7
$\not{p}_T$	95 GeV	120 GeV	100 GeV	90 GeV	90 GeV	150 GeV	90 GeV
$M_{\rm min}$	235 GeV	270 GeV	220 GeV	220 GeV	300 GeV	240 GeV	200 GeV
$p_{T,\tau\tau}$	20 GeV	80 GeV	20 GeV	50 GeV	20 GeV	20 GeV	20 GeV
$\Delta R_{\tau,\tau}$	$(0.1, 2.9)$	$(0.1, 2.9)$	$(0.1, 2.9)$	$(0.1, 2.9)$	$(0.1, 2.9)$	$(0.1, 2.9)$	$(0.1, 2.9)$
$\Delta R_{\tau\tau,\ell}$	$(0.1, 2.6)$	$(0.1, 2.5)$	$(0.1, 2.6)$	$(0.1, 2.6)$	$(0.1, 2.6)$	$(0.1, 2.6)$	$(0.1, 2.6)$

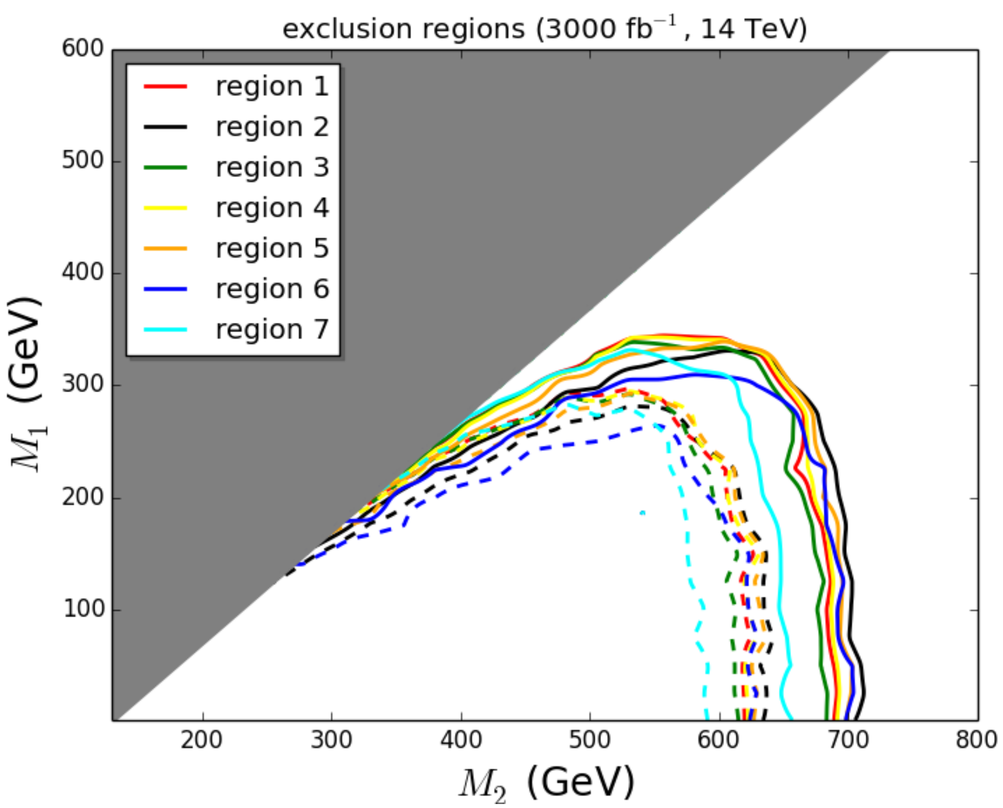

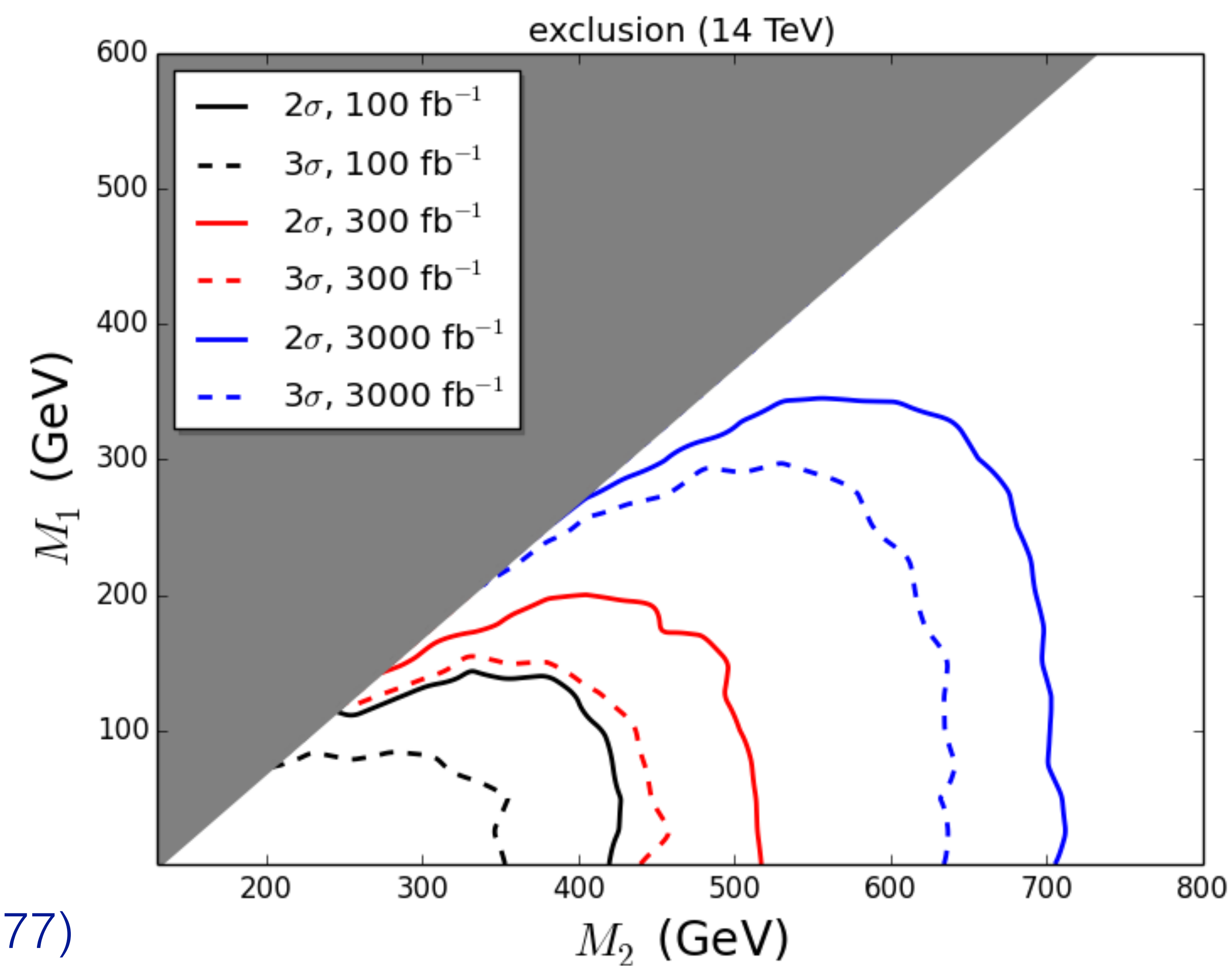

A.Papaefstathiou, KS, M.Takeuchi (1404.1077)

Chargino-Neutralino at a 100TeV *pp* collider

Wino, Higgsino cross section

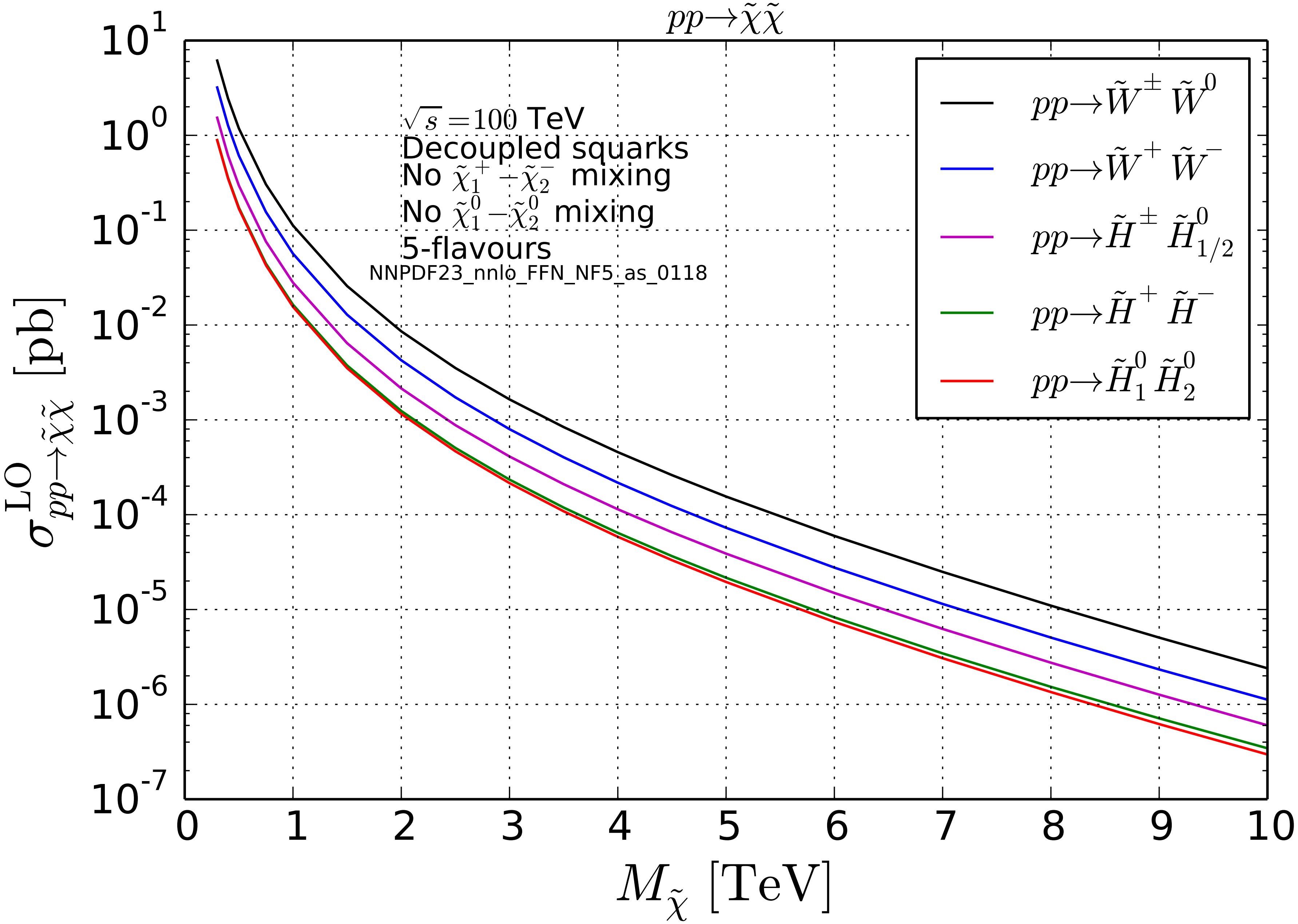

B.Acharya, K.Bozek, C.Pongkitivanichkul KS (1410.1532)

Wino → Higgsino decay

- In Higgsino LSP case, both chagino and neutralino can decay to W, Z and h.

$$\tilde{W}^{\pm} \to W^{\pm}\tilde{H}^{0}, Z\tilde{H}^{\pm}, h\tilde{H}^{\pm} \qquad \tilde{W}^{0} \to W^{\pm}\tilde{H}^{\mp}, Z\tilde{H}^{0}, h\tilde{H}^{0}$$

- The decay rates are related through the *Goldstone equivalence theorem*.

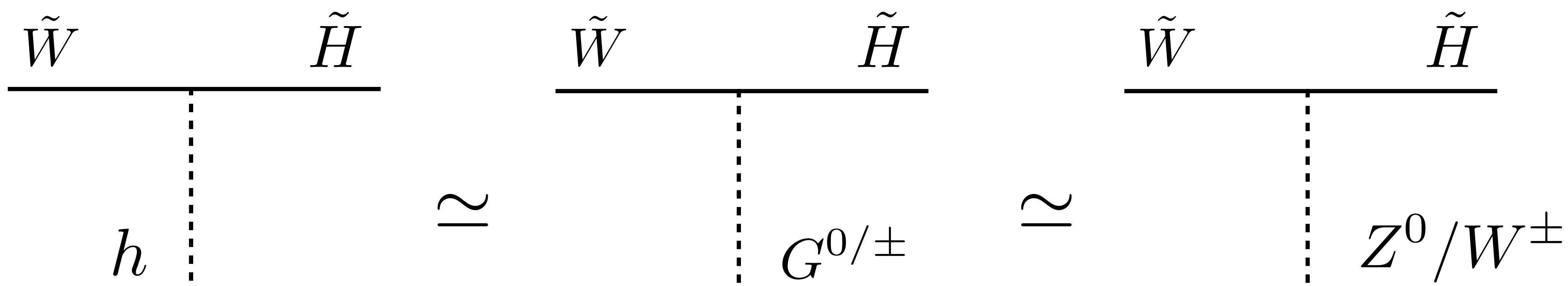

Wino → Higgsino decay

$$\mathrm{BR}(\widetilde{W}^{\pm}) \simeq \begin{cases} 0.5 & \to W^{\pm}\widetilde{H}^{0} \\ 0.25 & \to h\widetilde{H}^{\pm} \\ 0.25 & \to Z\widetilde{H}^{\pm} \end{cases} \qquad \mathrm{BR}(\widetilde{W}^{0}) \simeq \begin{cases} 0.5 & \to W^{\pm}\widetilde{H}^{\mp} \\ 0.25 & \to h\widetilde{H}^{0} \\ 0.25 & \to Z\widetilde{H}^{0} \end{cases}$$

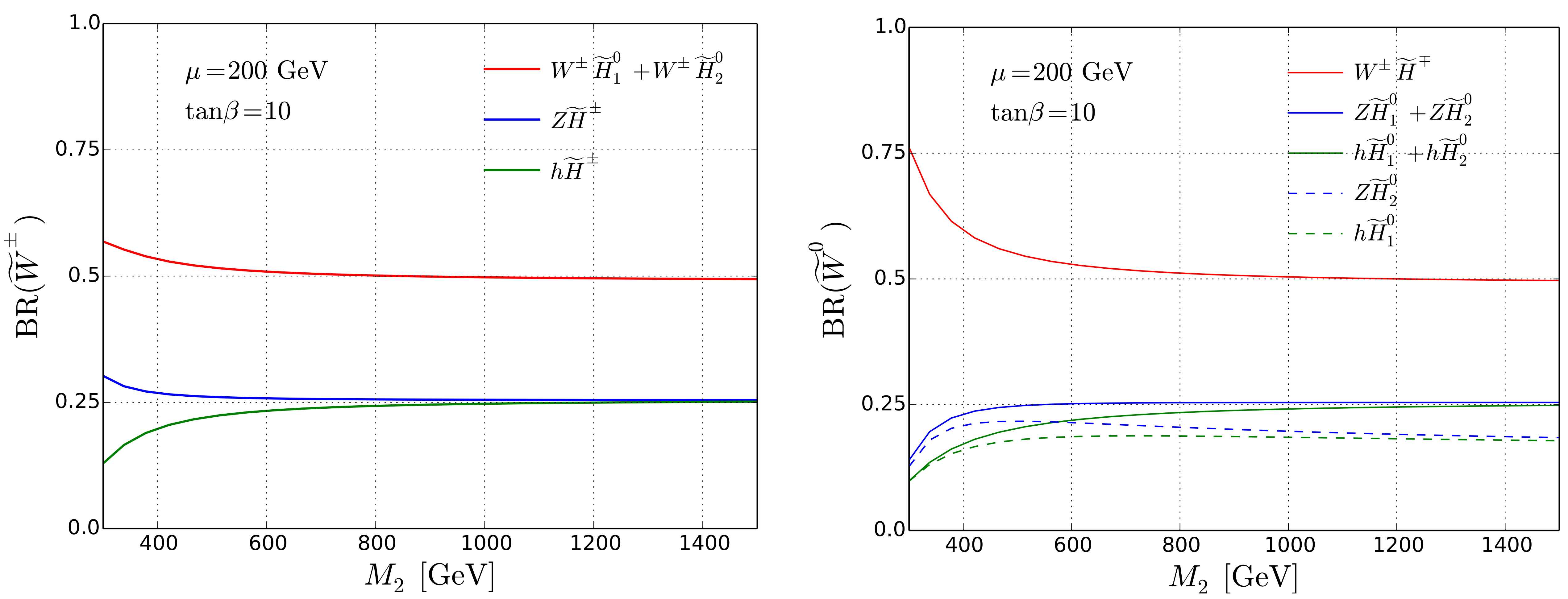

B.Acharya, K.Bozek, C.Pongkitivanichkul KS (1410.1532)

3 lepton channel in *WZ* mode

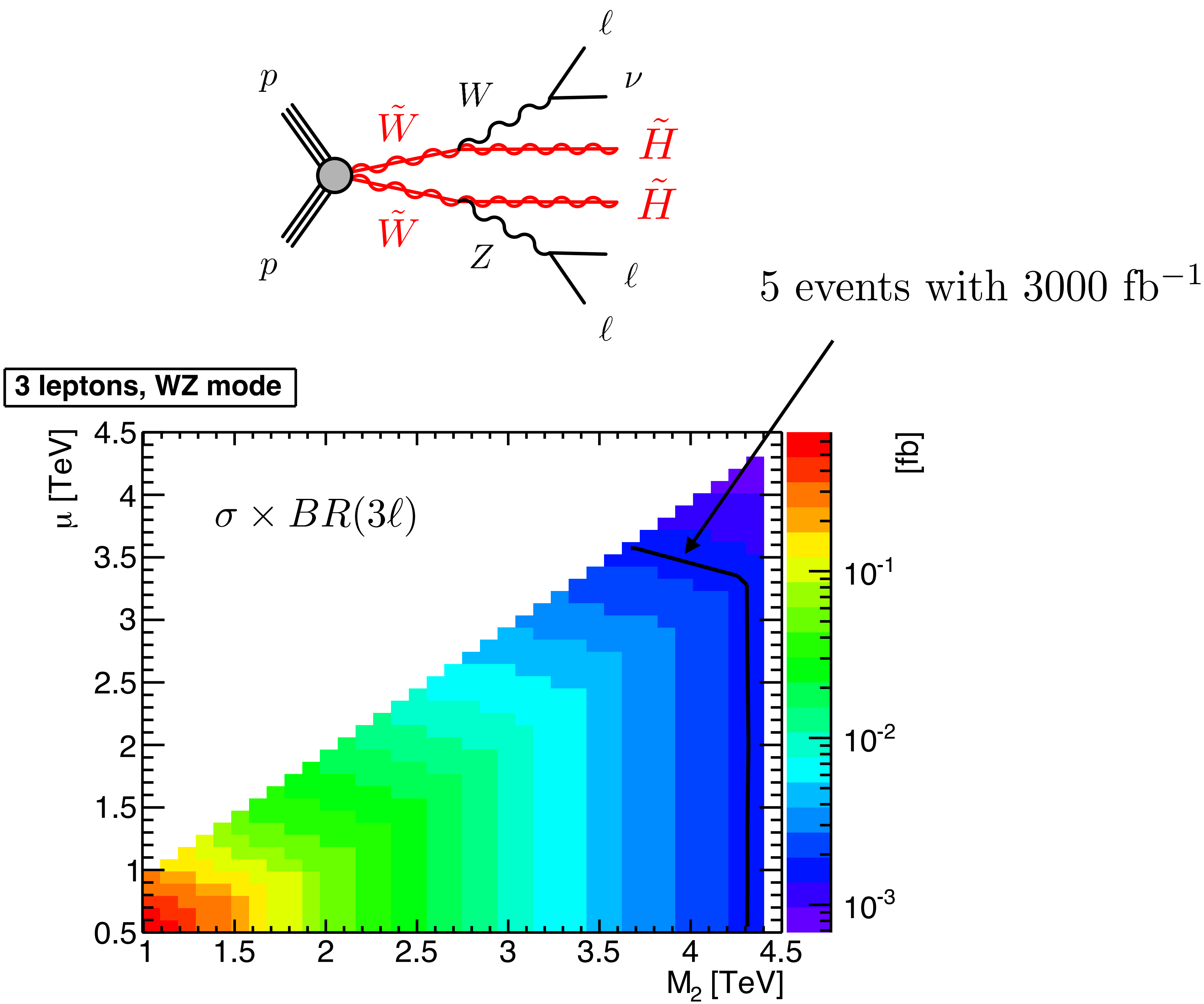

B.Acharya, K.Bozek, C.Pongkitivanichkul KS (1410.1532)

Distributions

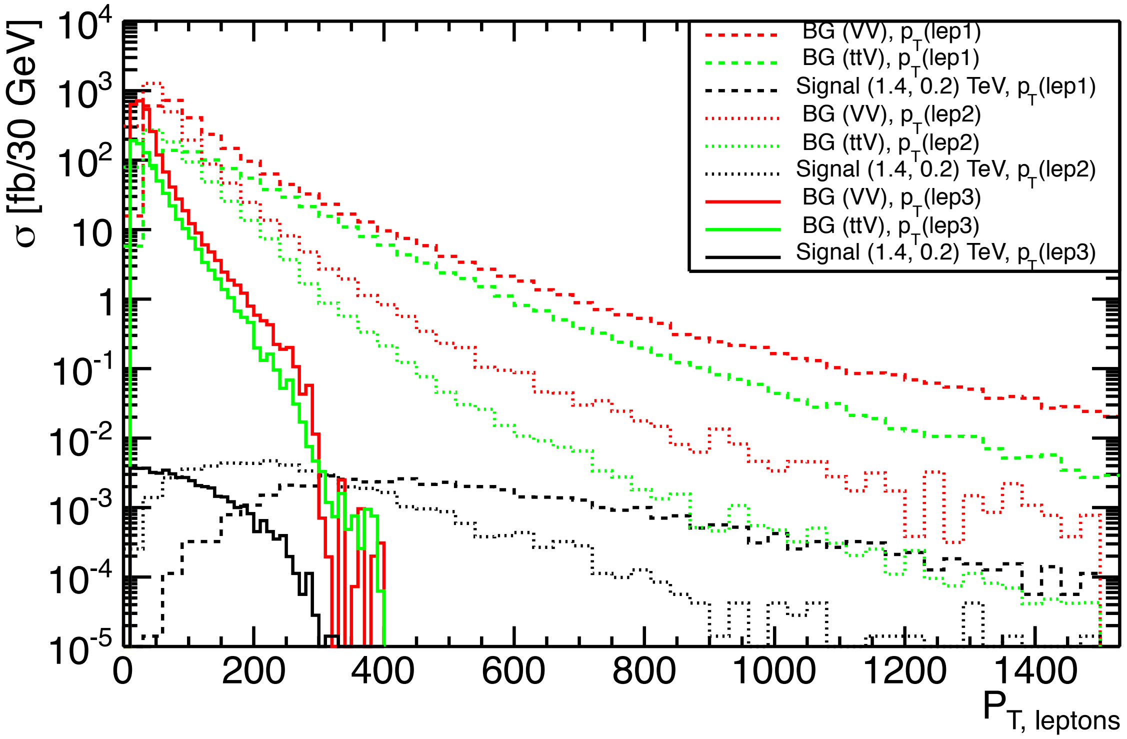

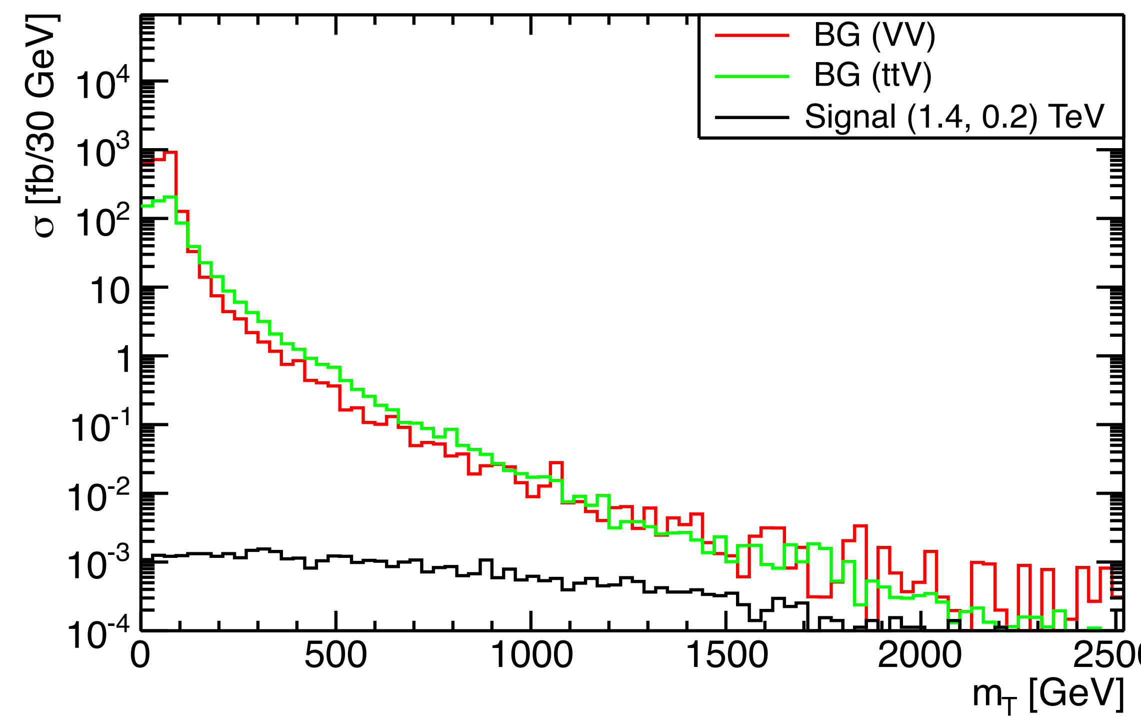

$$m_T \equiv \sqrt{2|p_T(\ell')||E_T^{\rm miss}|(1-\cos\Delta\phi)},$$

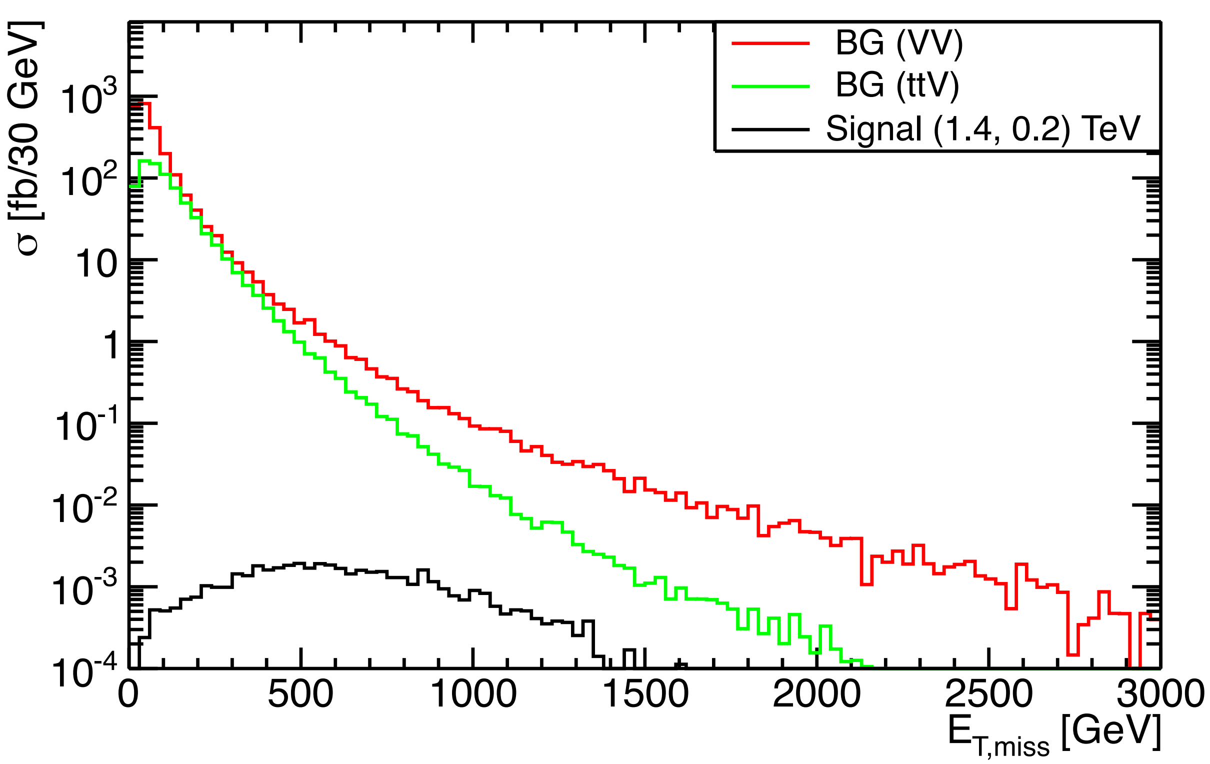

B.Acharya, K.Bozek, C.Pongkitivanichkul KS (1410.1532)

Event selection

preselection

- exactly three isolated leptons with $p_T > 10$ GeV and $|\eta| < 2.5$
- a same-flavour opposite-sign (SFOS) lepton pair with $|m_{\ell\ell}^{\mathrm{SFOS}} - m_Z| < 10$ GeV
- no b-tagged jet

signal regions

Signal Region	3 lepton p_T [GeV]	E_T^{miss} [GeV]	m_T [GeV]
Loose	$> 100, 50, 10$	> 150	> 150
Medium	$> 250, 150, 50$	> 350	> 300
Tight	$> 400, 200, 75$	> 800	> 1100

Cut-flow

- Cut-flows for the signal and background processes in fb

Process	No cut	$= 3$ lepton	$\lvert m_{\ell\ell}^{\rm SFOS} - m_Z \rvert < 10$	no-b jet
VV	3025348	2487	2338	2176
ttV	220161	792	552	318
tV	2764638	68.9	6.07	4.12
VVV	36276	76.1	56.2	56.2
BG total	6046422	3424	2952	2554
$(M_2, \mu) = (800, 200)$	1.640	0.588	0.565	0.534
$(M_2, \mu) = (1200, 200)$	0.397	0.124	0.119	0.111
$(M_2, \mu) = (1800, 200)$	0.0863	0.0190	0.0179	0.0170

Process	$p_T^\ell > (400, 200, 75)$	$E_T^{\rm miss} > 800$	$m_T > 1100$	$S/\sqrt{B}$
VV	5.65	0.123	0.00166	
ttV	1.03	0.0056	0.00092	
tV	0.015	0.0001	0	
VVV	0.350	0.0109	0.00153	
BG total	7.05	0.140	0.00411	
$(M_2, \mu) = (800, 200)$	0.0460	0.0020	0.0012	1.00
$(M_2, \mu) = (1200, 200)$	0.0238	0.0070	0.0052	4.45
$(M_2, \mu) = (1800, 200)$	0.0053	0.0031	0.0026	2.22

Result

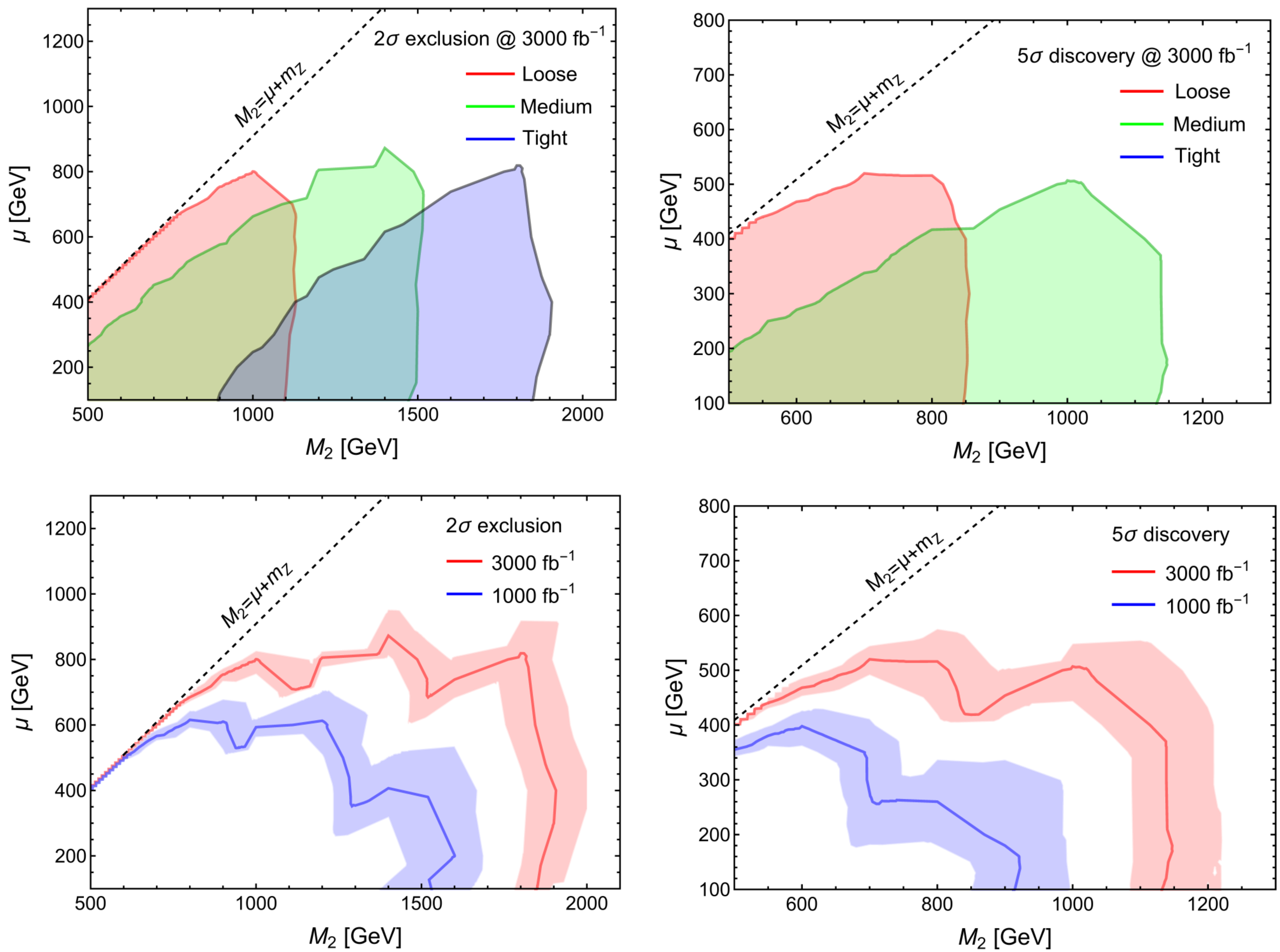

B.Acharya, K.Bozek, C.Pongkitivanichkul KS (1410.1532)

Summary

- The LHC will resume with 13 TeV CoM energy and the exciting time will start.
- It opens up new measurements of Higgs bosons:
  e.g. ttH, tHj productions
- The BSM direct searches: important to understand how to interpret the results.
- Split SUSY is an interesting scenario after LHC run1. Light gauginos may show up at 13 TeV LHC.

T.Cohen, et.al (1311.6480)

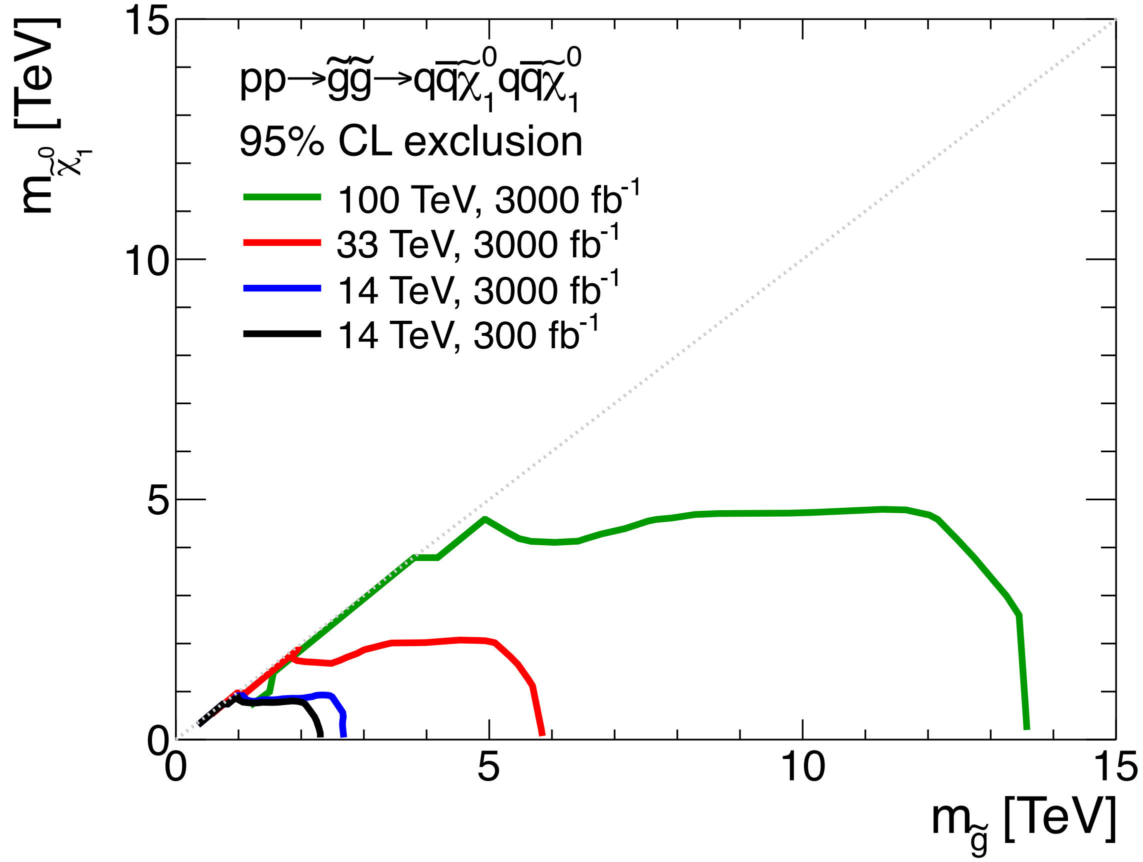

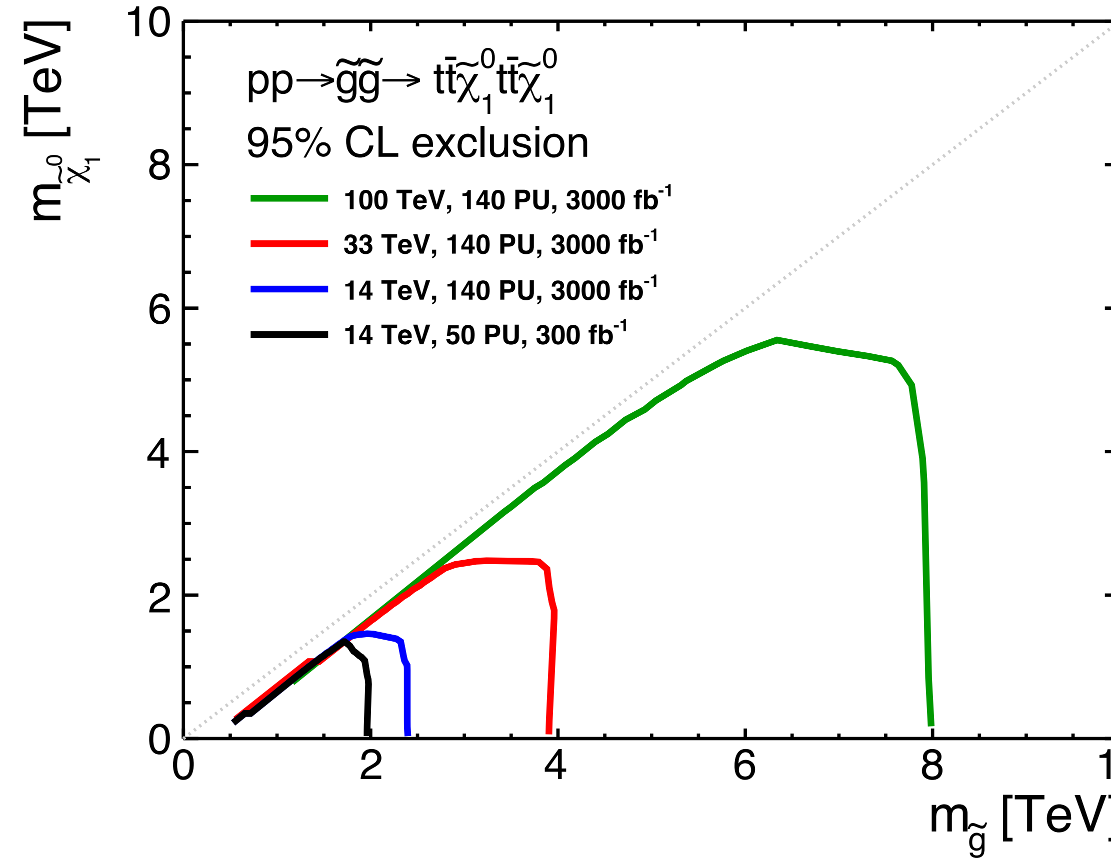

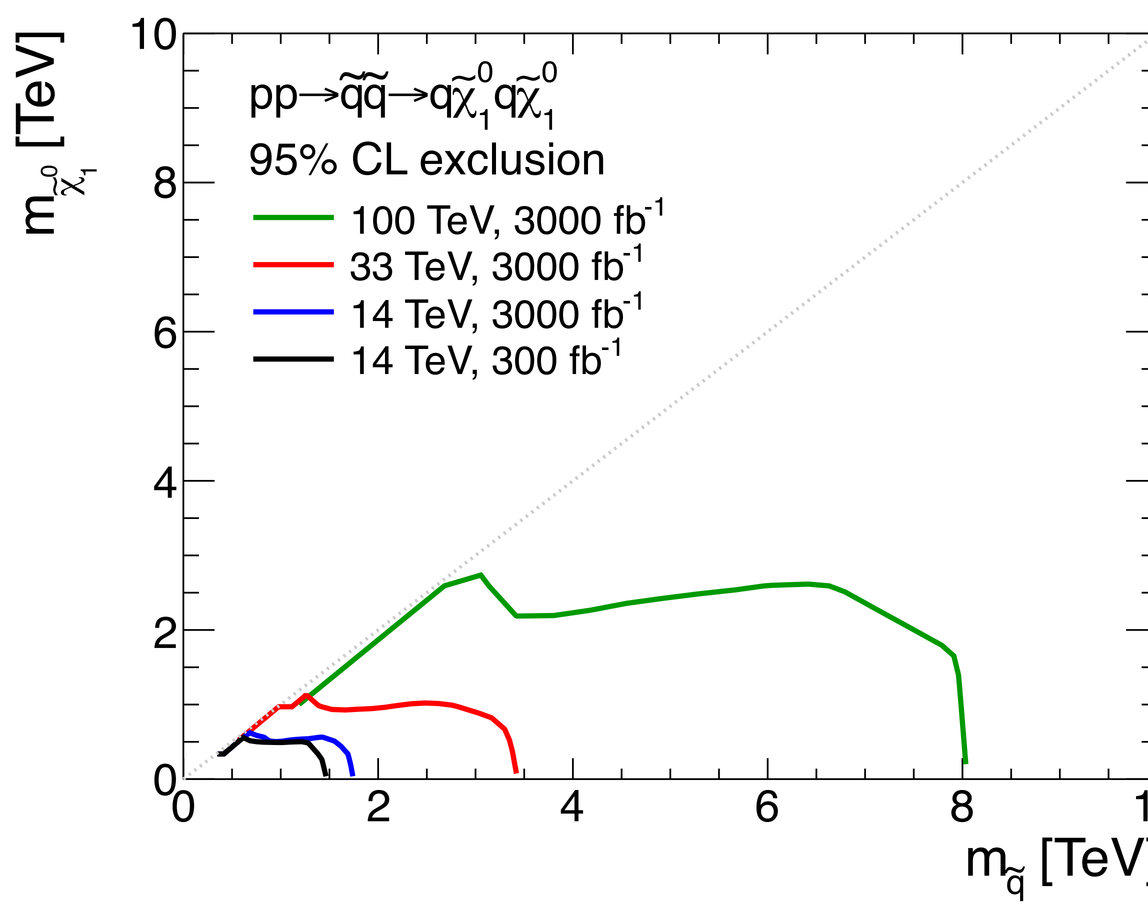

- $\Delta R_{\max}$: the distance to the track furthest away from the jet axis.
- f_{core}: the fraction of the total jet energy contained in the centre-most cone defined by $\Delta R < 0.1$.
- $\Delta R_{\max} < 0.05$.
- $f_{\text{core}} > 0.95$.

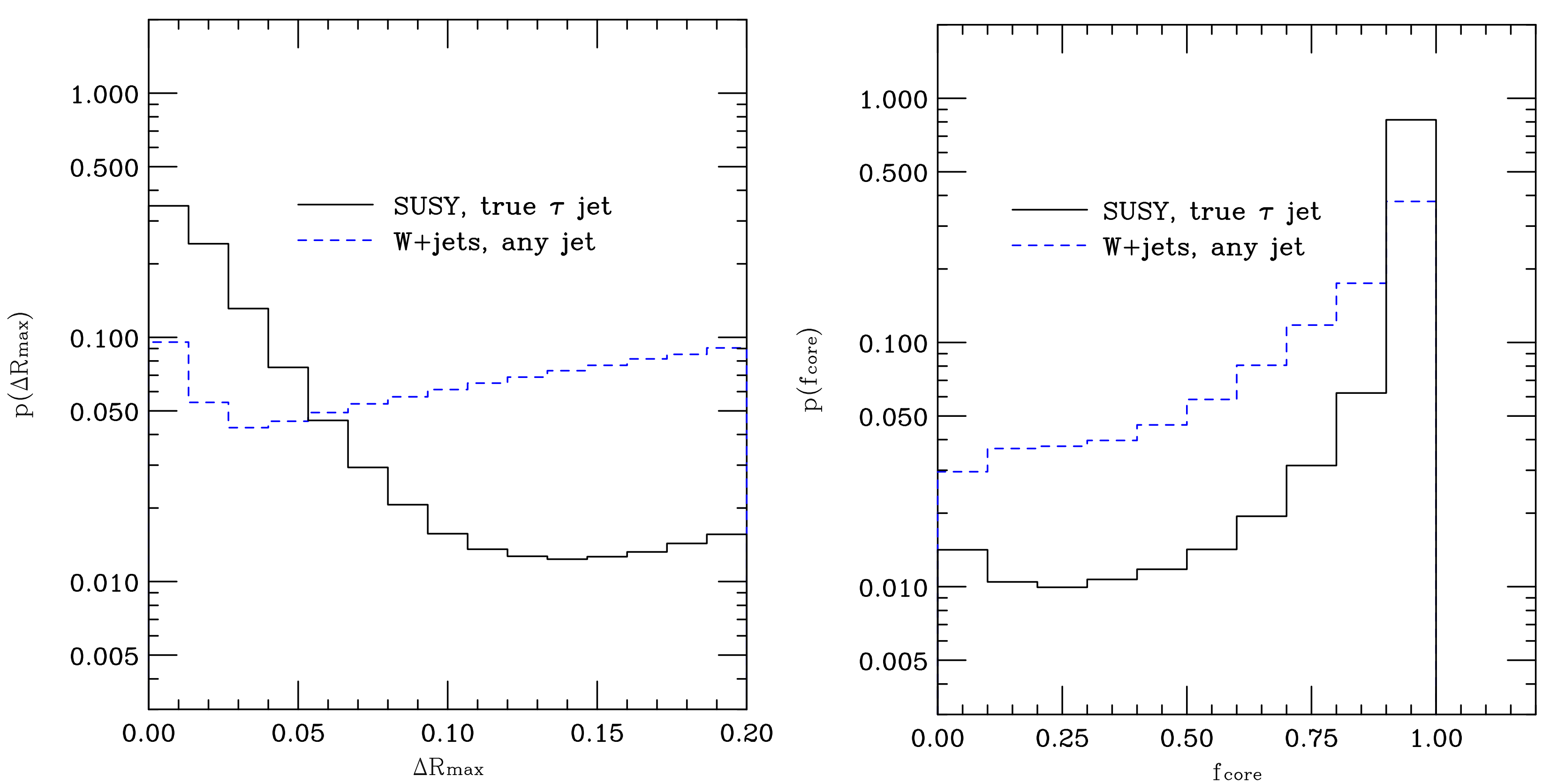

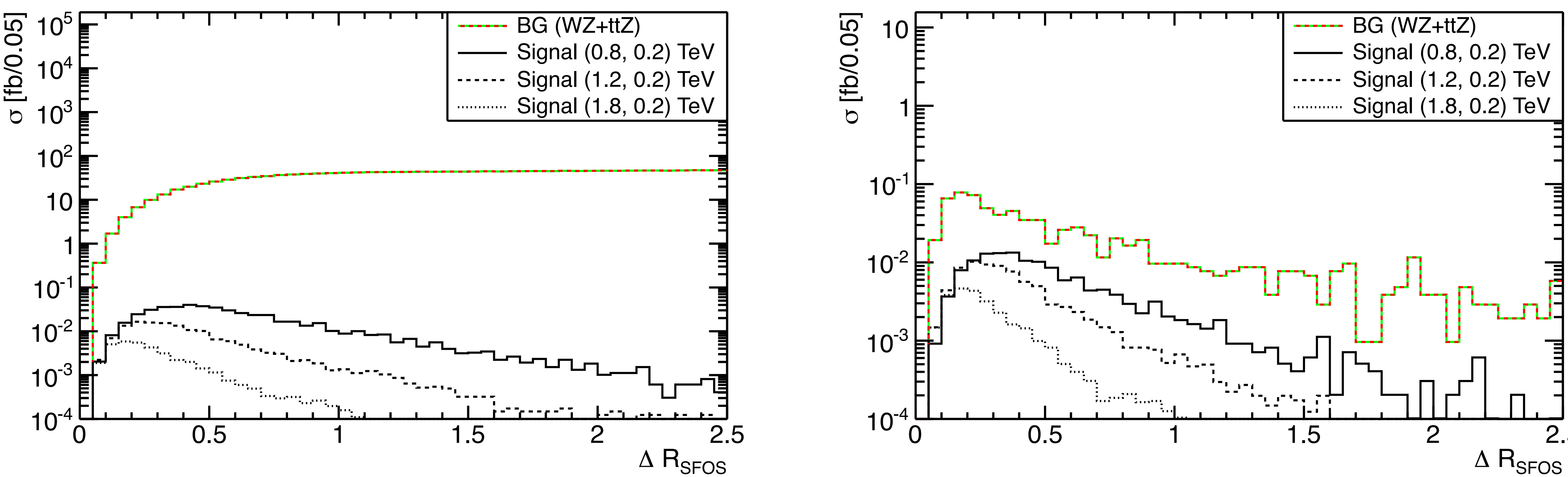

Figure 9. The distributions of $\Delta R_{\rm SFOS}$, the distance between the SFOS lepton pair, **(a)** after preselection cuts, **(b)** after additional cuts: $E_T^{\rm miss} > 500$ GeV and $m_T > 200$ GeV. For both plots, detector simulation has been done by `Delphes 3` using the same detector setup as the one used in Snowmass samples but with $R = 0.05$.

Process	No cut	$= 3$ lepton	$\lvert m_{\ell\ell}^{\rm SFOS} - m_Z \rvert < 10$	no-b jet
VV	3025348	2487	2338	2176
ttV	220161	792	552	318
tV	2764638	68.9	6.07	4.12
VVV	36276	76.1	56.2	56.2
BG total	6046422	3424	2952	2554
$(M_2, \mu) = (800, 200)$	1.640	0.588	0.565	0.534
$(M_2, \mu) = (1200, 200)$	0.397	0.124	0.119	0.111
$(M_2, \mu) = (1800, 200)$	0.0863	0.0190	0.0179	0.0170

Table 3. The (visible) cross sections (in fb) for the cuts employed in the *preselection*. The column marked "No cut" shows the cross sections for the background processes (defined in Table 1) and the cross section times branching ratio into 3 leptons via WZ for signal benchmark points.

Process	$p_T^\ell > (400, 200, 75)$	$E_T^{\rm miss} > 800$	$m_T > 1100$	$S/\sqrt{B}$
VV	5.65	0.123	0.00166	
ttV	1.03	0.0056	0.00092	
tV	0.015	0.0001	0	
VVV	0.350	0.0109	0.00153	
BG total	7.05	0.140	0.00411	
$(M_2, \mu) = (800, 200)$	0.0460	0.0020	0.0012	1.00
$(M_2, \mu) = (1200, 200)$	0.0238	0.0070	0.0052	4.45
$(M_2, \mu) = (1800, 200)$	0.0053	0.0031	0.0026	2.22

Table 6. The visible cross sections (in fb) used in the *Tight* signal region. The last column shows $S/\sqrt{B}$ assuming the 3000 fb^{-1} luminosity for different benchmark points.

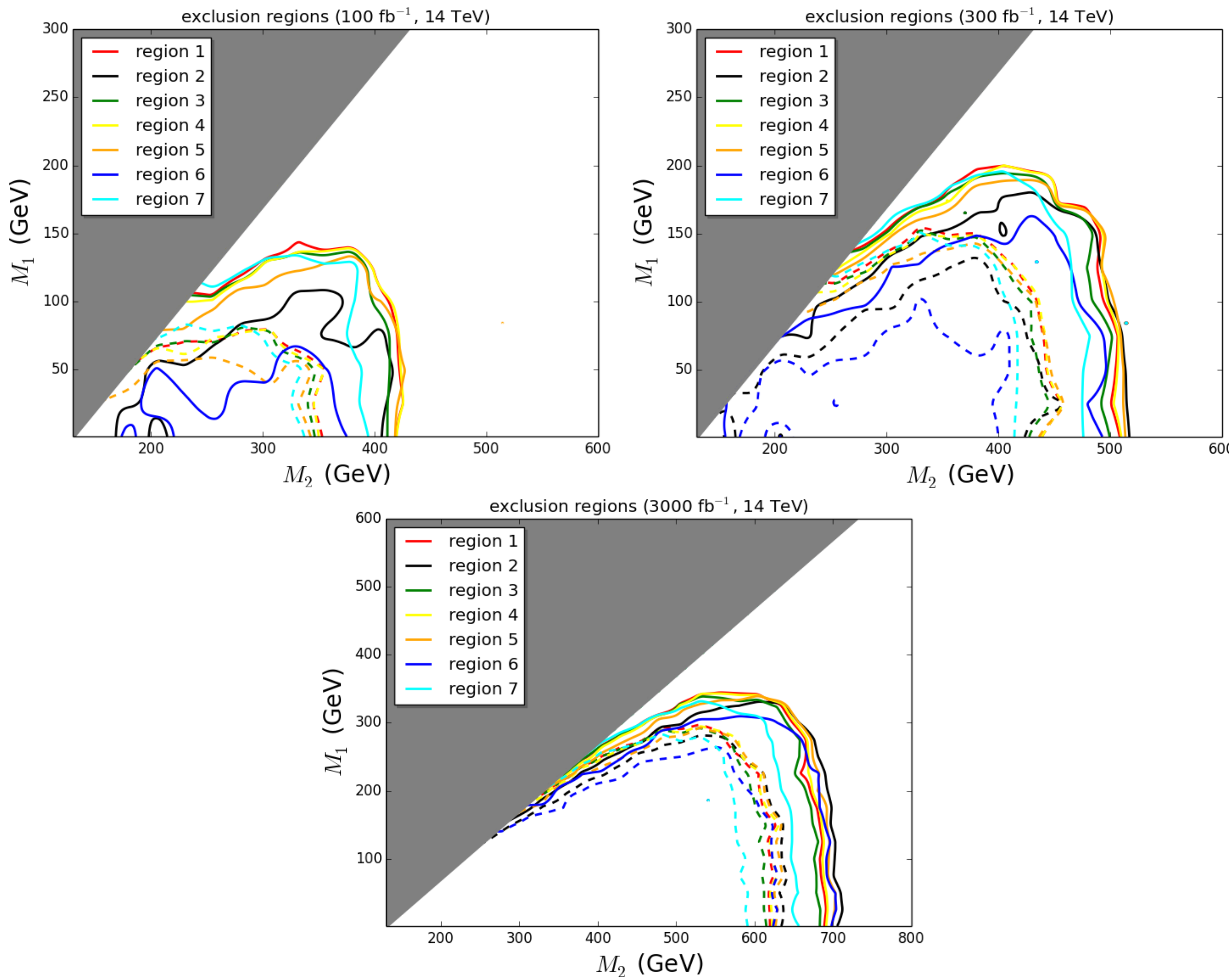

Figure 14. The exclusion on the M_2-M_1 plane obtained for the signal regions defined in Table 4 at integrated luminosities of 100 fb^{-1} (upper left), 300 fb^{-1} (upper right) and 3000 fb^{-1} (bottom). The solid curves show the 2σ exclusion boundary, whereas the dashed curves show the 3σ boundary.

$$|C_{\tilde{\chi}_1^0\tilde{\chi}_2^0 Z}| \simeq \frac{e}{2}\frac{m_Z^2}{|\mu|^2},$$

$$|C_{\tilde{\chi}_1^0\tilde{\chi}_2^0 h}| \simeq \frac{e}{2}\frac{m_Z}{|\mu|}\left|2\sin 2\beta + \frac{M_1+M_2}{\mu}\right|,$$

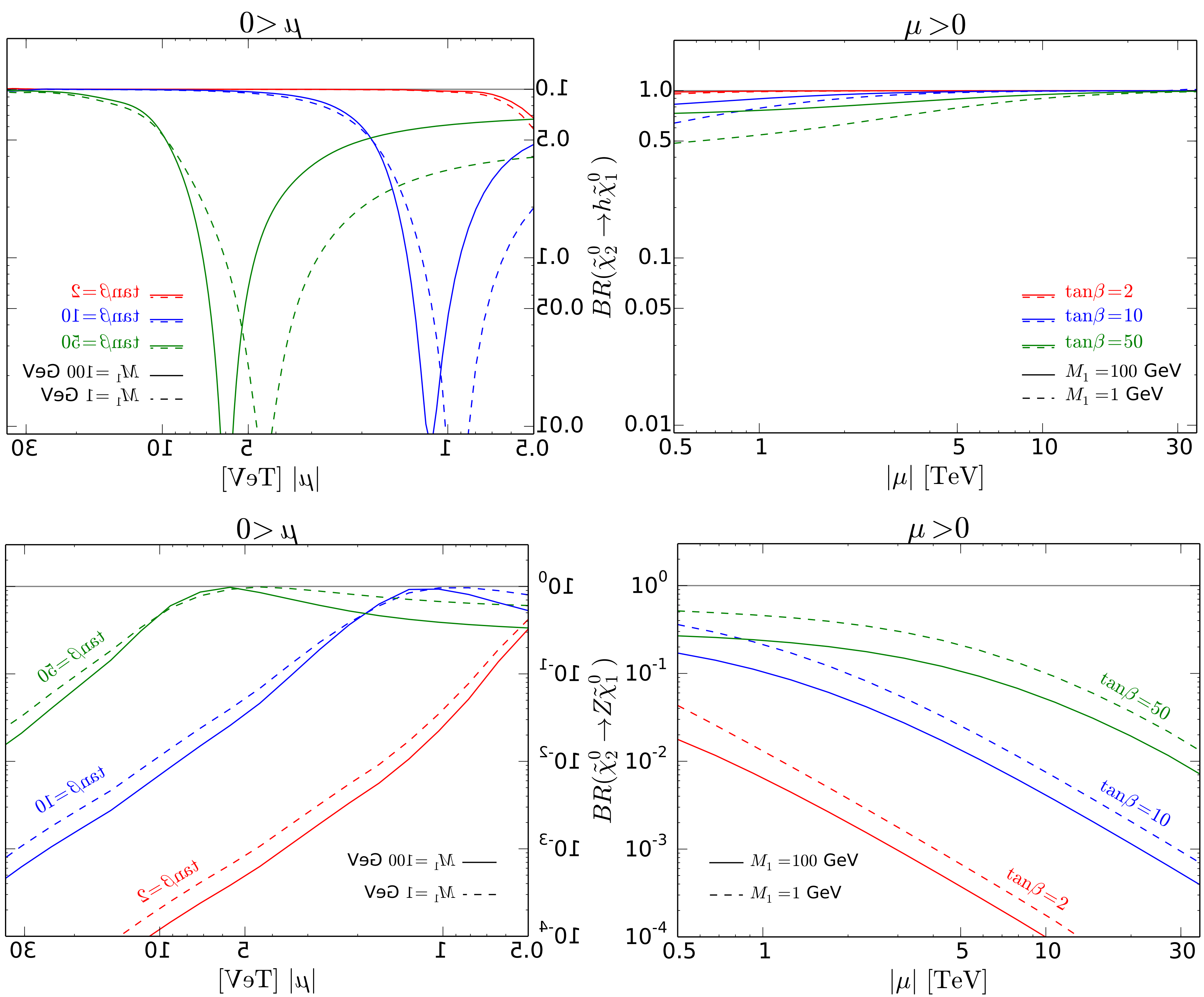

Invariant Mass

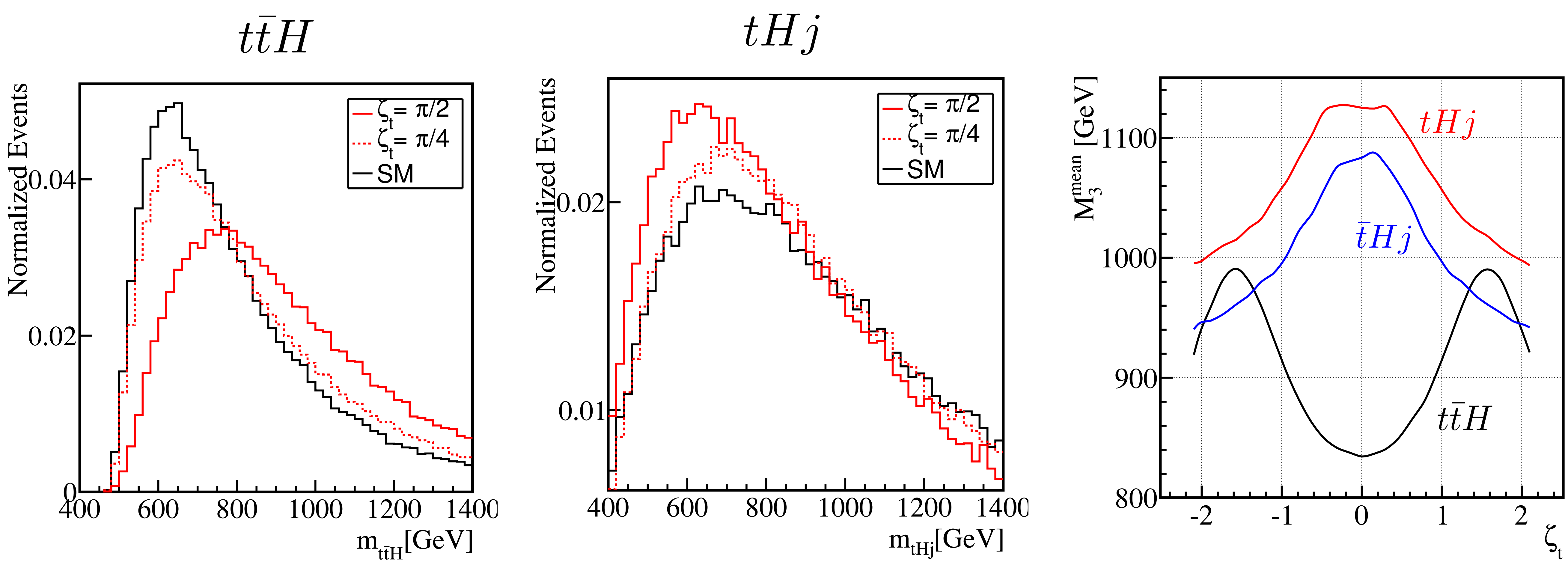

- For ttH, the total invariant mass increases as increasing the CP phase ζ_t.
- For tHj, the total invariant mass decreases as increasing ζ_t.

14 TeV, Parton Level